
Report No. BD-545 RPWO #7
FINAL REPORT

April 2005

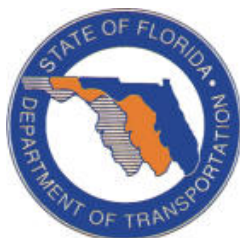
Contract Title: Field Verification of Camber Estimates for Prestressed Girders
UF Project No.: 00030896 (previously 4554 019 12)
Contract No.: BD-545 RPWO #7
UPN No.: 03040891

FIELD VERIFICATION OF CAMBER ESTIMATES FOR PRESTRESSED CONCRETE BRIDGE GIRDERS

Principal Investigator(s):	Ronald A. Cook, Ph.D., P.E. David Bloomquist, Ph.D., P.E.
Graduate Research Assistant:	Jonathan E. Sanek
Project Manager:	Marcus H. Ansley, P.E.

Department of Civil & Coastal Engineering
College of Engineering
University of Florida
Gainesville, Florida 32611

Engineering and Industrial Experiment Station



1. Report No. BD-545 RPWO #7		2. Government Accession No.		3. Recipient's Catalog No.	
4. Title and Subtitle Field Verification of Camber Estimates for Prestressed Girders				5. Report Date April 2005	
				6. Performing Organization Code	
				8. Performing Organization Report No. 00030896	
7. Author(s) R. A. Cook, D. Bloomquist, J. E. Sanek				10. Work Unit No. (TRAIS)	
9. Performing Organization Name and Address University of Florida Department of Civil Engineering 345 Weil Hall / P.O. Box 116580 Gainesville, FL 32611-6580				11. Contract or Grant No. BD545 RPWO #7	
				13. Type of Report and Period Covered Final Report	
				14. Sponsoring Agency Code	
12. Sponsoring Agency Name and Address Florida Department of Transportation Research Management Center 605 Suwannee Street, MS 30 Tallahassee, FL 32301-8064					
15. Supplementary Notes Prepared in cooperation with the Federal Highway Administration					
16. Abstract <p>Prestressed concrete girders are used on many of Florida's bridges. These girders are subject to camber, the upward deflection of the girder due to the eccentricity of the prestressing force. Differences have been found between camber predicted by the design program employed by the FDOT and the measured field camber for prestressed "Bulb-Tee" girders. These differences can cause changes and delays during construction because of corrections to build-up and/or bearings of the bridge superstructure. The focus of this investigation was to obtain field measurements of camber on large prestressed girders over an extended period of time. This information was used to evaluate the current camber prediction model used by the FDOT. Specifically, the types of girders monitored for this project were 1) the 78-inch Florida Bulb-Tee girder, 2) the AASHTO Type IV girder, and 3) the AASHTO Type V girder.</p>					
17. Key Words camber, prestressed, girder, beam			18. Distribution Statement No restrictions. This document is available to the public through the National Technical Information Service, Springfield, VA, 22161		
19. Security Classif. (of this report) Unclassified		20. Security Classif. (of this page) Unclassified		21. No. of Pages 129	22. Price

ACKNOWLEDGMENTS

Many imparted their own individual efforts toward the successful conclusion of this project. We would like to thank Isaac Canner, Xiaoming Wen, Michael Reponen, and Joe Liberman for the help they provided in the field. Also, we thank George Lopp for the guidance and help he offered in the operation of the *MTS*[®] concrete cylinder testing apparatus; Chuck Broward and Danny Brown for their help with the fabrication of the instrumentation used on this project; Richard DeLorenzo of the FDOT State Materials Office for his help with the supplemental materials testing; and Dr. Bon Dewitt for his help operating the surveying instrumentation implemented on this project. We would also like to offer our gratitude to John Jarrett and all those individuals at the *Durastress Inc.* precast facility. Without their cooperation, this project could not have taken place. We also appreciate the information provided by the *Gate Precast Company*.

TABLE OF CONTENTS

CHAPTER	<u>Page</u>
1 INTRODUCTION	1
2 PRESTRESSED BEAM CAMBER	3
2.1 Introduction.....	3
2.2 Construction Problems.....	3
2.3 Time Dependent Effects	4
2.4 Calculation of Camber	9
2.5 LRFD Prestress Loss.....	10
2.6 LRFD Creep Coefficient.....	14
2.7 Thermal Effects.....	15
2.8 Effect of Coarse Aggregate.....	17
2.8.1 Introduction.....	17
2.8.2 Mechanical Properties.....	17
2.8.3 Physical Properties.....	18
2.8.4 Effects of Coarse Aggregate on Differential Shrinkage	20
3 METHODOLOGY	21
3.1 Camber Measurement	21
3.2 Thermal Gradient Measurement and Camber Correction.....	25
3.3 Supplemental Material Testing.....	29
4 SUMMARY OF RESULTS	32
4.1 Camber Measurement at Release.....	32
4.2 Camber Measurement Summary.....	35
4.3 Supplemental Material Testing Summary	45
4.4 Florida Limerock Specimens	52
4.4.1 Camber Measurement at Release.....	53
4.4.2 Camber Measurement Summary.....	54
5 CONCLUSIONS AND RECCOMENDATIONS	57

APPENDIX

A	CAMBER AT RELEASE MEASUREMENTS	59
B	FIELD CAMBER MEASUREMENTS.....	60
C	EMPIRICAL THERMAL ANALYSIS.....	65
D	ANALYTICAL THERMAL ANALYSIS.....	72
E	TABULATED AMBIENT DATA	88
F	MIX DESIGNS	101
G	TABULATED MATERIAL TESTING DATA	106
H	78" BULB-TEE CAMBER CALCULATION	110
I	DOCUMENTED LIMEROCK SPECIMEN DATA.....	117
	REFERENCES	119

LIST OF TABLES

<u>Table</u>	<u>Page</u>
1 Angular measurement technique accuracy	23
2 <i>Pro-Level</i> TM measurement technique accuracy	25
3 Example of field measurements and thermally corrected cambers	28
4 Comparison of field measured camber to predicted camber	36
5 Girder pour identification summary.....	46
6 Tabular comparison of predicted and actual camber values for Limerock and granite specimens of the AASHTO Type IV girder	55
7 Comparison of field measured camber to predicted camber at 240 days for Bulb-Tee girders	56

LIST OF FIGURES

<u>Figure</u>	<u>Page</u>
1 Drying shrinkage vs. time	7
2 Concrete creep vs. time after loading	7
3 Camber at midspan vs. time	8
4 Effect of relative aggregate and cement stiffness on concrete stiffness	18
5 Optical target mounted on fixed ceramic magnet	21
6 Isometric view of a three-point resection analysis	22
7 <i>Pro-Level</i> TM water manometer schematic	24
8 <i>Pro-Level</i> TM water manometer measurement technique	25
9 Infrared temperature sensor	26
10 Example single day temperature profile of Bulb-Tee girder 3	27
11 Field cured 4"x 8" concrete test cylinders	29
12 Computerized <i>MTS</i> [®] concrete cylinder testing apparatus	30
13 Bar chart of 78" Bulb-Tee camber at release, after moving, and FDOT predicted values	33
14 Bar chart of AASHTO Type IV camber at release, after moving, and FDOT predicted values	34
15 Bar chart of AASHTO Type IV camber at release, after moving, and FDOT predicted values	34
16 AASHTO Type IV girder in storage	37
17 Field camber measurements for 78" Bulb-Tee girder 1	38
18 Field camber measurements for 78" Bulb-Tee girder 2	38
19 Field camber measurements for 78" Bulb-Tee girder 3	39
20 Field camber measurements for 78" Bulb-Tee girder 4	39
21 Field camber measurements for 78" Bulb-Tee girder 5	40
22 Field camber measurements for 78" Bulb-Tee girder 6	40
23 Summary of field camber measurements for all 78" Bulb-Tee girders	41
24 Field camber measurements for AASHTO Type IV girder 1	41
25 Field camber measurements for AASHTO Type IV girder 2	42

26	Field camber measurements for AASHTO Type IV girder 3.....	42
27	Summary of field camber measurements for all AASHTO Type IV girders	43
28	Field camber measurements for AASHTO Type V girder 1	43
29	Field camber measurements for AASHTO Type V girder 2	44
30	Field camber measurements for AASHTO Type V girder 3	44
31	Field camber measurements for AASHTO Type V girder 4.....	45
32	Summary of field camber measurements for all AASHTO Type V girders.....	45
33	78" Bulb-Tee pour "A" compressive strength vs. time	47
34	78" Bulb-Tee pour "A" elastic modulus vs. time	48
35	78" Bulb-Tee pour "B" compressive strength vs. time.....	48
36	78" Bulb-Tee pour "B" elastic modulus vs. time	49
37	AASHTO Type IV pour "A" compressive strength vs. time.....	49
38	AASHTO Type IV "A" elastic modulus vs. time.....	50
39	AASHTO Type V pour "A" compressive strength vs. time	50
40	AASHTO Type V "A" elastic modulus vs. time	51
41	AASHTO Type V pour "B" compressive strength vs. time	51
42	AASHTO Type V "B" elastic modulus vs. time	52
43	Limerock 72" Bulb-Tee and AASHTO Type IV camber at release	53
44	72" Bulb-Tee (Limerock) girder camber growth summary	54
45	AASHTO Type IV (Limerock) girder camber growth summary	54
46	Comparison of predicted camber to actual field camber for granite and limerock specimens of AASHTO Type IV girder	55

CHAPTER 1 INTRODUCTION

Prestressing of concrete, in general, is the introduction of an internal loading condition such that the performance of the structural member is improved in several ways. Specifically, a prestressing force is used in flexural members to lessen the concrete tensile stresses. This is done in order to prevent or reduce concrete cracking in the tensile zone due to tensile stresses exceeding the rupture strength of the concrete. The prestressing force is typically applied to a concrete beam section such that it creates an eccentric, axial loading condition resulting in an upward deflection or camber. Also, as a result of preventing cracking, this “preloading” reduces the amount the flexural member will deflect under service loads, thus improving the serviceability of the member. The prestressing force, however, does not increase the flexural strength of an element.

The prestressed beam design program currently implemented by the Florida Department of Transportation, *Eng LFRD PSBeam v.1.85*, includes calculations for the prediction of time-dependent camber growth that have not been field verified. This camber growth is obtained by calculating the elastic camber at the release of the prestressed girder (i.e., application of the prestressing force) and applying a time-dependent multiplication factor. The focus of this investigation was to obtain field camber measurements on different types of bridge girders with the goal of verifying or improving the present design methodology used by the FDOT for time-dependent camber estimation.

Periodic field camber measurements from initial prestress transfer to as much as six months after transfer were performed on:

- Six (6) Florida 78-inch Bulb-Tee were 162-feet in length with fifty-three (53) 0.60"-diameter, 270-ksi, "Lo-Lax" prestressing strands, and used FDOT Class VI coarse granite aggregate concrete with a specified 28-day compressive strength of 8,500-psi.
- Three (3) AASHTO Type IV girders were 91-feet in length with thirty (30) ½"-diameter, 270-ksi, "Lo-Lax" prestressing strands, and used FDOT Class IV coarse granite aggregate concrete with a specified 28-day compressive strength of 5,500-psi.
- Four (4) AASHTO Type V girders were 81-feet in length with twenty-eight (28) ½"-diameter, 270-ksi, "Lo-Lax" prestressing strands, and used a FDOT Class IV coarse granite aggregate concrete with a specified 28-day compressive strength of 5,500-psi.

CHAPTER 2 PRESTRESSED BEAM CAMBER

2.1 Introduction

Camber is the upward deflection of a flexural member due the eccentricity of the prestressing force. The prestressing force is placed eccentrically to counteract the downward deflection of the flexural member caused by gravity loads and service loads. The amount of camber is dependent upon several factors: the tendon profile, the prestress magnitude, the span, the section properties, and the elastic modulus of the concrete (Nawy 2003).

2.2 Problems with Construction

The need for accurate predictions of estimated camber in prestressed structural members can not be overstated. However, even in controlled conditions, predictions of element deflections to a high degree of accuracy are difficult (Tadros, Ghali, and Meyer 1985). Discrepancies between the predicted and the actual measured field camber can cause delays in construction because of corrections to build-up and/or bearings of the prestressed structure. In the FDOT structural design guidelines, the haunch between the slab and the girder can be adjusted in order to compensate for variation between the required and provided deck profile and maintain a constant slab thickness (Yazdani, Mtenga, and Richardson 1999). These solutions cause construction delays which can be costly and cause additional problems throughout later construction stages.

2.3 Time-Dependent Effects

One important characteristic of camber is that it increases with time. This camber growth begins immediately following the application of the prestressing force to the flexural element. This is known as the prestress “transfer” or “release.” The element first deflects upward due to the elastic strain in the pre-compressed tensile zone. Strains due to concrete creep and shrinkage then begin to grow with time (at a higher rate in the pre-compressed tensile zone than in the compressive zone), thus creating a time-dependent relationship of camber growth (Sinno and Furr 1970). These strains bring about losses in the prestressing force, or what are referred to as “prestress losses.” These prestress losses cause a reduction in the prestressing force which leads to an overall reduction in the amount of camber a prestressed element will exhibit.

These prestress losses can be calculated one of several ways: lump sum estimates of the total prestress loss, refined estimates of each contributing factor (as outlined by *ACI 209R Committee Report* and *AASHTO LRFD Bridge Design Specification*), or a rigorous analysis using the “time-step procedure” (Naaman and Hamza 1993). The time-step procedure is the most accurate method for determining long-term prestress losses when the material properties and environmental conditions are well-known. This method takes into account the interdependent effects of the long-term prestress losses upon one another. For example, the relaxation of the prestressing steel reduces the amount of stress applied to the pre-compressed tensile zone of the flexural element. This reduced stress then affects the amount that the concrete will creep and shrink. The time-step procedure discretizes these effects into time increments, at the end of which a prestress loss is then calculated and accumulated (Naaman and Hamza 1993). Prestress losses to be

considered in an analysis of a pre-tensioned flexural member are loss due to; anchorage of prestressing steel (*ANC*), deflecting device for draped strands in pre-tensioned construction (*DEF*), elastic shortening (*ES*), creep of concrete (*CR*), shrinkage of concrete (*SH*), and relaxation of the prestressing steel (*RET*) (Preston 1975). The total prestress loss (*TL*) is defined by the equation:

$$TL = ANC + DEF + ES + \sum_{ii} (CR + SH + RET) \quad (1)$$

For analysis of a post-tensioned flexural member, loss due to friction of the prestressing tendon (*FR*) would be included in the total prestress loss calculation (Naaman and Hamza 1993). In this equation, time-dependent losses from creep, shrinkage, and steel relaxation are lumped together because they are interdependent upon one another.

Although long-term prestress losses include the effect due to relaxation of the prestressing steel, the more dominant factors are those due to creep and shrinkage of the concrete. The bulk of the prestress loss due to relaxation occurs before the transfer of the prestressing force. Thus, there are few provisions made to include the effects of the prestress loss due to relaxation for calculations of the long-term prestress loss and camber because they are relatively small (Magura, Sozen, and Siess 1964). Generally, 30-40% of the steel relaxation takes place within the first two days following the application of the prestressing force. Therefore, prestress losses due to creep and shrinkage of the concrete are overwhelmingly the more influential factors in affecting the long-term behavior of prestressed elements.

Creep is an increase in strain with time under a sustained stress condition (Neville 1971). The amount of creep a concrete structural element will undergo depends primarily

on the magnitude of the applied load, the time for which the load is applied, and the strength of the concrete at which the load is first introduced (Kostmatka and Panarese 1988). Additional factors affecting the creep of a concrete specimen are the curing history of the concrete; type, amount and maximum size of aggregate; type of cement; amount of cement paste; size and shape of concrete specimen; volume to surface area ratio; amount of non-prestressed steel reinforcement; and the temperature and humidity at which the concrete specimen is stored (Kostmatka and Panarese 1988).

Shrinkage is the volumetric deformation of a concrete specimen with time in an unstressed condition (Illston and England 1970). Shrinkage is caused by ambient relative humidity that is below the point of saturation of the concrete (i.e., relative humidity < 100%).

Both creep and shrinkage of concrete result mainly from the removal of absorbed water from the calcium-silicate-hydrate (CSH) portion of the cement matrix. This causes a strain in the concrete which, in turn, results in a volumetric deformation (Mehta 1986). The difference between these two is that creep is stress induced while shrinkage is induced by ambient conditions. Because these phenomena are based on a common origin, it is stated that they are interrelated to one another and occur simultaneously (Mindness, Young, and Darwin 2003). Also, because concrete creep and shrinkage occur simultaneously, it is impossible to test for each of them independently. Instead, shrinkage strain must be tested for alone and then subtracted from the strain resulting from the combined effect of creep and shrinkage (Lybas 1990).

A strong validation of concrete creep and shrinkage's interdependence upon one another is the evidence that the time-dependent behavior of creep is very similar to that of

shrinkage. Both shrinkage and creep curves grow logarithmically with time with some portion of the resultant strain being irreversible or plastic due to rewetting or unloading, respectively. Fig. 1 below shows the time-dependent behavior of shrinkage and Fig. 2 shows the time-dependent behavior of creep.

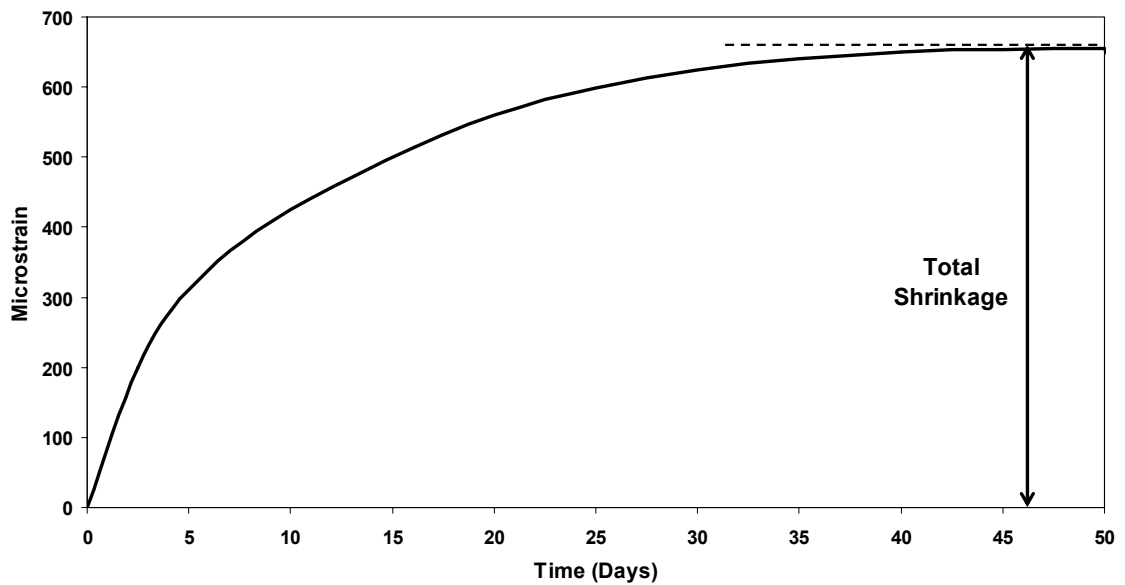


Figure 1. Drying shrinkage vs. time.

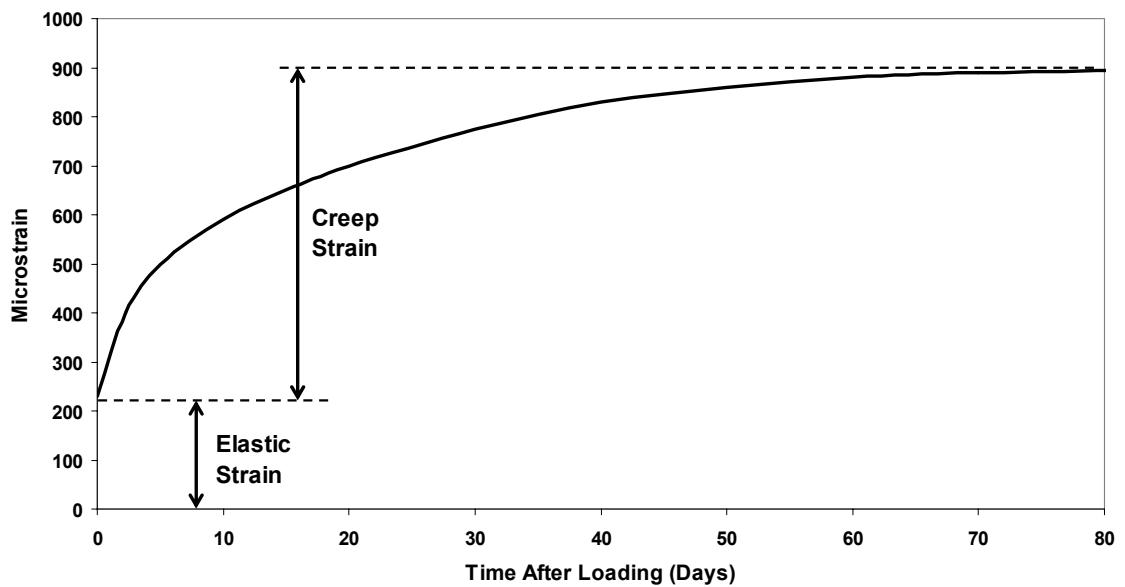


Figure 2. Concrete creep vs. time after loading.

It is also interesting to note that the camber growth curve also follows a similar trend (see Fig. 3).

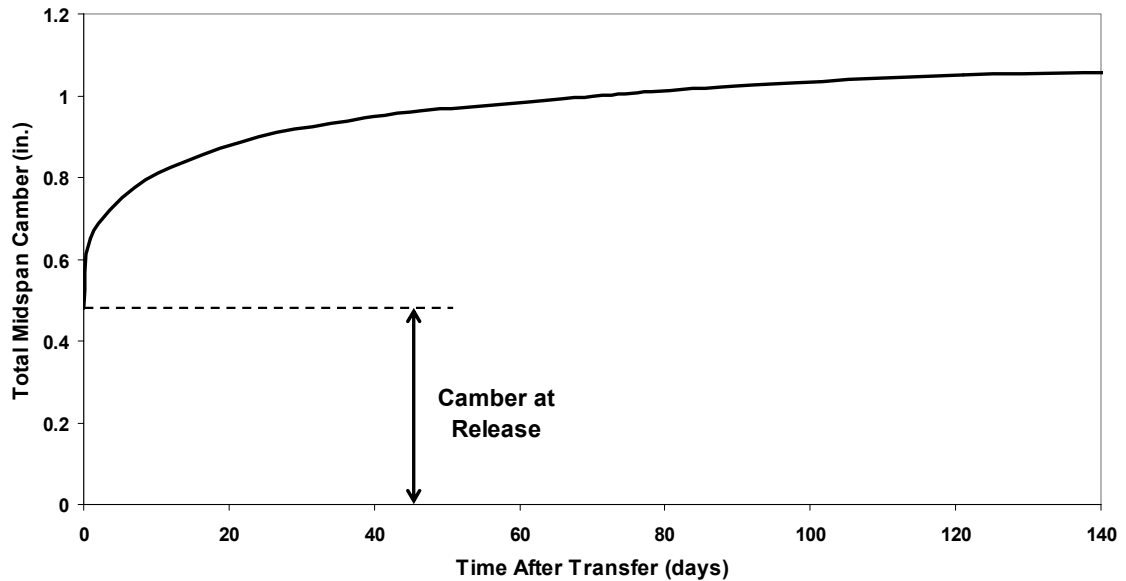


Figure 3. Camber at midspan vs. time.

These figures help substantiate the importance of concrete creep and shrinkage effects on the time-dependent behavior of prestressed flexural elements.

Another consideration is differential shrinkage. Differential shrinkage is solely influenced by the geometry of the prestressed element's cross-section. Because it is caused by the rate of water loss from the CSH portion of the cement matrix, it is apparent that the rate at which water is transported from the interior of the concrete section to the atmosphere would be controlled by the length of the diffusion path traveled by the water (Mehta 1986). This factor is taken into account when calculating the amount of shrinkage that will occur using the *ACI 209R* correction factors based on either the average-thickness method or the volume-to-surface area ratio (V/S) method. Typically, the average-thickness method tends to compute correction factors that are greater than those calculated using the volume-to-surface area method (*ACI 209R*).

These numerical representations of the geometry of a section appear to have a linear relationship with the logarithm of shrinkage (Neville 1971). Generally, a higher volume-to-surface area ratio or theoretical-thickness will produce less ultimate shrinkage in concrete. However, considering the geometry of some AASHTO girders, specifically the Florida Bulb-Tee girder, shrinkage may occur at different rates between the top flange, which has a “T-shape,” and the bottom bulb. Evidence has shown that members with small cross-sections result, initially, in faster rates of shrinkage, but lower ultimate shrinkage values, and vice-versa for members with large cross-sections (Mindness, Young, and Darwin 2003). A “T-shaped” section, with a lower V/S ratio, will dry and shrink more rapidly than a square-shaped section (Mindness, Young, and Darwin 2003), such as the bulb portion of the Florida Bulb-Tee, but have less ultimate shrinkage. This is known as differential shrinkage and could account for errors in the calculation of the long-term camber growth of Florida Bulb-Tee girder. Also, uneven drying conditions due to poorly ventilated areas of the girder during storage could also cause differential shrinkage. When the concrete section of a prestressed element dries asymmetrically, warping can occur (Neville 1971), thus altering the camber.

2.4 Calculation of Camber

Nilson suggests that the effects of creep and shrinkage should not only affect the long-term loading due to the prestress force but it should also affect that due to the self-weight of the member (Nilson 1987). Taking this into account, the calculation of camber after all long-term losses in the prestress force is given by Equation 2 below.

$$\Delta = \Delta_{pe} + \frac{\Delta_{pi} + \Delta_{pe}}{2} \cdot \phi(t, t_i) - \Delta_o [1 + \phi(t, t_i)] \quad (2)$$

where:

Δ_{pi} = Camber due to initial prestress force after steel relaxation- and elastic shortening-related losses (in.)

Δ_{pe} = Camber due to effective prestress force after all prestress losses, (in.)

Δ_o = Deflection due to self-weight of member (in.)

$\phi(t, t_i)$ = *LRFD* time-dependent creep coefficient.

The calculation of the initial prestress force, effective prestress force, and the creep coefficient, as outlined by the *AASHTO LRFD Bridge Design Specification*, are discussed in the sections below.

2.5 LRFD Prestress Loss Calculations

The Florida Department of Transportation's prestressed beam design program, *Eng LRFD PSBeam v.1.85*, uses refined estimates of time-dependent prestress losses as outlined by the *AASHTO LRFD Bridge Design Specification* in section 5.9.5.4. These estimates provide a more accurate representation of creep-, shrinkage-, and steel relaxation-related losses than those obtained using the lump-sum estimate approach. These prestress losses for pretensioned members are calculated using the equations listed below.

Elastic Shortening (*ES*):

$$\Delta f_{pES} = \frac{E_p}{E_{ci}} \cdot f_{cgp} \quad (3)$$

where:

f_{cgp} = sum of concrete stresses at center of gravity of the prestressing tendons due to the prestress force at transfer and the self-weight of the member at

the sections of maximum moment (ksi)

E_p = elastic modulus of prestressing tendons (ksi)

E_{ci} = elastic modulus of concrete at transfer (ksi)

$$\Delta f_{pES} = \frac{A_{ps} \cdot f_{pbt} \cdot (I_g + e_m^2 \cdot A_g) - e_m \cdot M_g \cdot A_g}{A_{ps} \cdot (I_g + e_m^2 \cdot A_g) + \frac{A_g \cdot I_g \cdot E_{ci}}{E_p}} \quad (4)$$

$$f_{pbt} = 0.75 \cdot f_{pu} \quad \text{for low relaxation strands} \quad (5)$$

$$f_{pbt} = 0.70 \cdot f_{pu} \quad \text{for stress-relieved strands} \quad (6)$$

where:

A_{ps} = area of prestressing steel (in²)

A_g = gross area of section (in²)

E_{ci} = elastic modulus of concrete at transfer (ksi)

E_p = elastic modulus of prestressing tendons (ksi)

e_m = average eccentricity of prestressing tendons at midspan (in)

f_{pbt} = stress in prestressing tendons immediately prior to transfer (ksi)

f_{pu} = ultimate tensile stress of prestressing tendons (ksi)

I_g = moment of inertia of the gross concrete section (in⁴)

M_g = moment at midspan due to member self-weight (kip·in)

Relaxation of the Prestressing Tendon at Transfer (*RET*):

$$\Delta f_{pR1} = \frac{\log(24.0 \cdot t)}{40.0} \cdot \left[\frac{f_{pj}}{f_{py}} - 0.55 \right] \cdot f_{pj} \quad (7)$$

for low-relaxation strands

$$\Delta f_{pR1} = \frac{\log(24.0 \cdot t)}{10.0} \cdot \left[\frac{f_{pj}}{f_{py}} - 0.55 \right] \cdot f_{pj} \quad (8)$$

for stress-relieved strands

where:

t = estimated time from jacking to transfer (days)

f_{pj} = jacking stress of the tendon (ksi)

f_{py} = specified yield strength of prestressing steel (ksi)

Drying Shrinkage (SR):

$$\Delta f_{pSR} = (17.0 - 0.150 \cdot H) \quad (9)$$

where:

H = average annual ambient relative humidity (%)

Concrete Creep (CR):

$$\Delta f_{pCR} = 12.0 \cdot f_{cgp} - 7.0 \cdot \Delta f_{cdp} \geq 0 \quad (10)$$

where:

f_{cgp} = concrete stress at center of gravity of prestressing steel at transfer (ksi)

Δf_{cdp} = change in concrete stress at center of gravity of prestressing steel due to permanent loads except load from prestressing force (i.e., gravity loads) calculated at same section as f_{cgp} (ksi)

Relaxation of the Prestressing Tendon after Transfer (RET):

$$\Delta f_{pR2} = [20.0 - 0.4 \cdot \Delta f_{pES} - 0.2 \cdot (\Delta f_{pSR} + \Delta f_{pCR})] \cdot 0.30$$

for low relaxation strands

(11)

$$\Delta f_{pR2} = 20.0 - 0.4 \cdot \Delta f_{pES} - 0.2 \cdot (\Delta f_{pSR} + \Delta f_{pCR})$$

for stress relieved strands

(12)

The *Eng LFRD PSBeam v.1.85* program first calculates the prestress loss due to the relaxation in the prestressing steel using either Equation 7 or 8, depending on the type of prestressing strands used (i.e., low-relaxation strands or stress-relieved strands). Then, assuming an initial value of 5% for the prestress loss due to elastic shortening of the concrete and considering the initial prestress loss due to relaxation, it calculates an estimated value of the prestress at transfer (i.e., $f_{pe} = f_{pj} - (0.05 \cdot f_{pj} + \Delta f_{R1})$). Using this estimated prestress, a second value for the prestress loss due to elastic shortening is calculated using Equation 3. This procedure is then repeated, iteratively, once more to determine the final prestress loss due to elastic shortening. The program then calculates the prestress losses due to shrinkage and creep of the concrete using Equations 9 and 10. A final value of the prestress loss due to the relaxation of the prestressing steel is then calculated using Equation 11 or 12, depending on the type of prestressing strands used, using the values calculated in the previous steps. Using these calculated prestress losses, the initial prestress force, P_i , can be obtained by subtracting the steel relaxation loss ($R1$) and the elastic shortening loss from the jacking force. This is used to determine the camber immediately after transfer, or Δ_{pi} . The effective prestress force, P_e , is the force in the tendons after all of the prestress losses. It is calculated by subtracting time-dependent losses due to creep, shrinkage, and steel relaxation ($R2$) from the initial prestress force. The effective prestress force is used to calculate the reduced camber after the long-term

prestress losses, or Δ_{pe} . Example calculations of this method can be found in Appendix H.

2.6 LRFD Creep Coefficient

Section 5.4.2.3.2 of the *1998 AASHTO LRFD Bridge Design Specification* uses equations from the *ACI 209R Committee Report* and empirical data as the basis for the calculation of what is known as the “creep coefficient.” The creep coefficient is the ratio of creep strain to elastic strain at some time after loading. The time-dependent equation given below was introduced by Collins and Mitchell (1991) and adopted by the *AASHTO LRFD Bridge Design Specification*.

$$\phi(t, t_i) = 3.5 \cdot k_c \cdot k_f \cdot \left(1.58 - \frac{H}{120}\right) \cdot t_i^{-0.118} \cdot \frac{(t - t_i)^{0.6}}{10 + (t - t_i)^{0.6}} \quad (13)$$

where:

t = time, in days, after loading

t_i = time, in days, time at which load is applied after casting

k_c = correction factor for V/S ratio

k_f = correction factor that accounts for lower creep of high-strength concrete

H = relative humidity, in percent

Correction Factors:

$$k_f = \frac{1}{0.67 + \left(\frac{f'_c}{9000}\right)} \quad (14)$$

where:

f'_c = 28-day compressive strength of the concrete (psi)

$$k_c = \left[\frac{\frac{t}{26 \cdot e^{0.36(V/S)} + t}}{\frac{t}{45 + t}} \right] \cdot \left[\frac{1.80 + 1.77 \cdot e^{-0.54(V/S)}}{2.587} \right] \quad (15)$$

where:

V/S = volume to surface area ratio (in.)

The correction factor, k_f , (Equation 14) accounts for the influence of concrete strength (Collins and Mitchell, 1991). Ngab, Nilson, and Slate found in a 1981 study that concrete with a compressive strength in the range of 9,000 to 12,000 psi (i.e., high-strength concrete) tended to exhibit a creep coefficient of about 50 to 75 percent that of normal-strength concrete under normal drying conditions. The correction factor, k_c , (Equation 15) accounts for the effects of the volume-to-surface ratio and is based on empirical data given in the *PCI Design Handbook* and the *CPCI Metric Design Manual*.

The design program, *Eng LFRD PSBeam v.1.85*, used by the Florida Department of Transportation uses magnification factors in order to obtain a time-dependent camber estimate. The values listed in the program are an average of the creep coefficients calculated using the LFRD method specified above and values taken from an older program once used by the FDOT. These factors are multiplied by the elastic camber, or camber immediately after transfer, to obtain a time-dependent value of the camber at 30-, 60-, 120-, and 240-days.

2.7 Thermal Effects

The prestressed beam camber can be significantly influenced by ambient conditions experienced during storage and at the time of measurement. Conditions such as ambient temperature, wind speed, relative humidity, solar radiation, as well as the composite material and section properties of the girder can influence how the beam's

internal temperature changes. Generally, if a structural member undergoes a uniform temperature increase, that member will experience a thermally induced strain and expand uniformly. However, due to the restraint provided by the prestress force, this movement is inhibited in the pre-compressed tensile zone in the base of the beam and not in the compressive zone in the flange of the beam, thus producing an increase in the girder's curvature. Also, from the field observations made, it is known that the temperature increase is not uniform. The girders often experienced higher internal temperatures in the top flange than in the bottom flange, creating a thermal gradient. This thermal gradient adds to the effect of an increase in beam curvature.

In a University of Texas study, this thermal effect was accounted for using an empirical analysis in which the beam's temperature gradient and camber were measured several times throughout the day in order to obtain a relationship between the two. The first camber reading was taken as the baseline reading, and an increase in camber was calculated by subtracting the subsequent readings from this initial value. A relationship between the increase in camber and thermal gradient was then used to correct these field measured values for thermally induced effects (Byle, Burns, and Carrasquillo 1997). This empirical method and an analytical method are used to account for any thermally induced changes in camber inherent in the field measurements.

The analytical method is outlined by the *NCHRP Report 276* which investigates thermal effects in concrete superstructures. This report organizes the United States into maximum solar radiation zones from which the predicted positive thermal gradient profile for a given concrete section can be determined using the tables provided. The actual thermal gradient profile obtained from the field measurements was used to account

for thermal effects on prestressed beam camber.

2.8 Effects of Coarse Aggregate

2.8.1 Introduction

It is not unexpected that the physical properties of the coarse aggregate strongly influence the behavior of concrete since coarse aggregate makes up nearly three quarters of concrete by volume (Sengul, Tasdemir, and Tasdemir 2002). Aggregate was originally considered an inert material added to the concrete mixture as a space filler for economical purposes (Neville 1963). However, the material properties of the coarse aggregate can strongly influence the physical behavior of concrete. Generally, aggregate properties are separated into three categories; physical properties, chemical properties, and mechanical properties. Concerning aggregates effect on creep and shrinkage of concrete, the mechanical and physical properties of coarse aggregate are of the most interest.

2.8.2 Mechanical Properties

Specifically, the most important mechanical property that affects the behavior of creep and shrinkage in concrete is the elastic modulus of the coarse aggregate (Mehta 1986). The elastic modulus of a material is defined as the change in stress with respect to elastic strain and is a measure of a materials resistance to deformation. Elastic modulus of concrete is of particular concern in prestressed and reinforced flexural elements (Baalbaki, Aicin, and Ballivy 1992). Concrete with a high modulus of elasticity will offer a higher degree of resistance against volumetric deformation. This results not only in a lower elastic strain, but also lower long-term strains due to creep and shrinkage, and hence causing lower long-term prestress losses. The influence of the aggregate properties

increase as the strength of the cement paste matrix grows close to that of the coarse aggregate, causing the concrete to act more monolithically (Giaccio and Zerbino 1998). This effect will be significant for the case of prestressed structural elements where high-strength concrete is used. Concordantly, a decrease in aggregate stiffness corresponds to a decrease in aggregate strength thus causing the strength of the aggregate to be closer to that of the high-strength cement matrix. The concrete stress-strain behavior acts linearly over a broader range, creating a concrete with a higher stiffness (Neville 1997) than expected using empirical relationships (see Fig. 4). However, a decrease in aggregate stiffness will, over all, lead to a total decrease in the stiffness of the concrete. For aggregates with a higher elastic modulus, this effect will not be as pronounced.

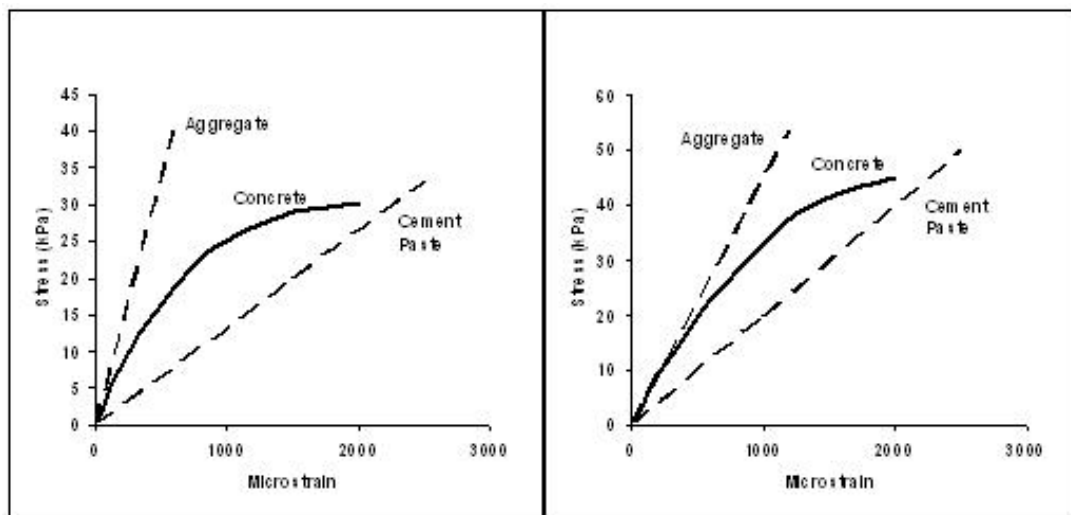


Figure 4. Effect of relative aggregate and cement stiffness on concrete stiffness (Neville 97)

2.8.3 Physical Properties

Of the physical properties of the coarse aggregate that influence the elastic modulus of the aggregate, porosity is the most significant (Mehta 1986). In a physical sense, an aggregate with a higher porosity, such as limestone, will have a lower density, therefore causing the aggregate to have a lower modulus of elasticity and thus, have a

lower stiffness. The result of this effect is a lower degree of restraint against deformation, and therefore, creep and shrinkage will have a more significant effect on the time-dependant deformation of concrete. Conversely, an increase in porosity of the aggregate actually increases its bond strength along the interfacial zone, thus increasing the concrete's compressive strength (Aïtcin and Mehta 1990). Other factors affecting the elastic modulus of the concrete are the maximum size, shape, surface texture, grading, and volume fraction of the aggregate; the porosity and water/cement ratio of the cement-paste matrix; the moisture state of the specimen at loading (Mehta 1986); age and curing conditions of the concrete specimen (Troxell, Davis, and Kelly 1968). Specimens tested in wet conditions had a tendency to present higher elastic moduli values than those tested in dry conditions. Also, the effect of age on the elastic modulus results in a rapid growth within the first few months and then begins to taper off. The elastic modulus may still continue to grow even after 3 years (Troxell, Davis, and Kelly 1968).

In particular, creep is influenced by the amount of aggregate the concrete contains and stiffness of the aggregate. Aggregate size, grading, and surface texture have little effect on creep (Mindness, Young, and Darwin 2003). Shrinkage is also influenced by the amount and stiffness of the coarse aggregate. In contrast, maximum aggregate size does have a significant effect on drying shrinkage in concrete (Mindness, Young, and Darwin 2003).

2.8.4 Effect of Aggregate on Differential Shrinkage

The effect of aggregate on differential shrinkage, aside from its direct influence on drying shrinkage, is the degree of restraint against volumetric deformation provided by the amount of coarse aggregate. Obviously an increase in aggregate content would significantly increase the concrete's ability to restrain any volumetric change due to

drying shrinkage (Neville 1971) thus differential shrinkage, overall, would become less of a factor. Another effect that the aggregate could have on differential shrinkage could be due to the asymmetric segregation of coarse aggregate during the casting process. A higher concentration of coarse aggregate at the bottom of a flexural element would cause a higher degree of restraint in the bottom than in the top, therefore creating the conditions of differential shrinkage.

CHAPTER 3 METHODOLOGY

3.1 Camber Measurement

The initial field measurements of the camber were made using a surveying theodolite and three optical targets. Three ceramic magnets were mounted to the top of each beam at the endpoints and midpoint to which the optical targets were temporarily affixed for each field measurement as seen in Fig. 5.



Figure 5. Optical target mounted on fixed ceramic magnet

The targets were always mounted in the same orientation to ensure consistency between readings and validate the zero reading for each girder. Vertical and horizontal angular readings from the theodolite were made and recorded a total of four times for each of the three targets (twice direct and twice reverse). This ensured that the angular readings were accurate and allowed for corrections to the zenith readings due to possible circle graduation errors inherent to the theodolite. This accounted for a total of twenty-four

angular readings for each field camber measurement.

Using these angular readings and the known distances between the endpoint targets and the target at midspan, the field camber could be calculated using a three-point resection analysis (see Fig. 6).

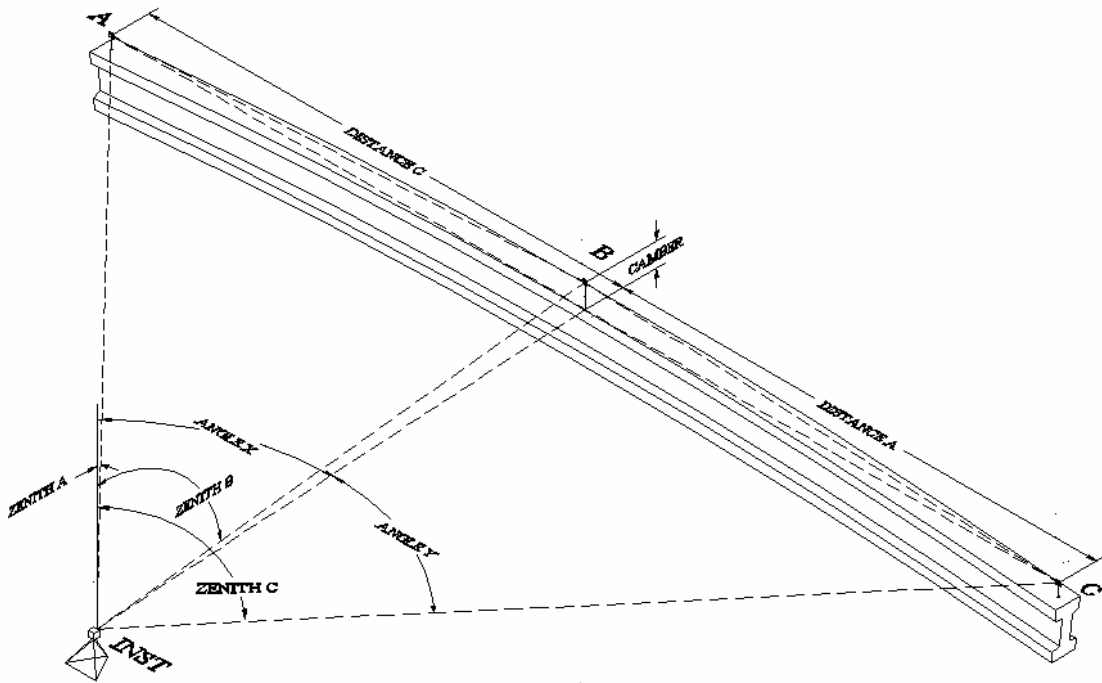


Figure 6. Isometric view of a three-point resection analysis

The resection procedure simply consists of a special case of triangulation. Using the measured distances, “A” and “C”, along with the measured angles; zeniths “A”, “B” and “C”, and horizontal angles “X” and “Y”, the relative vertical height of each target (relative to the instrument) can be triangulated. By subtracting the average relative height of the two endpoint targets from the relative height of the midspan target, we obtain the camber of the beam.

Before the prestressing tendons were cut, a zero reading was made on each girder to eliminate any systematic error inherent in the measuring process due to any surface irregularities or differential target heights. Immediately after the release of the

prestressing force, measurements using the surveying technique were compared to those measured directly off of the bed liner using a vernier caliper. The measurements using the vernier caliper were taken as the actual values for the percent difference calculations. The results are summarized in Table 1.

Table 1. Angular measurement technique accuracy

Beam No.	Surveying Technique (in)	Direct Measurement (in)	Difference (in)	Percent Difference (%)
FLBT 1	1.84	1.82	0.02	1.21%
FLBT 2	1.47	1.43	0.04	2.95%
FLBT 3	1.63	1.61	0.02	1.68%
FLBT 4	2.05	2.05	0.00	0.20%
FLBT 5	2.02	2.00	0.02	1.00%
FLBT 6	1.81	1.82	-0.01	-0.60%
TYPE IV 1	0.65	0.68	-0.03	-4.71%
TYPE IV 2	0.61	0.62	0.00	-0.65%
TYPE IV 3	0.67	0.64	0.03	3.91%

Although the accuracy of this method was acceptable, the actual field measurements were time consuming and the process of calculating the camber from angular measurements was very indirect. This method was used for the first four months of field measurements after which it was determined that a quicker, more direct method could be employed using a *Pro-Level*[™] water manometer.

The *Pro-Level*[™] water manometer is a surveying instrument which operates under the principle that water in a U-shaped tube will equalize to the same relative elevation due to the constant atmospheric pressure. The instrument's effective measuring resolution is 0.05-inches, which makes the accuracy of the measurements within the deliverable accuracy of 0.10-inches. The measuring system consists of an adjustable water reservoir, a 100-ft vinyl hose, and a graduated measuring rod or stadia with an adjustable length (see Fig. 7).

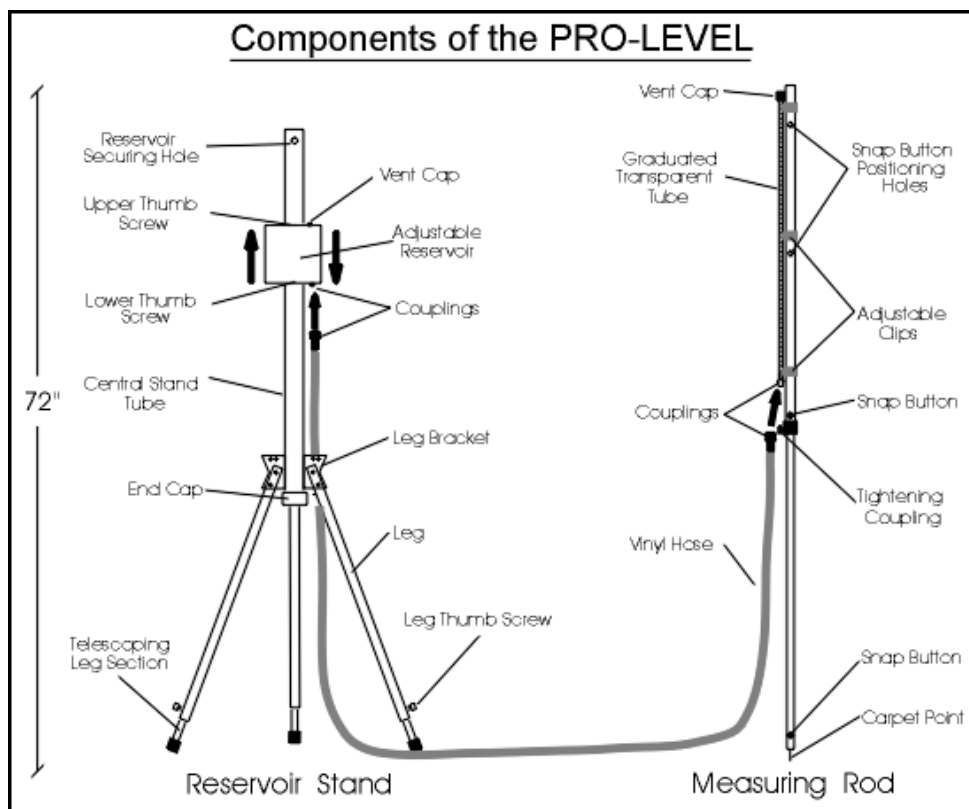


Figure 7. *Pro-Level*TM water manometer schematic (Source: <http://prolevel.com/operation.htm>, Last accessed November 30, 2004).

The reservoir is placed in a fixed location and the height is adjusted such that the meniscus reads somewhere near the middle of the stadia graduations. The stadia is then positioned at each target and the relative height is recorded to the nearest 0.05-inches. The camber is calculated by subtracting the average relative height of the endpoint readings from the relative height of the midspan reading (see Fig. 8). This instrument was used for the final three months of observations and was the only method of measurement used on the AASHTO Type V prestressed girders. Similarly, the measurements taken at release of these specimens using the *Pro-Level*TM water manometer were compared to those measured directly off of the bed liner using a vernier caliper to determine the accuracy. The measurements using the vernier caliper were taken as the

actual values for the percent difference calculations. These results are summarized in Table 3 below.

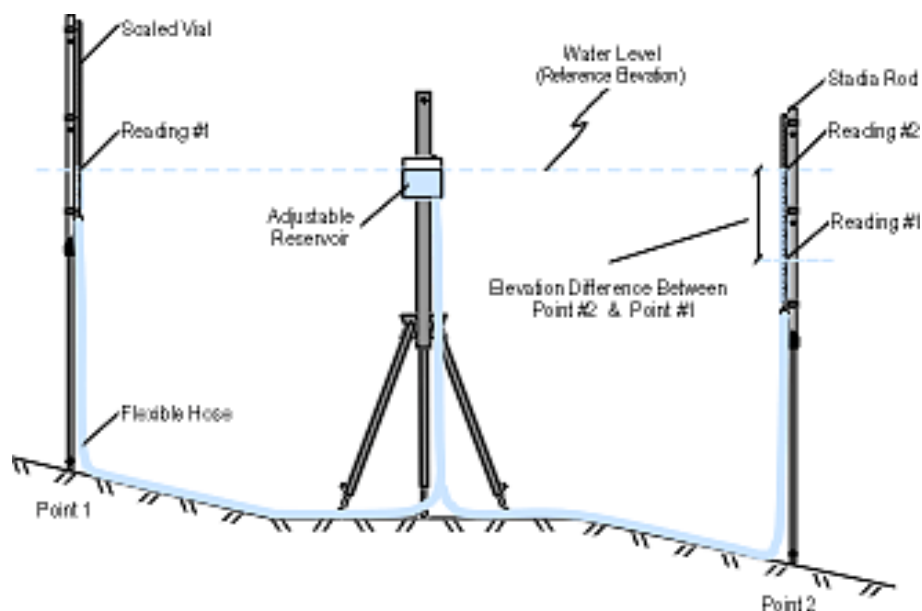


Figure 8. *Pro-Level*TM water manometer measurement technique (Source: <http://prolevel.com/operation.htm>, Last accessed November 30, 2004)

Table 2. *Pro-Level*TM measurement technique accuracy

Beam No.	<i>Pro-Level</i> TM (in)	Direct Measurement (in)	Difference (in)	Percent Difference (%)
TYPE V 1	0.85	0.82	0.03	3.66%
TYPE V 2	0.90	0.85	0.05	5.88%
TYPE V 3	0.85	0.85	0.00	0.00%
TYPE V 4	0.70	0.65	0.05	7.69%

3.2 Thermal Gradient Measurement and Camber Correction

To account for the influence of the thermal gradient on the camber measurements, an infrared temperature sensor was used to measure the surface temperature of each girder (Fig. 9). As shown in the example provided in Fig. 10 and in detail in Appendix B, this was done at several points along the profile of the section at the midspan of the girder

coinciding with the time of the camber measurements.



Figure 9. Infrared temperature sensor

In order to properly account for the effect of the thermal gradient, the surface temperature profile and camber were measured three times on single days (i.e., the effect of camber change relative to time since strand release was eliminated). This was done twice for the first three 78-inch Florida Bulb-Tee girders and one time each for the second three 78-inch Florida Bulb-Tee, AASHTO Type IV, and AASHTO Type V girders. A sample of the single day thermal gradient readings for a 78-inch Florida Bulb-Tee girder is shown in Fig. 10. The corresponding camber measurements for this girder were 2.99 in. at 7:30 AM, 3.13 in. at 9:30 AM, and 3.65 in. at 12:30 PM. This clearly indicates that the thermal gradient has a significant influence on camber. As discussed in Section 2.7, an empirical method and an analytical method were investigated for correcting the camber measurements to account for the thermal gradient.

The empirical method was based on approximating a linear thermal gradient over the depth of the beam. The linear differential temperature used in the empirical method is indicated by “ Δ Temperature” shown in Fig. 10. This was calculated by subtracting the average temperature of the bottom bulb from the average temperature of the top flange.

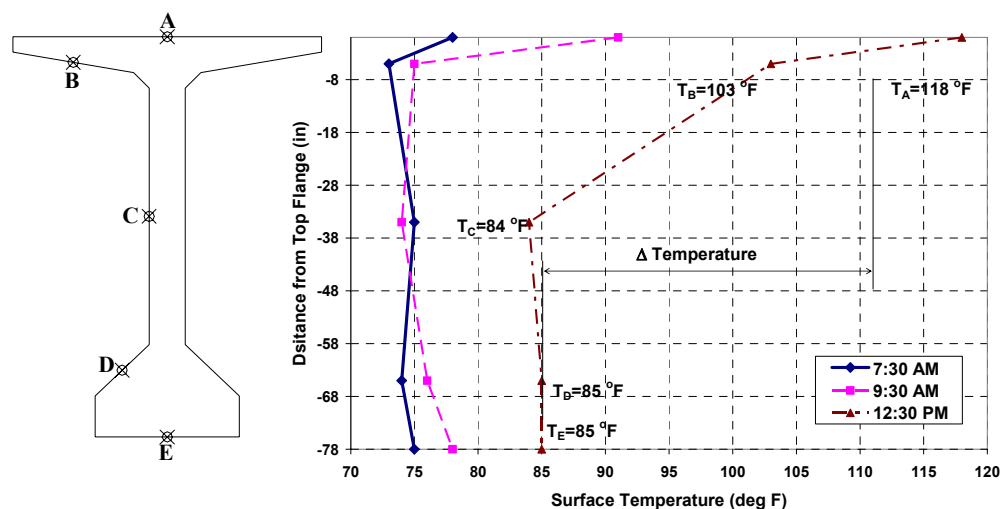


Figure 10: Example single day temperature profile of Bulb-Tee girder 3.

By determining the linear relationship between the change in thermal gradient and the change in camber, a correction factor was established to account for the thermal gradient. Details of the empirical method for correction of camber are presented in Appendix C.

Cambers were also corrected using the analytical thermal analysis. Using the thermal coefficient of the concrete provided in Table 5 of *NCHRP Report 276*, the mechanical properties of the concrete, and the section properties, the thermally induced internal stresses due to the gradient can be determined. Assuming the thermal gradient does not change along the length of the girder, a resisting internal moment can be calculated by integrating these stresses over the depth of the girder. Then, the deflection due to this moment can then be calculated using Equation 16 below.

$$\Delta_{therm} = \frac{M_{int} \cdot L^2}{8 \cdot E_c \cdot I_g} \quad (16)$$

where:

M_{int} = internal moment due to thermally induced stresses (kip*in)

L = length of girder (in)

E_c = elastic modulus of concrete (ksi)

I_g = gross moment of inertia of girder (in⁴)

A MathCAD worksheet was developed for the analytical method and is presented in Appendix D.

Table 3 presents the actual field measurements and the corrected cambers resulting from both the empirical and analytical methods for the example shown in Fig. 10. Appendix B provides full information on all field measurements and the resulting correction for both the empirical and analytical methods to account for the thermal gradient.

Table 3. Example of tabularized field measurements and thermally corrected cambers.

78" Florida Bulb-Tee 3											
CF _{therm} = 0.0090 1/°F											
Date	Time	Time After Release (Days)	Field Camber (in)	Top Flange Temp (°F)	Bottom Flange Temp (°F)	Web Temp (°F)	Top Bulb Temp (°F)	Bottom Bulb Temp (°F)	ΔT (°F)	Empirical Corrected Camber (in)	Analytical Corrected Camber (in)
6/7/2004	7:30 AM	58.98	2.99	78	73	75	74	75	1	2.96	2.97
6/7/2004	9:30 AM	59.06	3.13	91	75	74	76	78	6	2.96	2.98
6/7/2004	12:30 PM	59.19	3.65	118	103	84	85	85	25.5	2.81	2.79

As indicated by the example shown in Table 4 and by Appendix B, there is an insignificant difference between the corrected cambers for thermal gradient using the empirical method and the analytical method. Since the analytical method, based on *NCHRP Report 276*, better represents the actual camber changes caused by the thermal gradient, the corrections resulting from this method were used for developing camber versus time relationships. The empirical method would appear to be appropriate for future use in field applications where the detailed analytical method is not available.

In addition to measuring the surface temperature of the girder at the time of each camber reading, data regarding ambient conditions was also collected from a nearby weather station operated by the University of Florida Institute of Food and Agricultural

Sciences, or IFAS. The data collected included the ambient temperature at 60-cm and at 200-cm, the relative humidity, and the solar radiation all collected in one hour intervals throughout the day. The weather station data was taken from a unit located in Tavares, Florida (approximately 5 miles from the storage facility). This data is presented in Appendix E.

3.3 Supplemental Material Testing

The field camber measurements were supplemented with periodic material testing in order to obtain a time relationship with both the actual compressive strength and the elastic modulus of the concrete used in the girders. These cylinders were stripped of their molds once the forms were removed from the girders. They were then stored near the girders and “field cured” under the same conditions as the girders (see Fig. 11).



Figure 11. Field cured 4"x 8" concrete test cylinders.

This ensured that when the cylinders were tested, the results would provide an accurate representation of the actual concrete material properties of the girders. A series of three 4-inch x 8-inch cylinders were used for each test. The cylinders were tested in a computerized *MTS*[®] testing apparatus in accordance with *ASTM C39-96* and *ASTM*

C469-94. The elastic modulus was obtained using the strain measurements from two *MTS*[®] extensometers connected to a computerized data acquisition system in conjunction with the load data from the load cell (see Fig. 12).

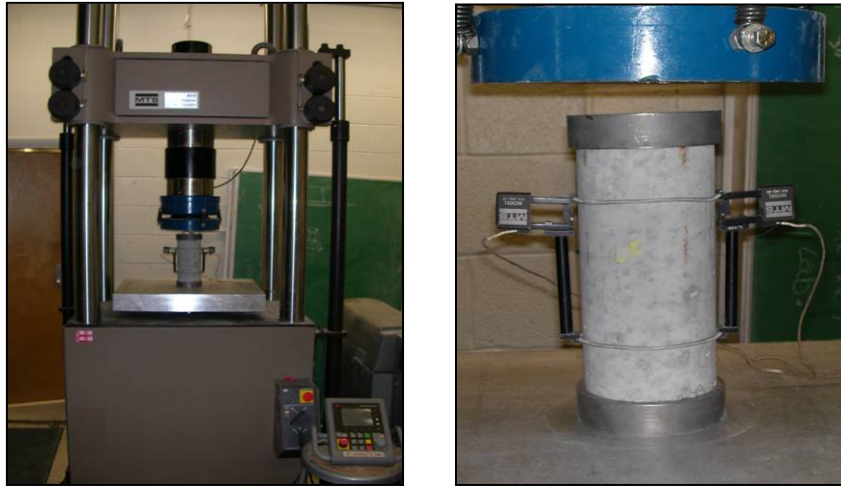


Figure 12. Computerized *MTS*[®] concrete cylinder testing apparatus.

The tests were made approximately every seven days until 28-days after the prestressing tendons were cut. Subsequently, the cylinders were tested more sparsely to show the long-term behavior of the concrete compressive strength and elastic modulus. The elastic modulus was obtained four different ways:

1. A linear regression of the stress-strain data.
2. The outlined procedure in *ASTM C469-94* (Equation 17).

$$E_c = \frac{\sigma_2 - \sigma_1}{\epsilon_2 - \epsilon_1} \quad (17)$$

where:

σ_1 = stress at 500-microstrain (psi)

σ_2 = 40% of f_c (psi)

ϵ_1 = 500-microstrain (ϵ)

ε_2 = strain at 40% of f'_c (ε)

3. The empirical relationship given by *ACI 318 02*, section 8.5.1 (Equation 18);

$$E_c = w_c^{1.5} * 33\sqrt{f'_c} \quad (18)$$

where:

w_c = unit weight of the concrete (pcf)

f'_c = compressive strength of the concrete (psi).

4. The empirical relationship given by *AASHTO LRFD Bridge Design Specification* in section C5.4.2.4 (Equation 19).

$$E_c = 1820 \cdot \sqrt{f'_c} \quad (19)$$

where:

f'_c = compressive strength of the concrete (ksi).

The results of those four methods for determining the modulus of elasticity are presented in Appendix G.

CHAPTER 4 SUMMARY OF RESULTS

4.1 Camber Measurement at Release

The camber measurements taken after the girders had been relocated to the storage area of the precast yard were generally larger than those measurements taken immediately after the release of the prestress force. The increase in camber from release to relocation for each prestressed girder is illustrated in Figs. 13 through 15. The camber values shown in these figures have been analytically corrected for thermal gradient effects as discussed in Section 3.2. The increase in camber after removal from the casting beds is most likely due to the horizontal restraint at the endpoints of the girder provided by the frictional force between the girder and the bed liner at transfer. One would surmise this effect to be more pronounced in heavier beams with larger span-to-depth ratios. This is clearly shown in Fig. 13 for the 162 ft. 78-inch Florida Bulb-Tee girders. Fig. 14 also indicates a very substantial change for the 91 ft. Type IV girders.

The substantial increase in camber from transfer to relocation for the AASHTO Type IV girders could have been affected by the procedure used for relocation of these girders. A permanent storage location was unavailable after the prestressing tendons had been cut so the girders were temporarily stored upon dunnage next to the casting bed until some space could be freed. As indicated in Appendix B, two hours elapsed from the camber measurement at the time of transfer and the camber measurement after the beams were stored. This is comparable to the three hours for 78-inch Bulb-Tee girders 1-3, two

and one-half hours for 78-inch Bulb-Tees 4-6, and one hour for the AAHSTO Type V girders. A comparison of the span-to-depth ratio of the AASHTO Type IV girders versus that of the 78-inch Bulb-Tee girders indicates that these values are close suggesting that perhaps the AASHTO Type IV girders are subject to a frictional restraining force at transfer as well. For tabulated values of the camber at release versus the camber after moving including percent increase calculations, refer to Appendix A.

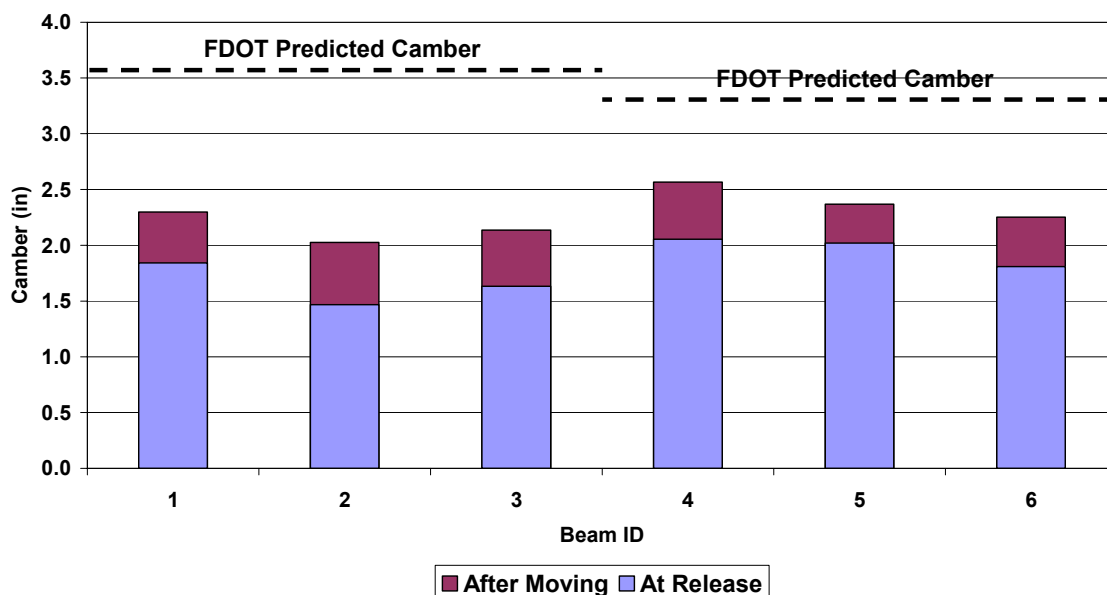


Figure 13. Bar chart of 78” Bulb-Tee camber at release, after moving, and FDOT predicted values.

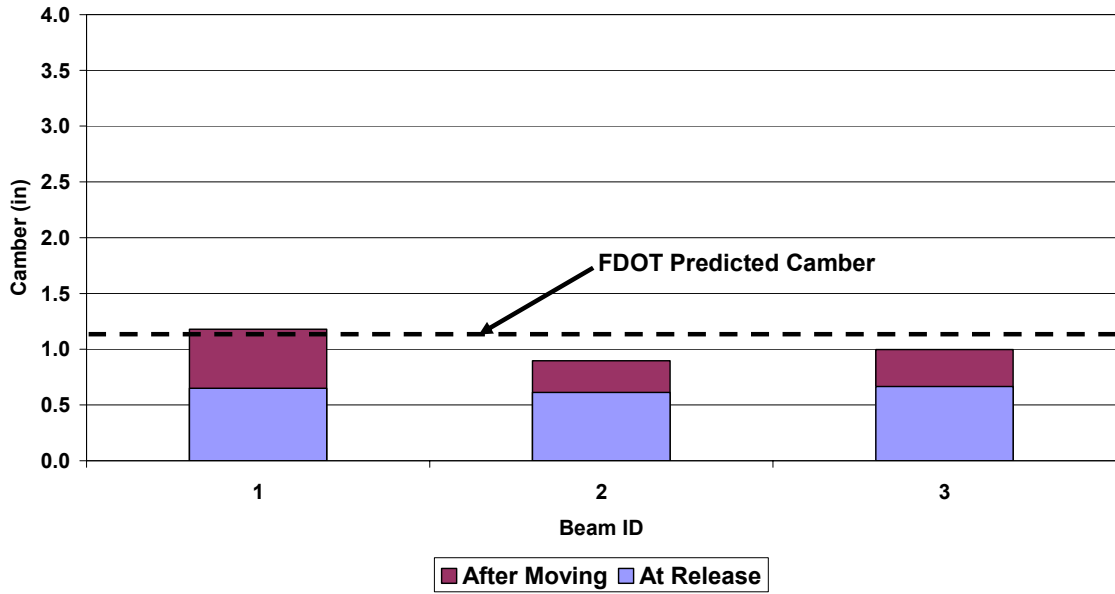


Figure 14. Bar chart of AASHTO Type IV camber at release, after moving, and FDOT predicted values.

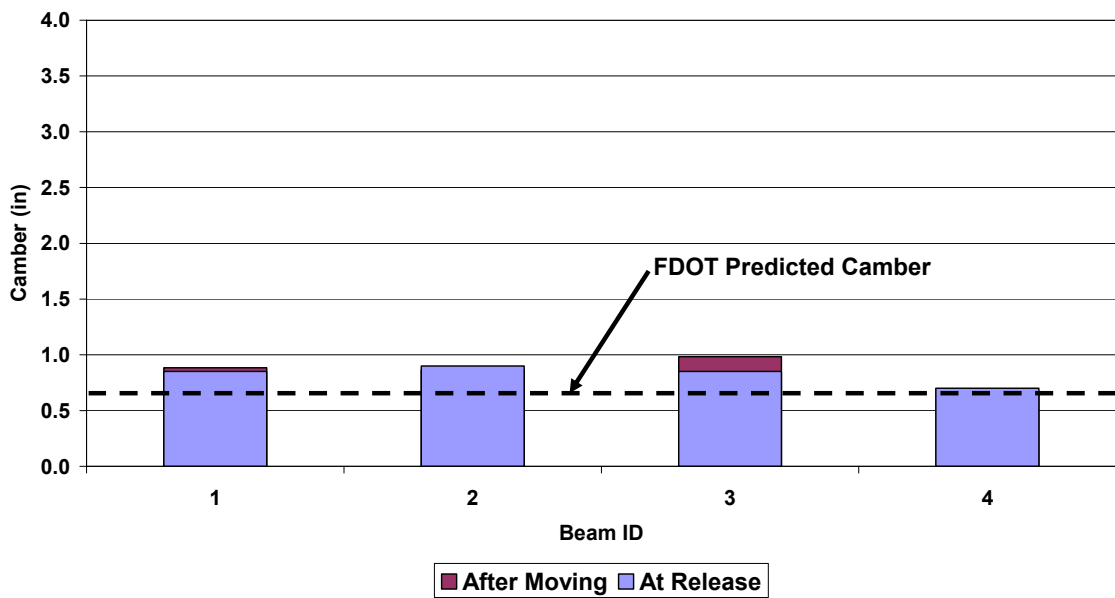


Figure 15. Bar chart of AASHTO Type V camber at release, after moving, and FDOT predicted values.

4.2 Camber Measurement Summary

The field camber measurements made on the 78-inch Bulb-Tee girders were on the order of 55-percent that of the predicted values--obtained from the *Eng LFRD PSBeam v.1.85* program--within the first few weeks of measurements to about 35-percent of the predicted values near the end of data collection. The program generally overestimated the time-dependent camber growth. The field camber measurements for each 78-inch Bulb-Tee girder and the predicted values using the *Eng LFRD PSBeam v.1.85* design program are presented below in Fig. 17 through Fig. 23. The estimated camber values for each girder obtained using the design program were calculated using:

1. The specified 28-day compressive strength and the AASHTO empirically calculated elastic moduli (at release and at 28-days).
2. The measured 28-day compressive strength and the measured elastic moduli (at release and at 28-days).

The temperature corrected camber values were calculated using the analytical thermal analysis.

The method employed by the *Eng LFRD PSBeam v.1.85* design program produced camber estimates that exceeded the 78-inch Bulb-Tee girder field measurements by as much as 180-percent. For this reason, it is suggested that the method described in section 2.4 for the time-dependent camber estimate be considered in place of the current method. A MathCAD worksheet, incorporating the use of the LFRD refined prestress loss calculation method described in section 2.5, the LFRD creep coefficient calculation described in section 2.6, and Nilson's camber calculation method described in section 2.4, can be found in Appendix H. A comparison between the mean interpolated field measurements, the predicted values taken from *Eng LFRD PSBeam v.1.85*, and the

predicted values using the Nilson method as provided in Appendix H for the 78-inch Bulb-Tee girder using the actual tested material properties is given in Table 4. .

Table 4. Comparison of field measured camber to predicted camber.

Time After Transfer (day)	Mean Interpolated Field Camber (in)	Mean FDOT Predicted Camber (in)	% Difference (%)	Nilson Method for Predicted Camber after Long-Term Prestress Loss (in)	% Difference (%)
0	1.80	3.44	90.7%	1.92	6.65%
30	3.00	5.95	98.6%	2.95	-1.47%
60	3.04	6.88	126%	3.35	9.99%
120	3.07	8.02	161 %	3.83	24.8%
200	3.10	8.66	179%	4.34	39.8%

It should be noted that although the Nilson method as presented in Appendix H gives a better prediction of the actual measured data its use should be carefully considered since it is based on using the effective prestress force after all long-term losses are considered. The method certainly deserves consideration for long term camber but its use for determining early camber (prior to long-term losses occurring) should only be considered if the value used for the effective prestress force is developed to be time dependent. In other words, at release the effective prestress force should be equal to the initial prestress force, after all loses it should be equal to that used in the Nilson method given in Appendix H, between these two points it should vary with time.

The field camber measurements made on the AASHTO Type IV girders were very close to the predicted values--obtained from the *Eng LFRD PSBeam v.1.85* program--within the first few weeks of measurements. Then, the field measured values began to diverge from the predicted values, becoming about 50-percent of the predicted values near the end of data collection. These girders were properly stored upon dunnage, but were left with little clearance between the ground and the bottom flange unlike the

other types of girders which were stored with about 18-inches of clearance between the ground and the bottom flange. In addition, vegetation growth surrounded the bottom flange and the girders were stored with little space in-between. The lack of ventilation surrounding the bottom flange could have caused more water to be trapped, thus creating a condition of differential shrinkage, and causing long-term effects (such as creep and shrinkage) to be less pronounced resulting in lower camber. Figure 16 shows the storage of the AASHTO Type IV girders. The field camber measurements for each AASHTO Type IV girder and the predicted values using the *Eng LFRD PSBeam v.1.85* design program are presented in Fig. 24 through Fig. 27.



Figure 16. AASHTO Type IV girder in storage.

The AASHTO Type V girders observed for this investigation were monitored for 28-days past the release of the prestress force. During this period, the field camber measurements adhered very closely to the predicted values obtained from the *Eng LFRD PSBeam v.1.85* program. The 30-day predicted camber from the design program was essentially the same as that measured in the field. The field camber measurements for each AASHTO Type IV girder and the predicted values using the *Eng LFRD PSBeam*

v.1.85 design program are presented in Fig. 28 through Fig. 32. For a tabular summary of the field camber measurements including empirically and analytically corrected values as well as surface temperature values, refer to Appendix B.

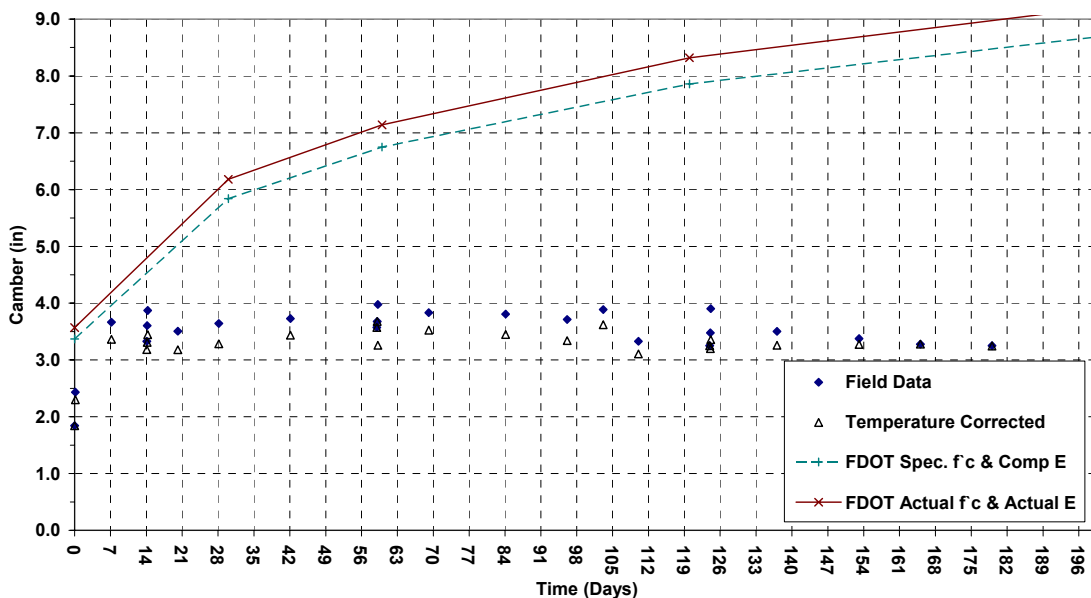


Figure 17. Field camber measurements for 78" Bulb-Tee girder 1.

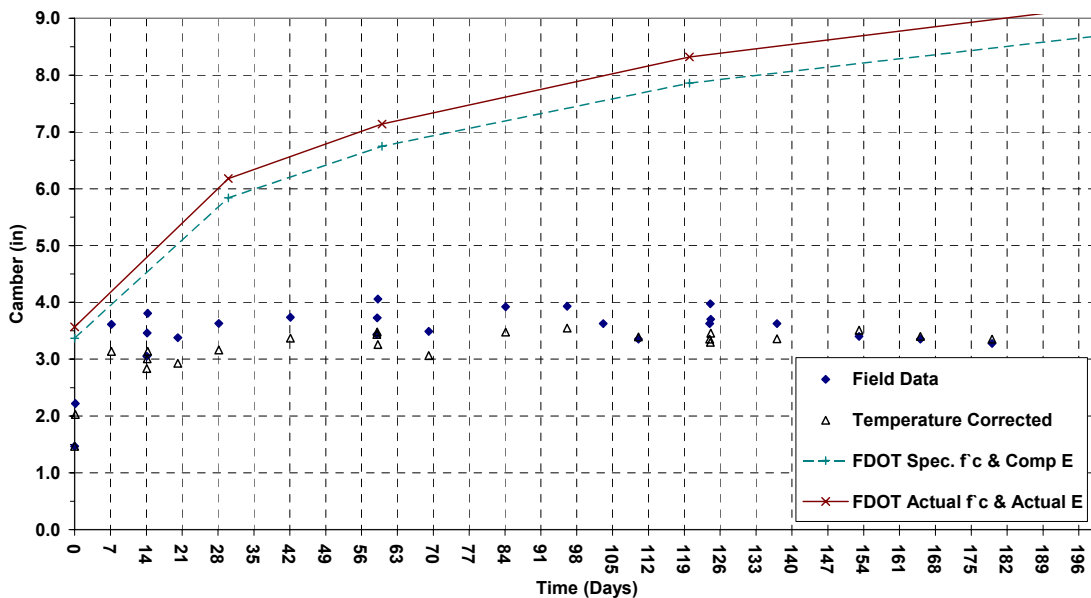


Figure 18. Field camber measurements for 78" Bulb-Tee girder 2.

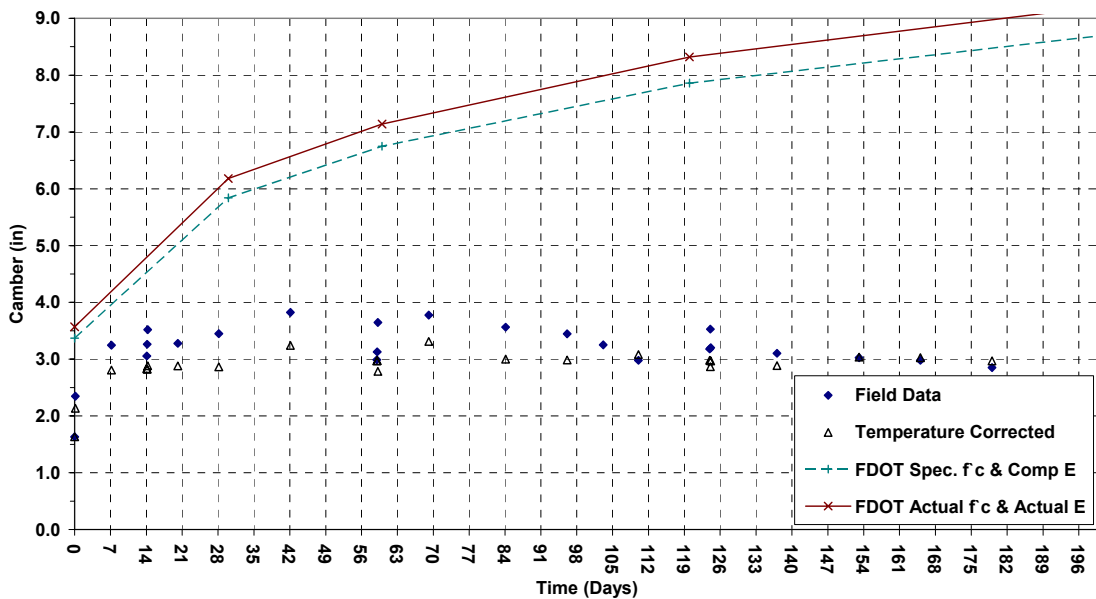


Figure 19. Field camber measurements for 78" Bulb-Tee girder 3.

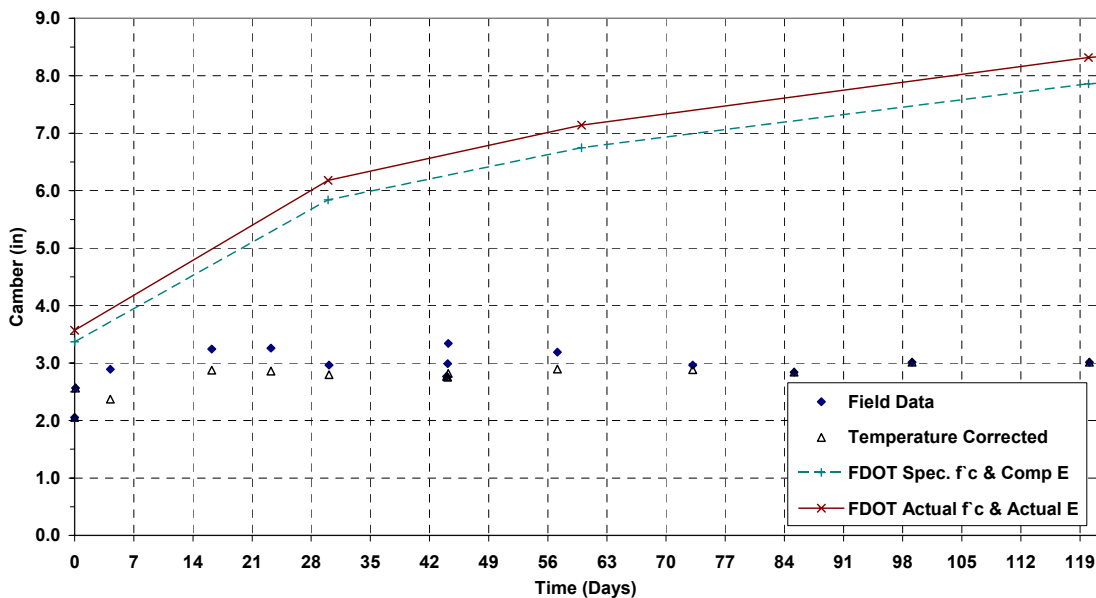


Figure 20. Field camber measurements for 78" Bulb-Tee girder 4.

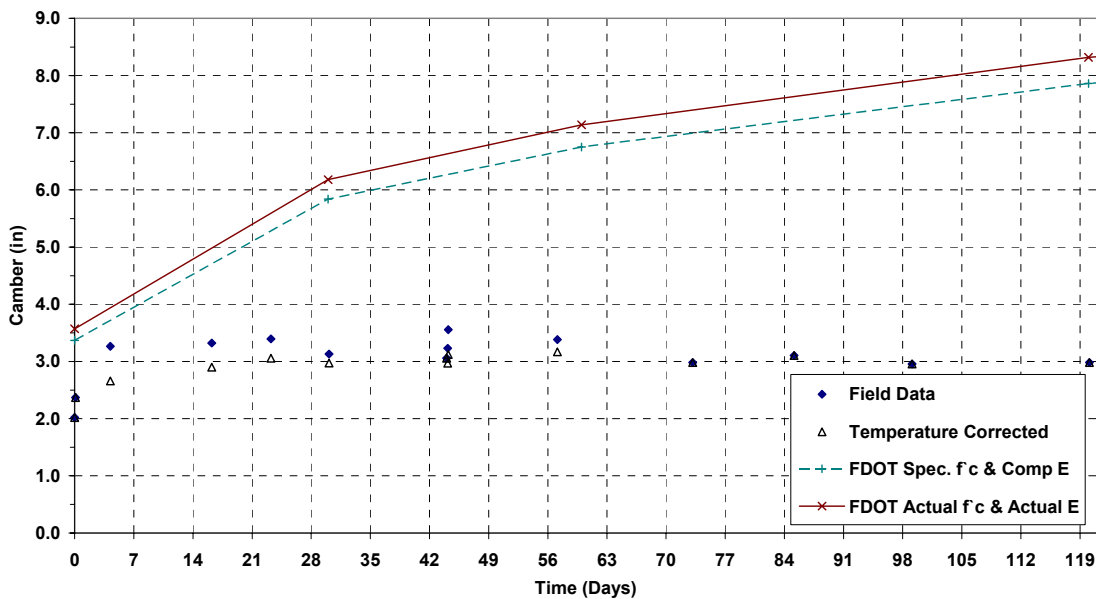


Figure 21. Field camber measurements for 78" Bulb-Tee girder 5.

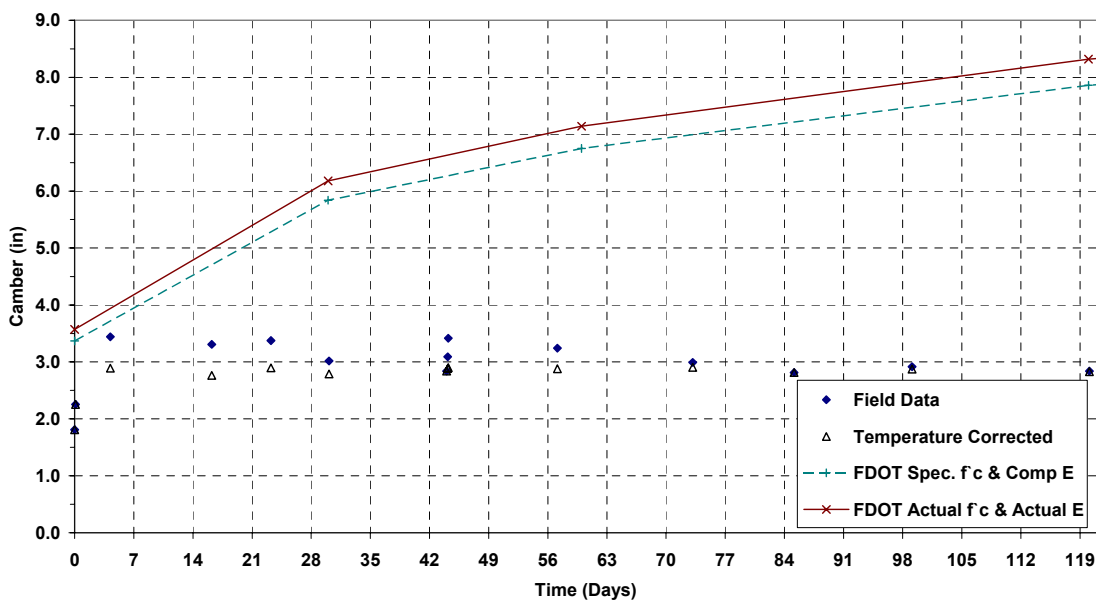


Figure 22. Field camber measurements for 78" Bulb-Tee girder 6.

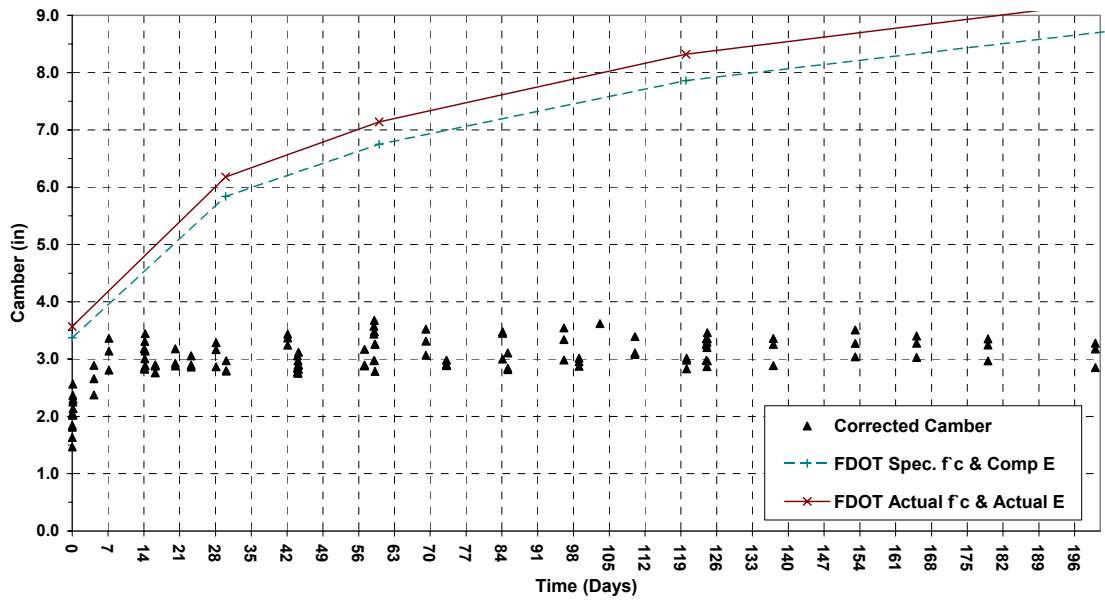


Figure 23. Summary of field camber measurements for all 78" Bulb-Tee girders.

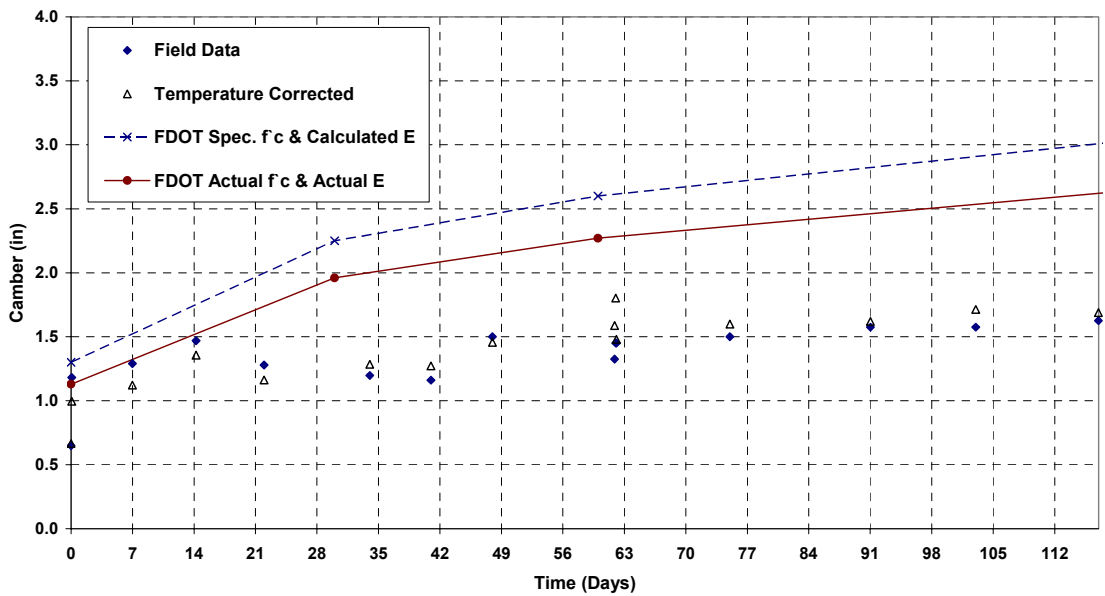


Figure 24. Field camber measurements for AASHTO Type IV girder 1.

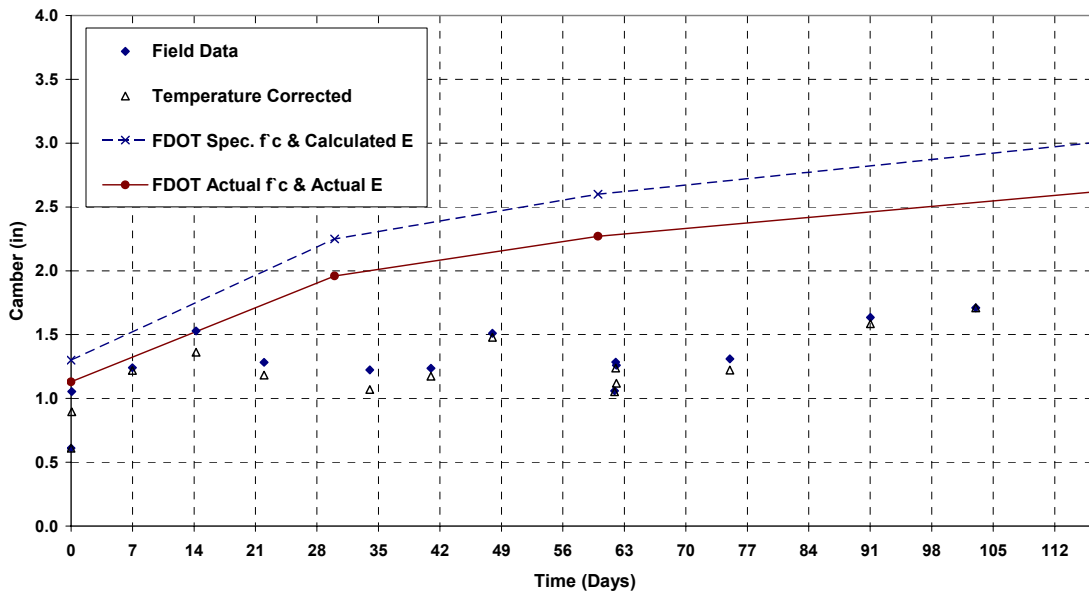


Figure 25. Field camber measurements for AASHTO Type IV girder 2.

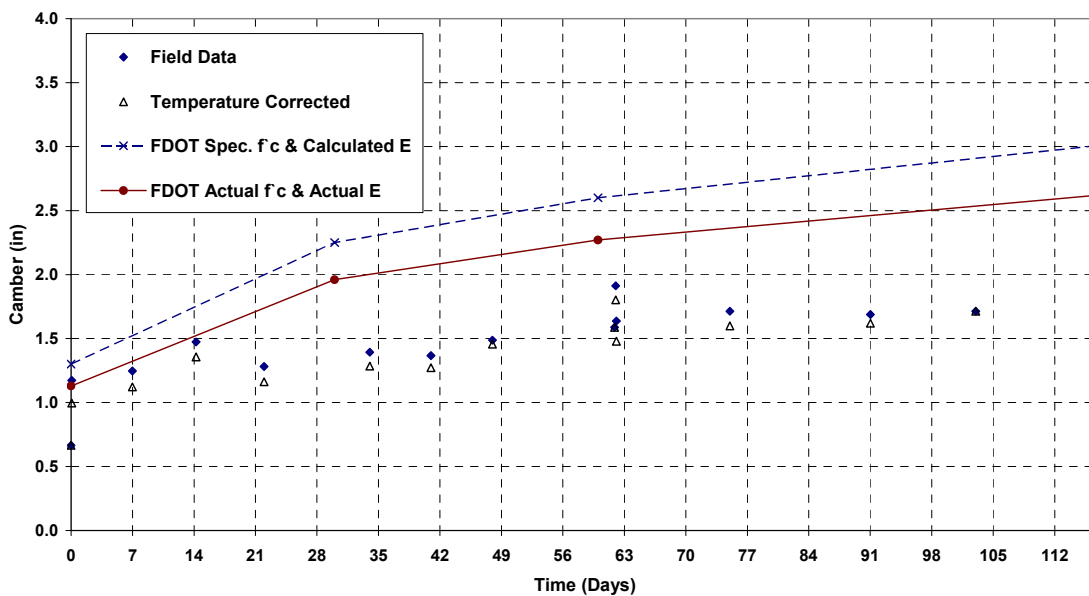


Figure 26. Field camber measurements for AASHTO Type IV girder 3.

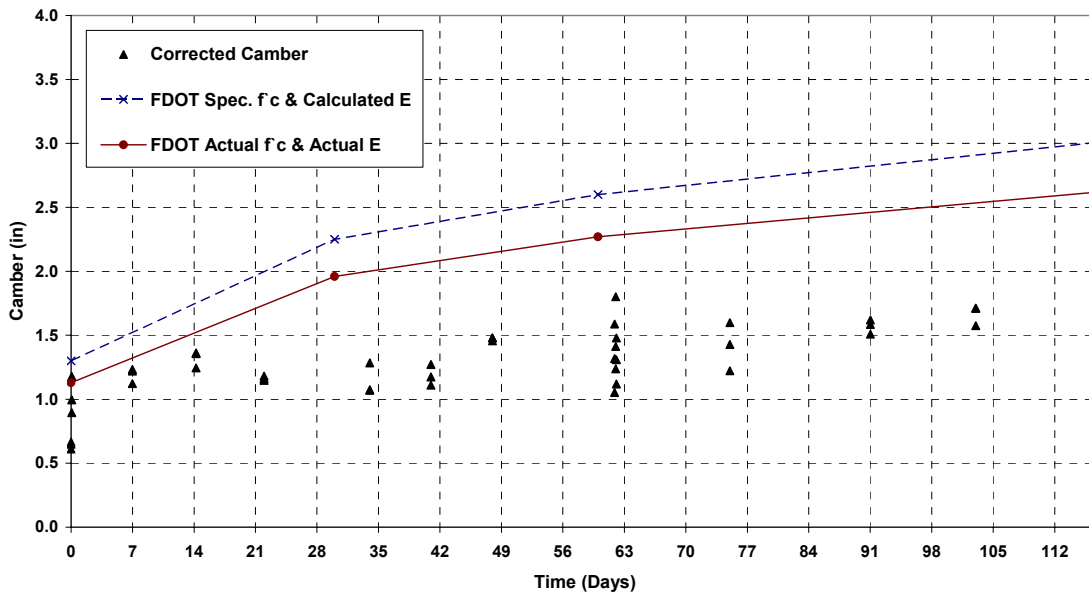


Figure 27. Summary of field camber measurements for all AASHTO Type IV girders.

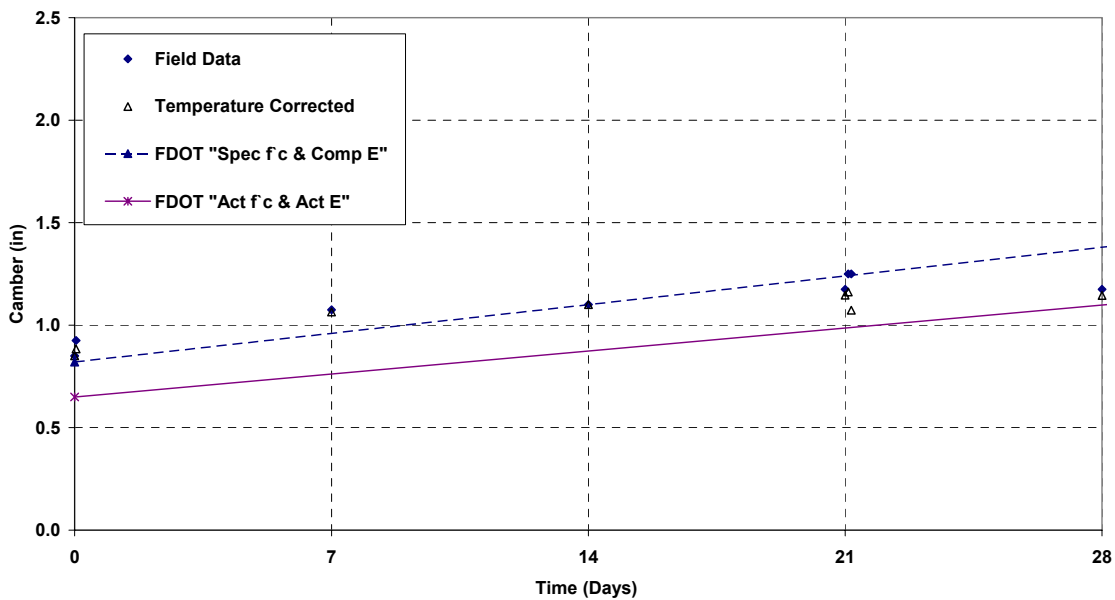


Figure 28. Field camber measurements for AASHTO Type V girder 1.

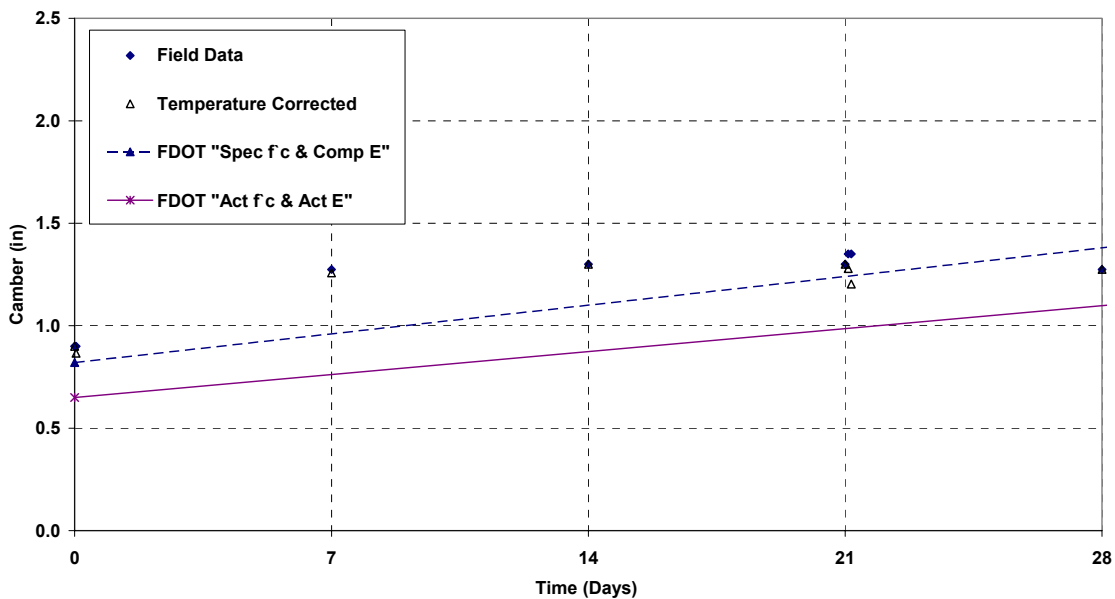


Figure 29. Field camber measurements for AASHTO Type V girder 2.

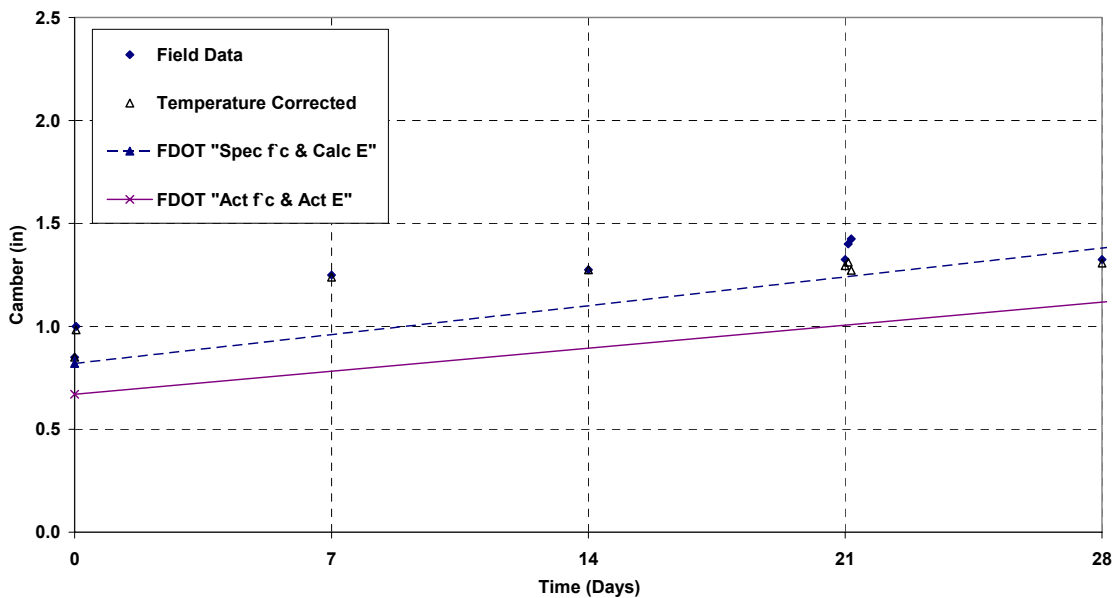


Figure 30. Field camber measurements for AASHTO Type V girder 3.

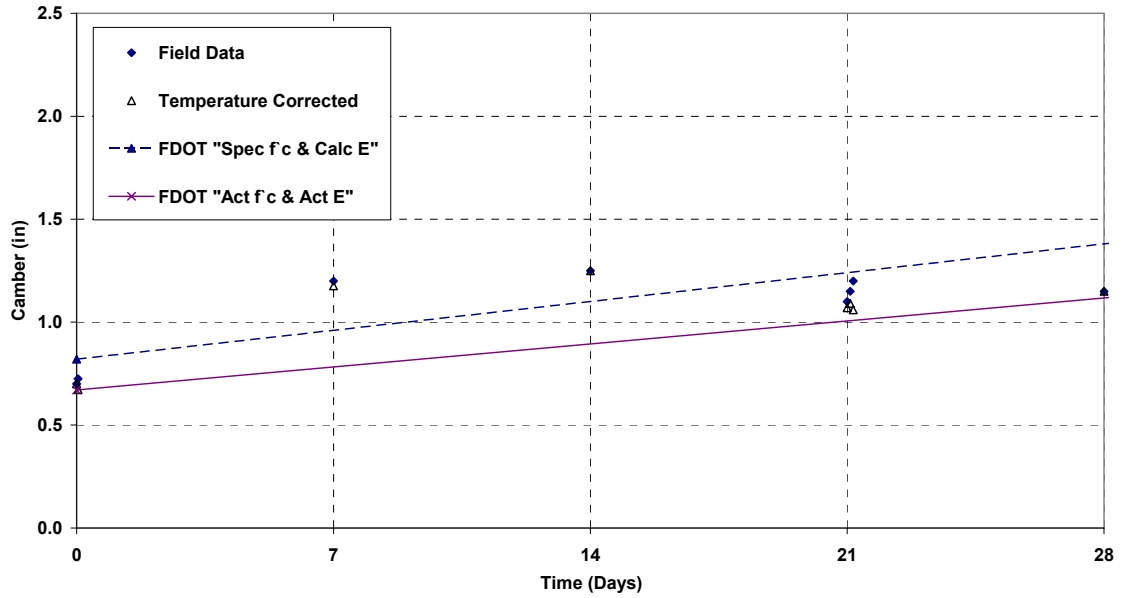


Figure 31. Field camber measurements for AASHTO Type V girder 4.

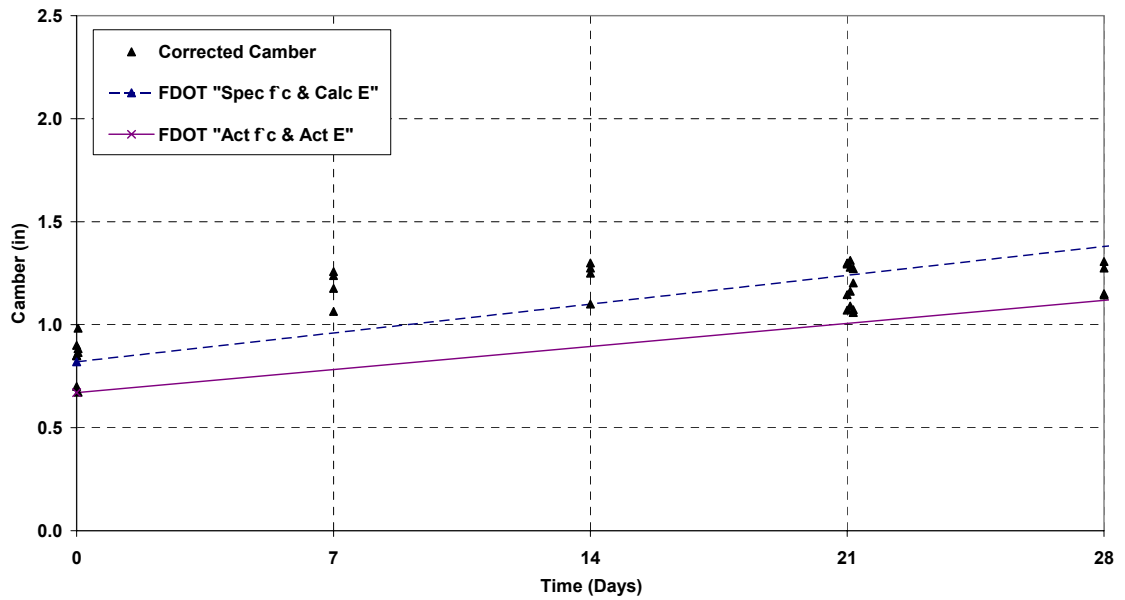


Figure 32. Summary of field camber measurements for all AASHTO Type V girders.

4.3 Supplemental Material Testing Summary

The supplemental material testing was performed periodically in conjunction with the field camber measurements in order to observe the relationship between the actual material properties and the time-dependent camber growth. Cylinders were made for

each pour of the girders being observed for this investigation. The six 78-inch Bulb-Tee girders were produced in two pours, the three AASHTO Type IV girders were produced in one, and the four AASHTO Type V girders were produced in two. Each series of test cylinders is identified by the type of girder and a letter representing which pour they were made from. For example, the test cylinders made from the first pour of 78-inch Bulb-Tee girders is identified with the letter “A.” A table summarizing which pours represent which girders is given in Table 5. The material tests were performed each week for the first 28-days and were then tested more sparsely thereafter in order to obtain a long-term model of the compressive strength and elastic modulus growth.

Table 5. Girder pour identification summary.

	<u>Pour A</u>	<u>Pour B</u>
78" Florida Bulb-Tee	Girders 1-3	Girders 4-6
AASHTO Type IV	Girders 1-3	—
AASHTO Type V	Girders 1-2	Girders 3-4

In addition to the three 4-inch x 8-inch cylinders used for each test, a series of three 6-inch x 12-inch cylinders were also tested on a few occasions for comparison. The compressive strength and elastic modulus tests for the 6-inch x 12-inch cylinders were performed by the Florida Department of Transportation Materials office in Gainesville, Florida. Material data from the 6-inch x 12-inch cylinders was obtained for the 78-inch Bulb-Tee girders and the AASHTO Type IV girders. Because there was little discernable difference between the results of the 4-inch x 8-inch cylinder tests and the 6-inch x 12-inch cylinder tests, it was decided that testing of only the 4-inch x 8-inch cylinder specimens for the AASHTO Type V girders would be adequate. Graphic representations of the compressive strength and the elastic modulus, obtained using the linear regression

analysis, are presented in the figures below. For the tabularized version of the materials testing summary refer to Appendix G. For the mix design of each pour, refer to Appendix F. Graphical representations of the results of the supplemental materials testing are as follows:

- The results of the material tests for pours “A” and “B” of the 78-inch Bulb-Tee girders for both the 4-inch x 8-inch cylinder specimens and the 6-inch x 12-inch cylinder specimens are summarized in Fig. 33 through Fig. 36.
- The results of the material tests for pour “A” of the AASHTO Type IV girders for both the 4-inch x 8-inch cylinder specimens and the 6-inch x 12-inch cylinder specimens are summarized in Fig. 37 and Fig. 38.
- The results of the material tests for pours “A” and “B” of the AASHTO Type V girders for the 4-inch x 8-inch cylinder specimens are summarized in Fig. 39 through Fig. 42.

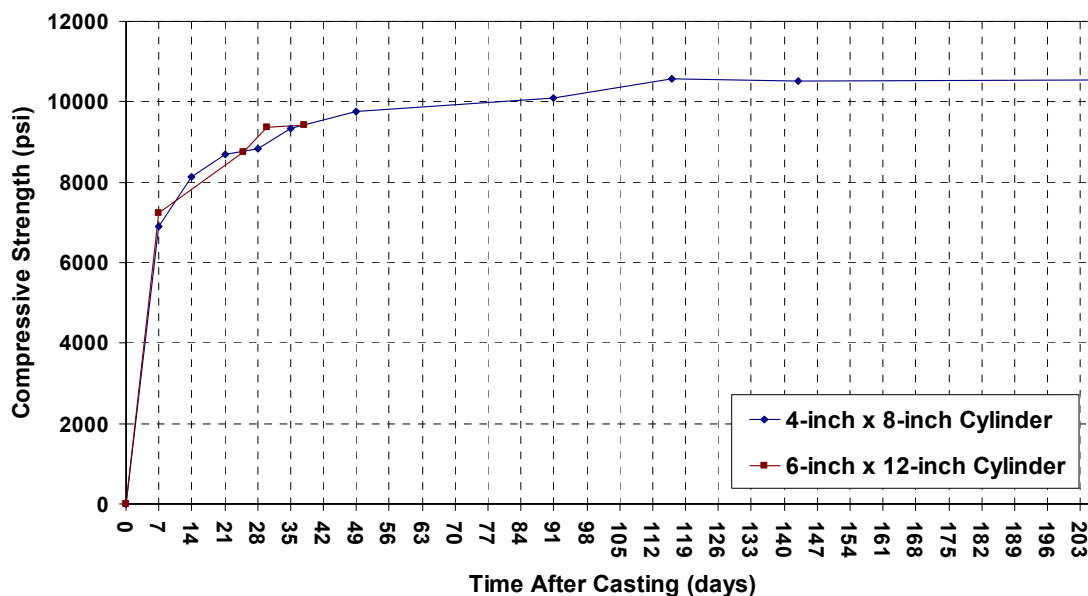


Figure 33. 78" Bulb-Tee pour "A" compressive strength vs. time.

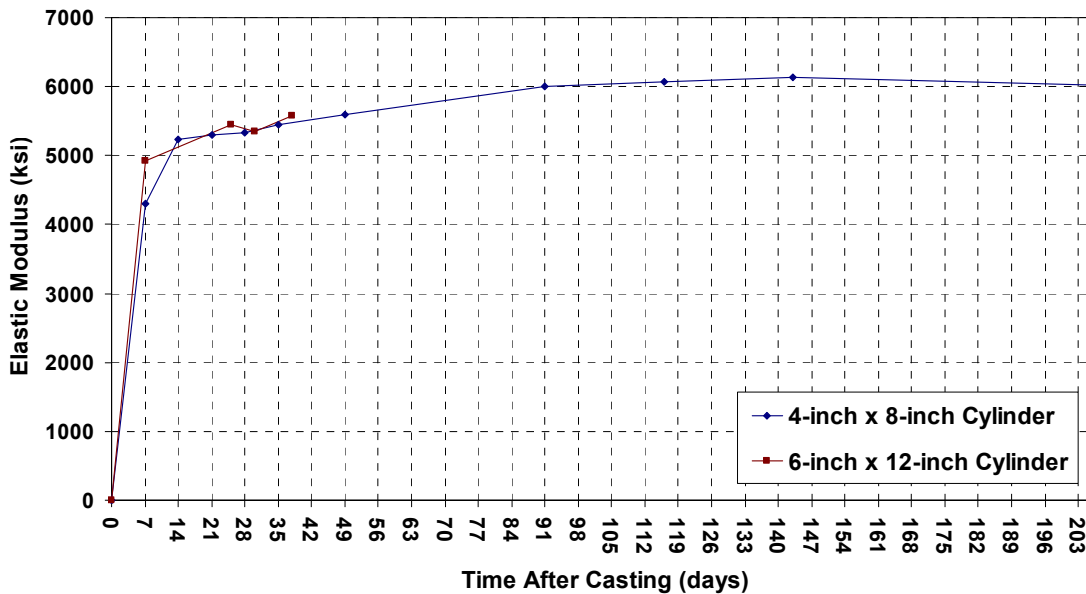


Figure 34. 78" Bulb-Tee pour "A" elastic modulus vs. time.

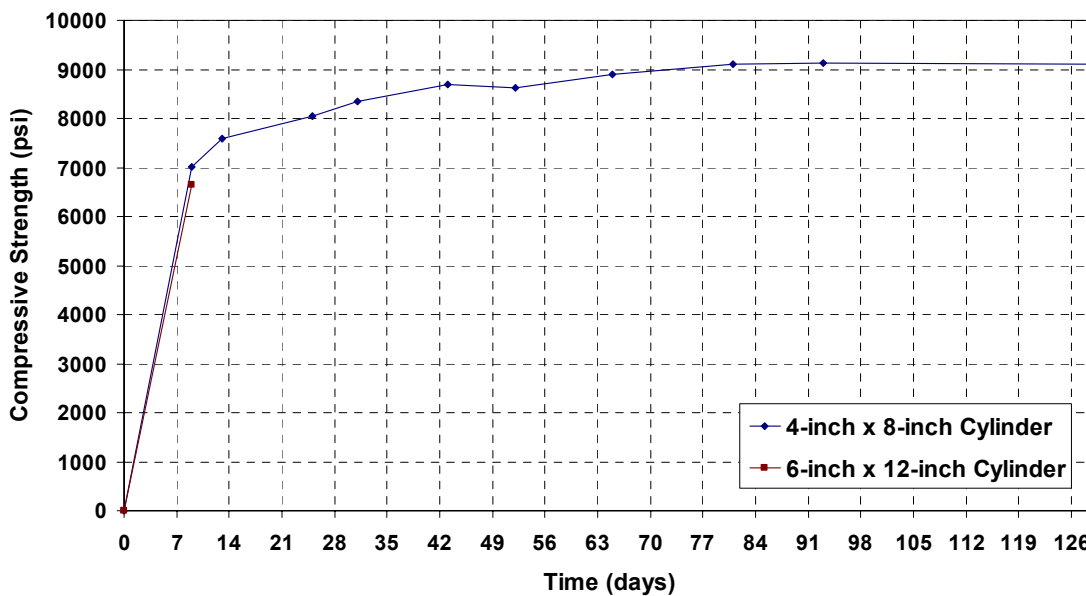


Figure 35. 78" Bulb-Tee pour "B" compressive strength vs. time.

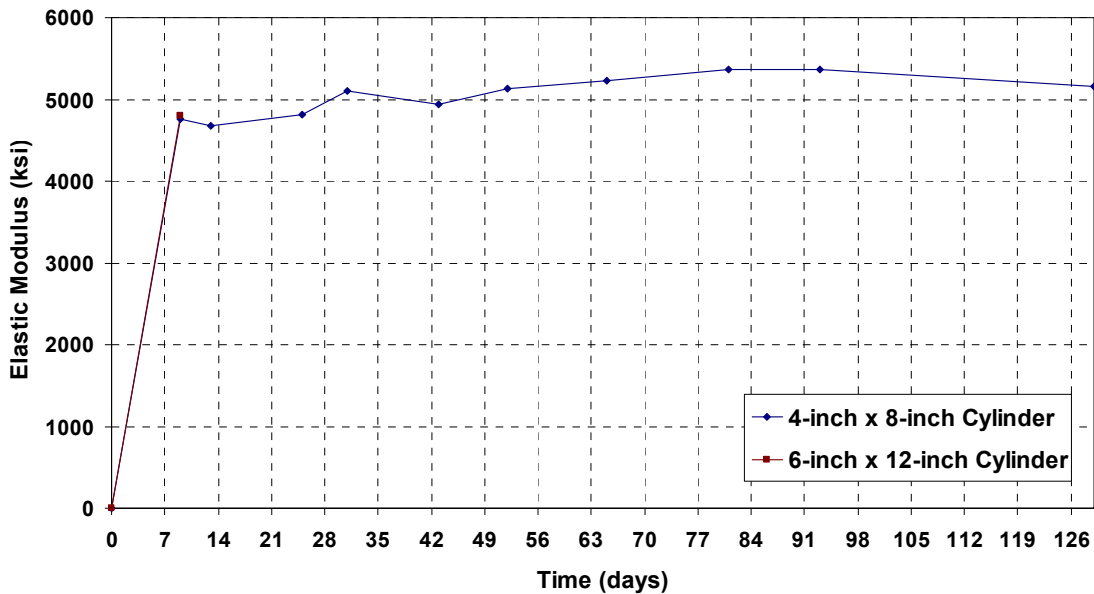


Figure 36. 78" Bulb-Tee pour "B" elastic modulus vs. time.

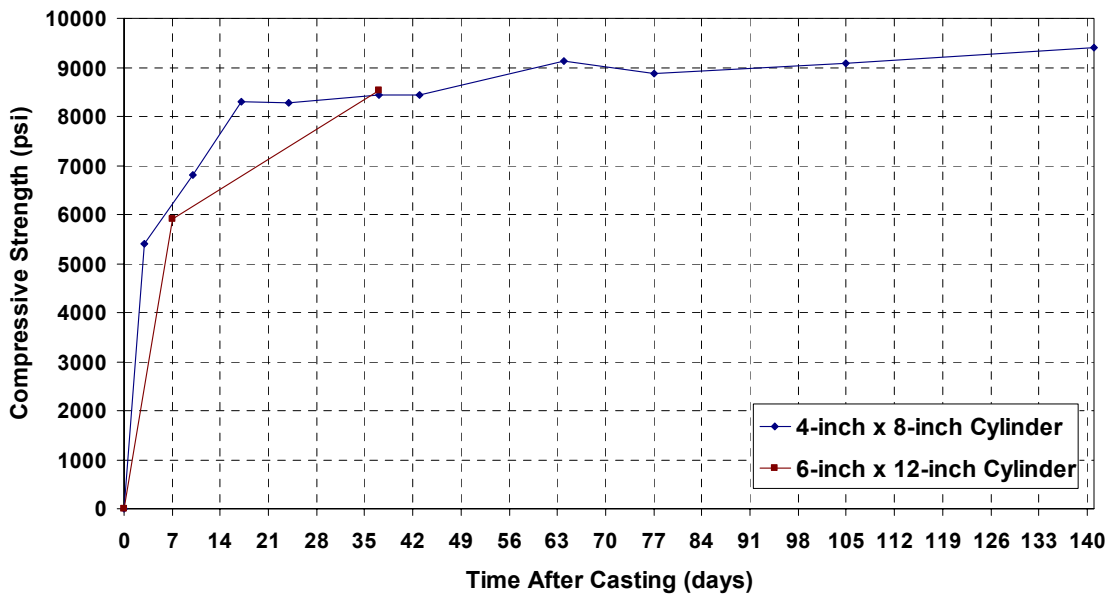


Figure 37. AASHTO Type IV pour "A" compressive strength vs. time.

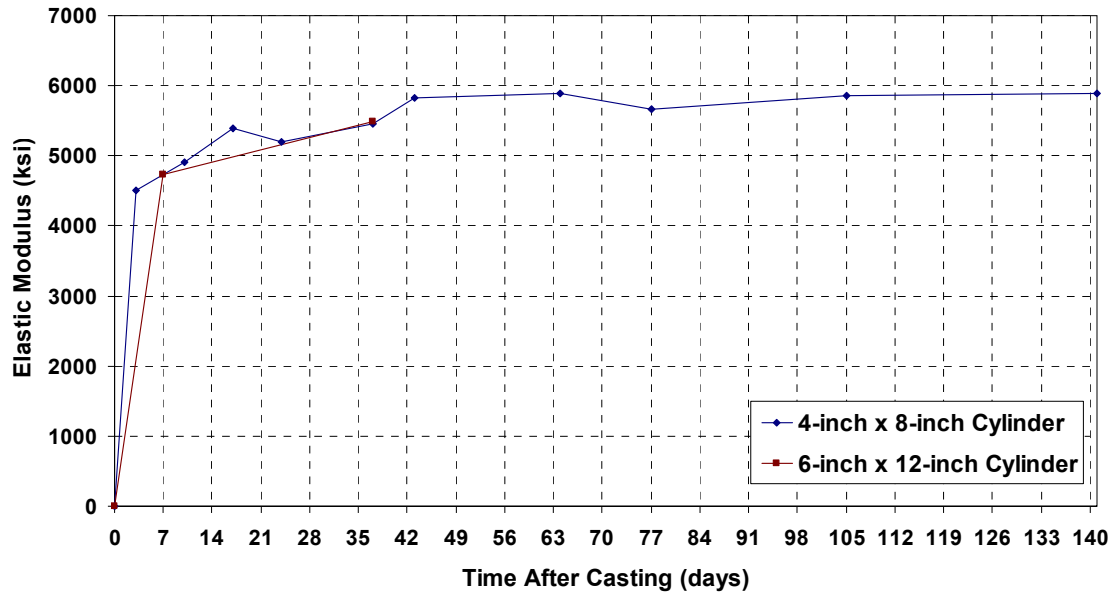


Figure 38. AASHTO Type IV pour "A" elastic modulus vs. time.

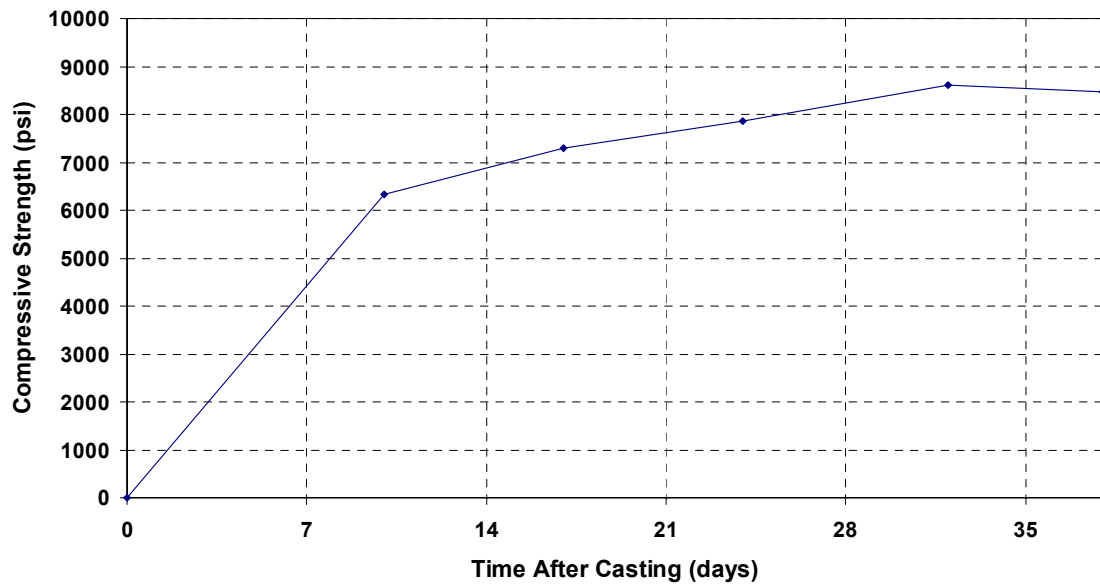


Figure 39. AASHTO Type V pour "A" compressive strength vs. time.

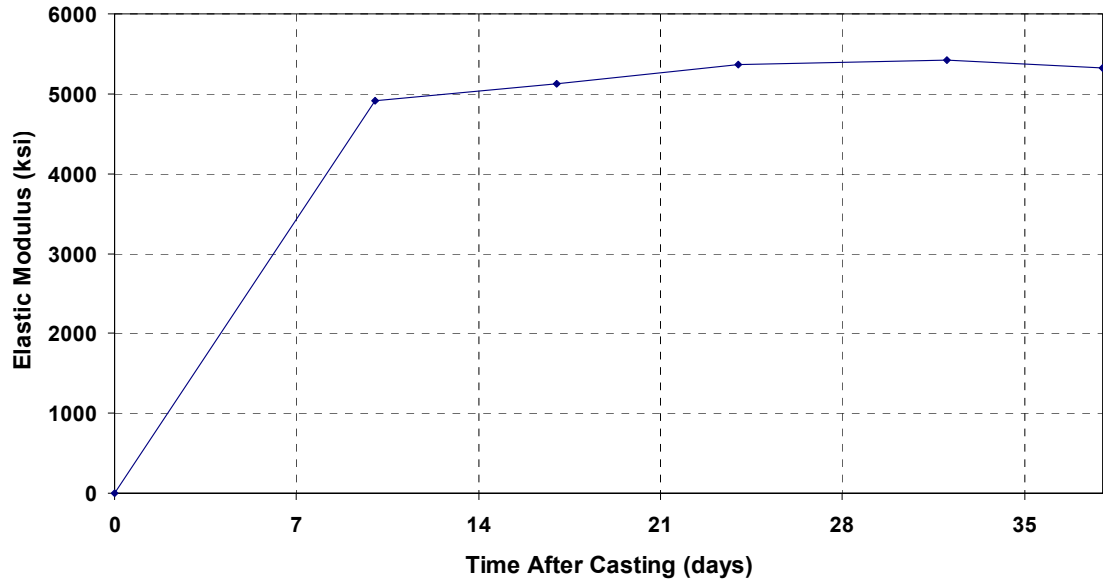


Figure 40. AASHTO Type V pour "A" elastic modulus vs. time.

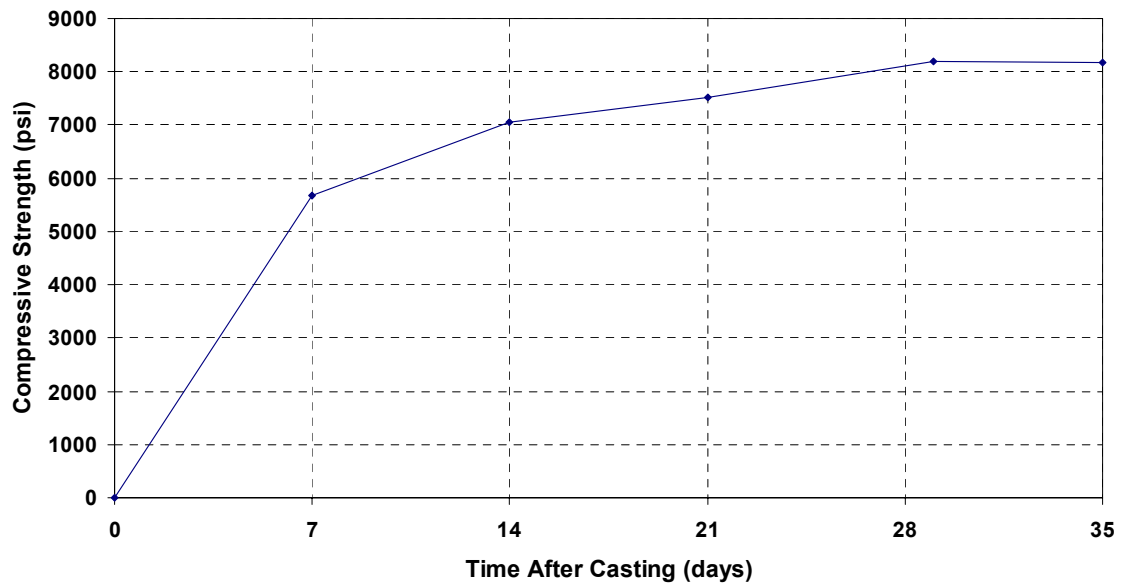


Figure 41. AASHTO Type V pour "B" compressive strength vs. time.

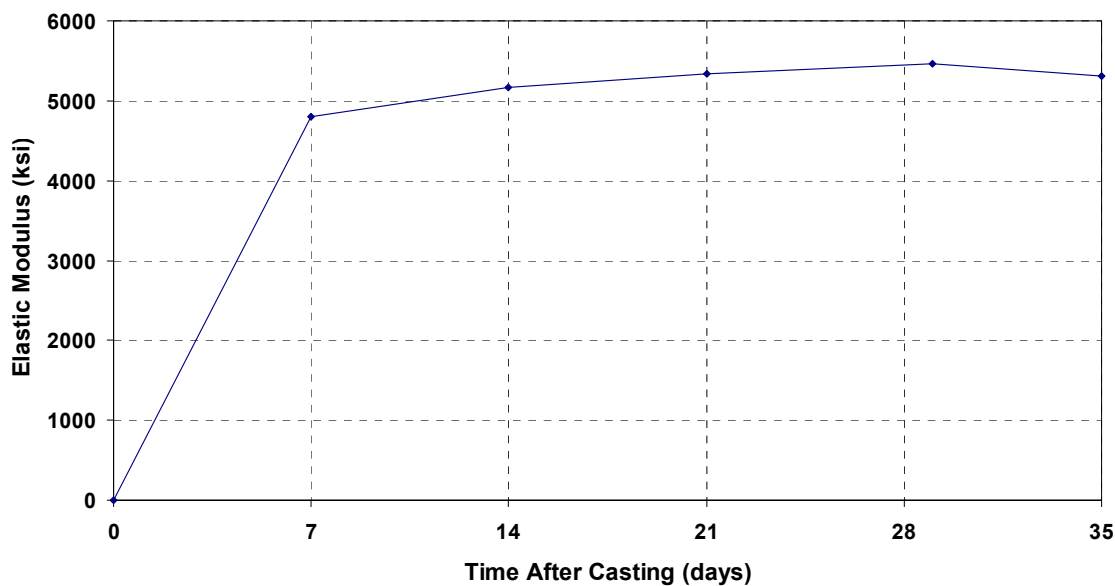


Figure 42. AASHTO Type V pour "B" elastic modulus vs. time.

4.4 Florida Limerock Specimens

In addition to the specimens using granite as a coarse aggregate, several specimens using Florida Limerock as a coarse aggregate were also investigated to determine the effects of the type of coarse aggregate content on long-term camber growth. The camber for these specimens was obtained from the prestressing yard inspection records and not from actual measurements performed using the procedures discussed in Chapter 3. These documented measurements were obtained for for:

- Ten (10) AASHTO Type IV girders were 95-feet in length with thirty-seven (37) 0.6"-diameter, 270-ksi, "Lo-Lax" prestressing strands, and used FDOT Class VI coarse limerock aggregate concrete with a specified 28-day compressive strength of 8,500-psi.
- Eight (8) 72-inch Florida Bulb-Tee girders were 129-feet in length with forty (40) 0.6"-diameter, 270-ksi, "Lo-Lax" prestressing strands, and used FDOT Class VI coarse limerock aggregate concrete with a specified 28-day compressive strength of 8,500-psi.

The measured field cambers for these specimens were compared to the predicted values obtained using the *Eng LFRD PSBeam v.1.85* design program. Detailed information on

the information obtained from the prestressing yard records is provided in Appendix I.

4.4.1 Camber Measurement at Release

The average initial camber measurement for the ten AASHTO Type IV girders and the eight 72-inch Florida Bulb-Tee girders fabricated using Florida Limerock as the coarse aggregate are shown in Fig. 43. It should be noted that the initial camber measurements were performed while the girders were in the forms and that no camber measurement was made after moving the girders to their storage location. As shown in Fig. 13 and Fig. 43 the initial camber for the Florida Bulb-Tee sections was much closer to that expected when using Florida Limerock as the coarse aggregate. One should note that the bed liner may have been greased prior to release to relieve the horizontal frictional restraint.

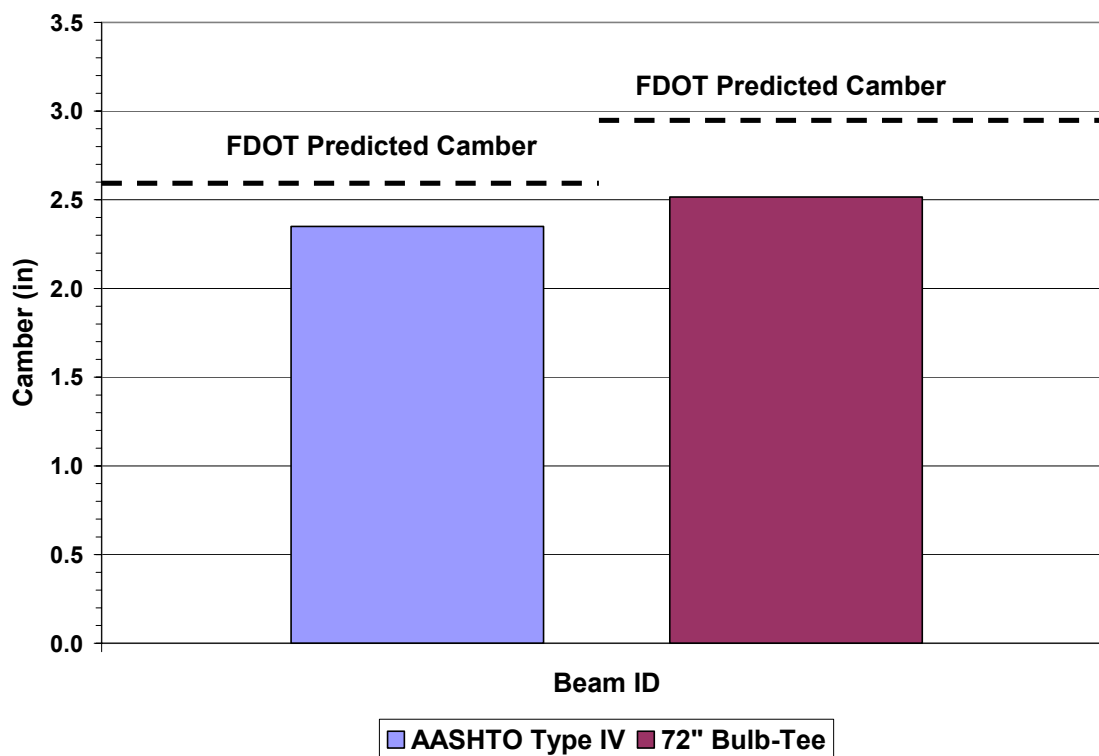


Figure 43. Limerock 72" Bulb-Tee and AASHTO Type IV camber at release.

4.4.2 Camber Measurement Summary

The time-dependent camber growth for the 72-inch Bulb-Tee girders and the AASHTO Type IV girders, both using Florida Limerock as a coarse aggregate, can be seen in Fig. 44 and Fig 45, respectfully. The predicted values from the design program were produced using the actual tested material properties given in Appendix I.

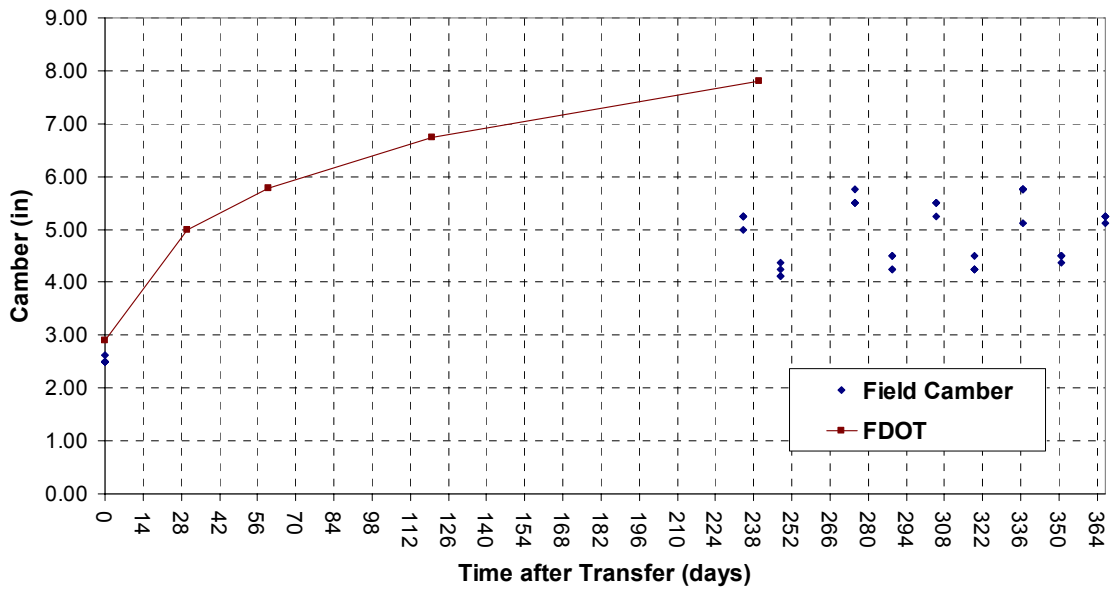


Figure 44. 72" Bulb-Tee (Limerock) girder camber growth summary.

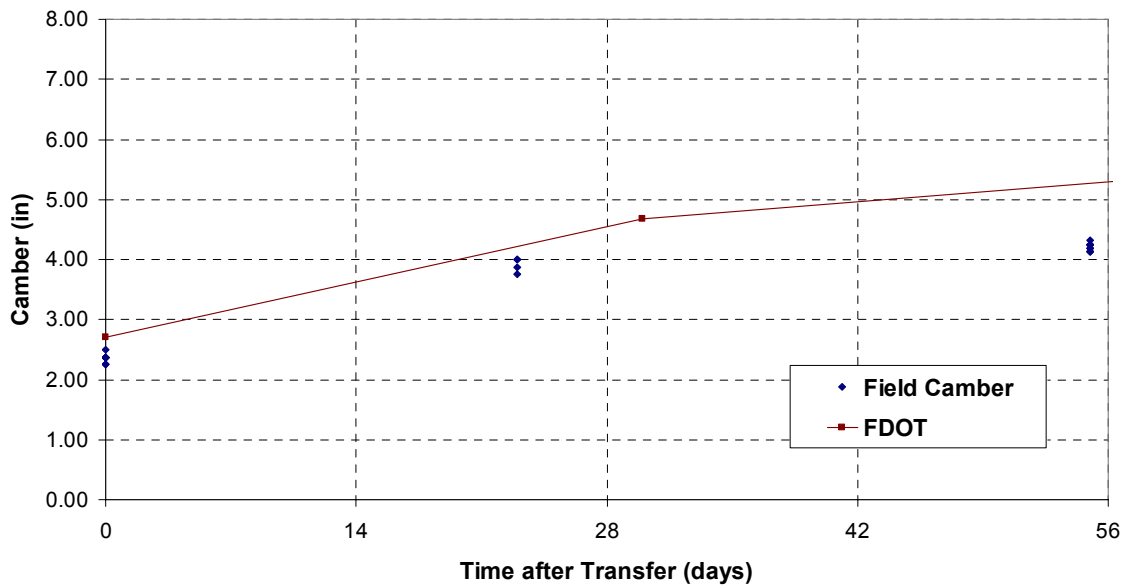


Figure 45. AASHTO Type IV (Limerock) girder camber growth summary.

This comparison is illustrated graphically for the AASHTO Type IV girders in Fig 46 and presented in tabular form in Table 6. From this figure, it can be stated that the coarse aggregate content has a significant effect on the long-term behavior of these prestressed girders. The design program overestimates the long-term camber by as much as 70% for the girders using granite as a coarse aggregate, but only 20% for the girders using Florida Limerock as a coarse aggregate.

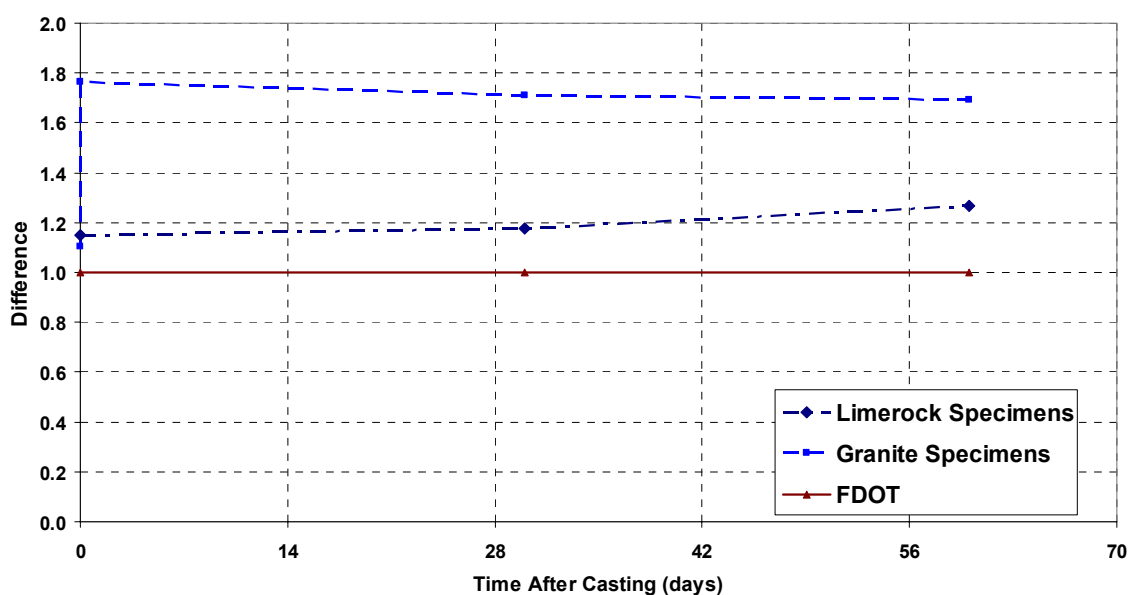


Figure 46. Comparison of predicted camber to actual field camber for granite and limerock specimens of AASHTO Type IV girder.

Table 6. Tabular comparison of predicted and actual camber values for Limerock and granite specimens of the AASHTO Type IV girder.

Limerock Specimens				Granite Specimens			
Time After Transfer (days)	(A) Field Camber (in)	(B) FDOT Predicted Camber (in)	Difference (B/A)	Time After Transfer (days)	(A) Field Camber (in)	(B) FDOT Predicted Camber (in)	Difference (B/A)
0	2.35	2.70	1.15	0	0.64	1.13	1.77
30	3.976	4.67	1.17	0	1.02	1.13	1.10
60	4.257	5.39	1.27	30	1.147	1.96	1.71
				60	1.34	2.27	1.69

For the 72-inch Florida Bulb-Tee girders, comparisons were made to the predicted values from the *Eng LFRD PSBeam v.1.85* design program and the recommended approach given by Equation 2 at 240-days after the transfer.

Table 7. Comparison of field measured camber to predicted camber at 240 days for Bulb-Tee girders.

	Mean Interpolated Field Camber (in)	Mean FDOT Camber (in)	% Difference (%)	Recommended Method (in)	% Difference (%)
Granite	3.10	9.29	199%	4.34	40.0%
Limerock	4.88	7.81	59.9%	3.48	-28.6%

CHAPTER 5 CONCLUSIONS AND RECCOMENDATIONS

The conclusions and recommendations presented in this report are based upon the data collected during this project, analysis of this data, and previous research literature related to this project.

- The observed camber increase with time was significantly less than what was estimated for the 162 ft. 78-inch Florida Bulb-Tees and the 91 ft. AASHTO Type IV girders when using the FDOT *LFRD PSBeam v.1.85* design program.
- It is recommended that the FDOT *LFRD PSBeam v.1.85* design program be modified to account for this. One possible approach would be the use of the time-dependent creep coefficient given by Section 5.4.2.3.2 of the *AASHTO LFRD Bridge Design Specification*. This creep coefficient should not only be applied to the camber due to the long-term loading of the prestress force, but it should also be applied to the deflection associated with the long-term loading due to the self-weight of the member. This can be done using the relationship proposed by Nilson in Eq. (2) (Appendix H provides example calculations showing this method). An improvement of the Nilson method presented in Eq. (2) and Appendix H would be to develop a time-dependent relationship for the effective prestressing force rather than assume that the effective prestressing force is determined after all time dependent losses have occurred.
- For the influence of the thermal gradient on camber, there was little difference between the empirically corrected camber measurements and the analytically corrected camber measurements in the majority of cases. Either method is suitable for the correction of camber due to thermal gradient effects.
- Both the AASHTO and the ACI methods for calculating the elastic modulus were fairly accurate for the 78-inch Bulb-Tee specimens for which an FDOT Class VI concrete was used, and also for the AASHTO Type IV and AASHTO Type V specimens for which an FDOT Class IV concrete was used.
- Guidelines for storage of the girders with instruction of the amount of clearance necessary between the ground and bottom flange should be implemented in order to reduce the effect of differential shrinkage in the field.
- Further investigation should be done with reference to the increase in camber from immediately after transfer to when the girders have been relocated to storage. This effect was consistently the most pronounced in heavy girders with a large span to depth ratio.

- Further investigation should be done on the effect of aggregate type on the long-term camber growth in prestressed girders to determine whether it is one of the possible causes for the discrepancy between the predicted and actual camber values.

APPENDIX A
CAMBER AT RELEASE

78" Bulb-Tee Girders					
Beam ID	FDOT Predicted Camber* (in)	Camber At Transfer (in)	Camber After Moving (in)	Camber Increase (in)	Percent Increase (%)
1	3.57	1.84	2.30	0.46	24.77%
2	3.57	1.47	2.03	0.56	38.07%
3	3.57	1.63	2.13	0.50	30.81%
4	3.31	2.05	2.57	0.51	24.98%
5	3.31	2.02	2.37	0.35	17.23%
6	3.31	1.81	2.25	0.44	24.49%
AASHTO Type IV Girders					
Beam ID	FDOT Predicted Camber* (in)	Camber At Transfer (in)	Camber After Moving (in)	Camber Increase (in)	Percent Increase (%)
1	1.13	0.65	1.18	0.53	81.94%
2	1.13	0.61	0.90	0.29	46.64%
3	1.13	0.67	1.00	0.33	49.77%
AASHTO Type V Girders					
Beam ID	FDOT Predicted Camber* (in)	Camber At Transfer (in)	Camber After Moving (in)	Camber Increase (in)	Percent Increase (%)
1	0.65	0.85	0.88	0.03	4.00%
2	0.65	0.90	0.87	-0.04	-3.89%
3	0.67	0.85	0.98	0.13	15.65%
4	0.67	0.70	0.67	-0.03	-4.00%
*FDOT predicted camber values based on actual tested material properties. ¹					

¹ Note: Cambers are analytically corrected for thermal effects.

APPENDIX B
FIELD CAMBER MEASUREMENTS

78" Florida Bulb-Tee 1											
$CF_{therm} = 0.0055 \text{ 1/}^\circ\text{F}$											
Date	Time	Time After Release (Days)	Field Camber (in)	Top Flange Temp ($^\circ\text{F}$)	Bottom Flange Temp ($^\circ\text{F}$)	Web Temp ($^\circ\text{F}$)	Top Bulb Temp ($^\circ\text{F}$)	Bottom Bulb Temp ($^\circ\text{F}$)	ΔT ($^\circ\text{F}$)	Empirical Corrected Camber (in)	Analytical Corrected Camber (in)
4/9/2004	8:00 AM	0.00	1.84						0	1.84	1.84
4/9/2004	11:00 AM	0.13	2.43						10	2.30	2.30
4/16/2004	12:00 PM	7.17	3.66						15	3.36	3.36
4/23/2004	10:00 AM	14.08	3.33						8	3.18	3.18
4/23/2004	12:00 PM	14.17	3.61						15	3.31	3.31
4/23/2004	2:00 PM	14.25	3.87						20	3.44	3.44
4/29/2004	11:00 AM	20.13	3.51	91	78	74	74	74	10.5	3.30	3.18
5/7/2004	11:00 AM	28.13	3.64	93	78	74	74	74	11.5	3.41	3.29
5/21/2004	11:00 AM	42.13	3.73	93	80	77	77	77	9.5	3.53	3.44
6/7/2004	7:30 AM	58.98	3.57	75	73	78	74	75	0	3.57	3.57
6/7/2004	9:30 AM	59.06	3.68	94	79	78	85	90	0	3.68	3.68
6/7/2004	12:30 PM	59.19	3.98	117	99	83	86	86	22	3.50	3.26
6/17/2004	11:00 AM	69.13	3.83	99	86	83	83	82	10	3.62	3.52
7/2/2004	11:00 AM	84.125	3.81	104	90	86	86	85	11.5	3.57	3.45
7/14/2004	11:00 AM	96.125	3.71	104	94	87	89	86	11.5	3.48	3.34
7/21/2004	12:00 PM	103.16667	3.89	100	90	82	84	81	12.5	3.62	3.62
7/28/2004	9:00 AM	110.04167	3.33	97	90	86	88	85	7	3.20	3.11
8/11/2004	7:00 AM	123.96	3.25	81	79	82	83	81	0	3.25	3.25
8/11/2004	10:00 AM	124.08	3.48	100	88	85	86	84	9	3.30	3.20
8/11/2004	12:00 PM	124.17	3.90	110	97	88	87	87	16.5	3.55	3.36
8/24/2004	10:00 AM	137.08333	3.50	97	86	84	84	83	8	3.35	3.26
9/9/2004	10:00 AM	153.08333	3.38	88	82	82	82	81	3.5	3.31	3.28
9/21/2004	10:00 AM	165.08333	3.28	72	73	74	74	75	0	3.28	3.28
10/5/2004	9:00 AM	179.04167	3.25	82	79	81	81	79	0.5	3.24	3.25
10/26/2004	9:00 AM	200.04167	3.18	70	69	74	73	69	0	3.18	3.18

78" Florida Bulb-Tee 2											
CF _{therm} = 0.0088 1/°F											
Date	Time	Time After Release (Days)	Field Camber (in)	Top Flange Temp (°F)	Bottom Flange Temp (°F)	Web Temp (°F)	Top Bulb Temp (°F)	Bottom Bulb Temp (°F)	ΔT (°F)	Empirical Corrected Camber (in)	Analytical Corrected Camber (in)
4/9/2004	8:00 AM	0.00	1.47						0	1.47	1.47
4/9/2004	11:00 AM	0.13	2.22						10	2.03	2.03
4/16/2004	12:00 PM	7.17	3.62						15	3.14	3.14
4/23/2004	10:00 AM	14.08	3.05						8	2.84	2.84
4/23/2004	12:00 PM	14.17	3.46						15	3.01	3.01
4/23/2004	2:00 PM	14.25	3.81						20	3.14	3.14
4/29/2004	11:00 AM	20.13	3.38	97	79	75	74	73	14.5	2.95	2.93
5/7/2004	11:00 AM	28.13	3.63	100	85	79	78	78	14.5	3.17	3.16
5/21/2004	11:00 AM	42.13	3.74	92	80	76	75	74	11.5	3.36	3.37
6/7/2004	7:30 AM	58.98	3.44	75	72	75	74	77	0	3.44	3.44
6/7/2004	9:30 AM	59.06	3.73	94	80	79	80	77	8.5	3.45	3.48
6/7/2004	12:30 PM	59.19	4.06	119	104	88	89	86	24	3.20	3.26
6/17/2004	11:00 AM	69.13	3.49	106	94	90	88	86	13	3.09	3.07
7/2/2004	11:00 AM	84.125	3.92	109	95	89	90	86	14	3.44	3.48
7/14/2004	11:00 AM	96.125	3.93	108	92	89	89	86	12.5	3.50	3.55
7/28/2004	9:00 AM	110.04167	3.63	98	90	86	88	85	7.5	3.39	3.39
8/11/2004	7:00 AM	123.96	3.35	81	79	82	83	81	0	3.35	3.35
8/11/2004	10:00 AM	124.08	3.63	101	89	85	85	84	10.5	3.29	3.30
8/11/2004	12:00 PM	124.17	3.98	110	95	88	87	86	16	3.42	3.46
8/24/2004	10:00 AM	137.08333	3.70	100	86	82	82	82	11	3.34	3.36
9/9/2004	10:00 AM	153.08333	3.63	89	82	82	81	82	4	3.50	3.51
9/21/2004	10:00 AM	165.08333	3.40	72	73	74	74	75	0	3.40	3.40
10/5/2004	9:00 AM	179.04167	3.35	80	78	81	80	79	0	3.35	3.35
10/26/2004	9:00 AM	200.04167	3.28	70	69	73	72	69	0	3.28	3.28
78" Florida Bulb-Tee 3											
CF _{therm} = 0.0090 1/°F											
Date	Time	Time After Release (Days)	Field Camber (in)	Top Flange Temp (°F)	Bottom Flange Temp (°F)	Web Temp (°F)	Top Bulb Temp (°F)	Bottom Bulb Temp (°F)	ΔT (°F)	Empirical Corrected Camber (in)	Analytical Corrected Camber (in)
4/9/2004	8:00 AM	0.00	1.63						0	1.63	1.63
4/9/2004	11:00 AM	0.13	2.35						10	2.13	2.13
4/16/2004	12:00 PM	7.17	3.25						15	2.81	2.81
4/23/2004	10:00 AM	14.08	3.05						8	2.83	2.83
4/23/2004	12:00 PM	14.17	3.26						15	2.82	2.82
4/23/2004	2:00 PM	14.25	3.52						20	2.88	2.88
4/29/2004	11:00 AM	20.13	3.28	94	80	76	75	74	12.5	2.91	2.88
5/7/2004	11:00 AM	28.13	3.45	102	89	80	78	78	17.5	2.90	2.87
5/21/2004	11:00 AM	42.13	3.82	101	87	80	77	76	17.5	3.22	3.24
6/7/2004	7:30 AM	58.98	2.99	78	73	75	74	75	1	2.96	2.97
6/7/2004	9:30 AM	59.06	3.13	91	75	74	76	78	6	2.96	2.98
6/7/2004	12:30 PM	59.19	3.65	118	103	84	85	85	25.5	2.81	2.79
6/17/2004	11:00 AM	69.13	3.78	106	95	87	86	87	14	3.30	3.31
7/2/2004	11:00 AM	84.125	3.56	112	96	87	88	85	17.5	3.00	3.00
7/14/2004	11:00 AM	96.125	3.45	106	95	87	87	86	14	3.01	2.98
7/28/2004	9:00 AM	110.04167	3.25	97	90	86	87	89	5.5	3.09	3.08
8/11/2004	7:00 AM	123.96	2.98	82	79	82	82	81	0	2.98	2.98
8/11/2004	10:00 AM	124.08	3.18	101	88	85	85	84	10	2.89	2.87
8/11/2004	12:00 PM	124.17	3.53	111	97	88	87	87	17	2.99	2.97
8/24/2004	10:00 AM	137.08333	3.20	98	86	83	82	82	10	2.91	2.89
9/9/2004	10:00 AM	153.08333	3.10	88	82	83	83	82	2.5	3.03	3.04
9/21/2004	10:00 AM	165.08333	3.03	72	73	74	74	75	0	3.03	3.03
10/5/2004	9:00 AM	179.04167	2.98	82	80	82	82	79	0.5	2.96	2.97
10/26/2004	9:00 AM	200.04167	2.85	71	70	75	74	69	0	2.85	2.85

78" Florida Bulb-Tee 4											
CF _{therm} = 0.0129 1/°F											
Date	Time	Time After Release (Days)	Field Camber (in)	Top Flange Temp (°F)	Bottom Flange Temp (°F)	Web Temp (°F)	Top Bulb Temp (°F)	Bottom Bulb Temp (°F)	ΔT (°F)	Empirical Corrected Camber (in)	Analytical Corrected Camber (in)
6/28/2004	6:30 AM	0.00	2.05	75	79	81	80	80	0	2.05	2.05
6/28/2004	9:00 AM	0.10	2.57	79	79	82	81	81	0	2.57	2.57
7/2/2004	12:00 PM	4.23	2.89	110	104	96	93	91	15	2.33	2.37
7/14/2004	12:00 PM	16.23	3.25	104	101	93	92	92	10.5	2.81	2.88
7/21/2004	12:00 PM	23.23	3.26	102	94	87	87	85	12	2.76	2.86
7/28/2004	9:00 AM	30.10	2.97	95	88	86	87	85	5.5	2.76	2.80
8/11/2004	7:00 AM	44.02	2.77	81	79	82	82	81	0	2.77	2.77
8/11/2004	10:00 AM	44.15	2.99	99	92	89	90	86	7.5	2.70	2.75
8/11/2004	12:00 PM	44.23	3.34	109	99	92	90	87	15.5	2.67	2.82
8/24/2004	10:00 AM	57.15	3.19	98	86	84	83	82	9.5	2.80	2.89
9/9/2004	10:00 AM	73.15	2.97	88	81	82	82	81	3	2.85	2.89
9/21/2004	10:00 AM	85.15	2.84	72	73	74	74	74	0	2.84	2.84
10/5/2004	9:00 AM	99.10	3.02	80	78	80	80	79	0	3.02	3.02
10/26/2004	9:00 AM	120.10	3.02	69	69	72	71	69	0	3.02	3.02
78" Florida Bulb-Tee 5											
CF _{therm} = 0.0106 1/°F											
Date	Time	Time After Release (Days)	Field Camber (in)	Top Flange Temp (°F)	Bottom Flange Temp (°F)	Web Temp (°F)	Top Bulb Temp (°F)	Bottom Bulb Temp (°F)	ΔT (°F)	Empirical Corrected Camber (in)	Analytical Corrected Camber (in)
6/28/2004	6:30 AM	0.00	2.02	75	78	81	80	80	0	2.02	2.02
6/28/2004	9:00 AM	0.10	2.37	79	80	82	82	81	0	2.37	2.37
7/2/2004	12:00 PM	4.23	3.26	114	103	94	92	89	18	2.64	2.66
7/14/2004	12:00 PM	16.23	3.32	111	95	91	90	89	13.5	2.85	2.90
7/21/2004	12:00 PM	23.23	3.39	100	89	84	84	84	10.5	3.02	3.06
7/28/2004	9:00 AM	30.10	3.13	94	89	86	87	86	5	2.96	2.97
8/11/2004	7:00 AM	44.02	3.06	80	79	85	83	82	0	3.06	3.06
8/11/2004	10:00 AM	44.15	3.23	98	87	84	84	84	8.5	2.94	2.97
8/11/2004	12:00 PM	44.23	3.56	107	94	88	87	87	13.5	3.05	3.12
8/24/2004	10:00 AM	57.15	3.38	95	84	83	82	83	7	3.13	3.17
9/9/2004	10:00 AM	73.15	2.98	85	83	84	86	83	0	2.98	2.98
9/21/2004	10:00 AM	85.15	3.11	72	73	74	74	75	0	3.11	3.11
10/5/2004	9:00 AM	99.10	2.96	81	79	81	82	79	0	2.96	2.96
10/26/2004	9:00 AM	120.10	2.98	71	69	74	74	69	0	2.98	2.98
78" Florida Bulb-Tee 6											
CF _{therm} = 0.0131 1/°F											
Date	Time	Time After Release (Days)	Field Camber (in)	Top Flange Temp (°F)	Bottom Flange Temp (°F)	Web Temp (°F)	Top Bulb Temp (°F)	Bottom Bulb Temp (°F)	ΔT (°F)	Empirical Corrected Camber (in)	Analytical Corrected Camber (in)
6/28/2004	6:30 AM	0.00	1.81	77	79	82	81	80	0	1.81	1.81
6/28/2004	9:00 AM	0.10	2.25	81	79	81	82	81	0	2.25	2.25
7/2/2004	12:00 PM	4.23	3.44	112	105	96	94	91	16	2.72	2.89
7/14/2004	12:00 PM	16.23	3.31	113	104	96	93	92	16	2.61	2.76
7/21/2004	12:00 PM	23.23	3.38	108	94	86	88	84	15	2.71	2.90
7/28/2004	9:00 AM	30.10	3.02	95	88	86	85	84	7	2.74	2.79
8/11/2004	7:00 AM	44.02	2.84	83	79	82	82	82	0	2.84	2.84
8/11/2004	10:00 AM	44.15	3.09	94	87	85	85	83	6.5	2.83	2.89
8/11/2004	12:00 PM	44.23	3.42	109	98	90	89	87	15.5	2.72	2.90
8/24/2004	10:00 AM	57.15	3.24	102	88	85	84	83	11.5	2.75	2.88
9/9/2004	10:00 AM	73.15	2.99	92	87	88	88	85	3	2.87	2.90
9/21/2004	10:00 AM	85.15	2.82	73	73	74	74	75	0	2.82	2.82
10/5/2004	9:00 AM	99.10	2.92	83	80	81	81	79	1.5	2.86	2.87
10/26/2004	9:00 AM	120.10	2.84	71	69	72	71	68	0.5	2.82	2.83

AASHTO Type IV 1											
CF _{therm} = 0.0132 1/°F											
Date	Time	Time After Release (Days)	Field Camber (in)	Top Flange Temp (°F)	Bottom Flange Temp (°F)	Web Temp (°F)	Top Bulb Temp (°F)	Bottom Bulb Temp (°F)	ΔT (°F)	Empirical Corrected Camber (in)	Analytical Corrected Camber (in)
6/10/2004	9:30 AM	0.00	0.65	83	83	85	88	85	0	0.65	0.65
6/10/2004	11:30 AM	0.08	1.18	104	88	87	98	92	1	1.17	1.18
6/17/2004	9:00 AM	6.98	1.29	87	85	85	84	82	3	1.24	1.23
6/24/2004	3:00 PM	14.23	1.47	117	100	95	96	95	13	1.22	1.25
7/2/2004	9:00 AM	21.98	1.28	98	88	87	86	85	7.5	1.15	1.15
7/14/2004	10:00 AM	34.02	1.20	101	90	90	89	88	7	1.09	1.08
7/21/2004	9:00 AM	40.98	1.16	92	85	86	86	85	3	1.12	1.11
7/28/2004	9:00 AM	47.98	1.50	92	85	86	87	87	1.5	1.47	1.48
8/11/2004	7:00 AM	61.90	1.33	79	82	83	82	79	0	1.33	1.32
8/11/2004	10:00 AM	62.02	1.45	95	87	87	88	89	2.5	1.40	1.41
8/11/2004	12:00 PM	62.10	1.45	107	91	90	90	91	8.5	1.29	1.31
8/24/2004	10:00 AM	75.02	1.50	93	86	87	87	84	4	1.42	1.43
9/9/2004	10:00 AM	91.02	1.58	94	86	86	86	86	4	1.49	1.51
9/21/2004	10:00 AM	103.02	1.58	75	74	75	75	75	0	1.58	1.58
10/5/2004	9:00 AM	116.98	1.63	88	84	85	84	80	4	1.54	1.55
10/26/2004	9:00 AM	137.98	1.75	81	74	74	73	70	6	1.61	1.64
AASHTO Type IV 2											
CF _{therm} = 0.0276 1/°F											
Date	Time	Time After Release (Days)	Field Camber (in)	Top Flange Temp (°F)	Bottom Flange Temp (°F)	Web Temp (°F)	Top Bulb Temp (°F)	Bottom Bulb Temp (°F)	ΔT (°F)	Empirical Corrected Camber (in)	Analytical Corrected Camber (in)
6/10/2004	9:30 AM	0.00	0.61	87	85	88	93	87	0	0.61	0.61
6/10/2004	11:30 AM	0.08	1.05	105	87	85	86	87	9.5	0.78	0.90
6/17/2004	9:00 AM	6.98	1.24	92	84	84	89	84	1.5	1.19	1.22
6/24/2004	3:00 PM	14.23	1.53	120	99	96	103	96	10	1.11	1.36
7/2/2004	9:00 AM	21.98	1.28	93	88	88	86	84	5.5	1.09	1.18
7/14/2004	10:00 AM	34.02	1.22	101	93	92	89	88	8.5	0.94	1.07
7/21/2004	9:00 AM	40.98	1.24	87	82	82	82	80	3.5	1.12	1.17
7/28/2004	9:00 AM	47.98	1.51	93	85	86	87	87	2	1.43	1.48
8/11/2004	7:00 AM	61.90	1.06	79	82	83	82	79	0	1.06	1.05
8/11/2004	10:00 AM	62.02	1.29	93	84	85	85	86	3	1.18	1.24
8/11/2004	12:00 PM	62.10	1.26	107	91	89	90	91	8.5	0.96	1.12
8/24/2004	10:00 AM	75.02	1.31	94	86	86	86	84	5	1.13	1.22
9/9/2004	10:00 AM	91.02	1.64	92	86	86	86	86	3	1.50	1.59
9/21/2004	10:00 AM	103.02	1.71	75	74	75	75	75	0	1.71	1.71
10/5/2004	3:36 AM	116.75	1.64	89	84	84	84	80	4.5	1.43	1.55
10/26/2004	9:00 AM	137.98	1.74	78	76	76	75	70	4.5	1.52	1.65
AASHTO Type IV 3											
CF _{therm} = 0.0123 1/°F											
Date	Time	Time After Release (Days)	Field Camber (in)	Top Flange Temp (°F)	Bottom Flange Temp (°F)	Web Temp (°F)	Top Bulb Temp (°F)	Bottom Bulb Temp (°F)	ΔT (°F)	Empirical Corrected Camber (in)	Analytical Corrected Camber (in)
6/10/2004	9:30 AM	0.00	0.67	86	84	87	95	89	0	0.67	0.67
6/10/2004	11:30 AM	0.08	1.17	104	88	85	84	87	10.5	1.02	1.00
6/17/2004	9:00 AM	6.98	1.25	95	87	86	84	84	7	1.14	1.12
6/24/2004	3:00 PM	14.23	1.47	116	103	99	105	100	7	1.35	1.36
7/2/2004	9:00 AM	21.98	1.28	95	89	89	87	84	6.5	1.18	1.16
7/14/2004	10:00 AM	34.02	1.39	101	88	88	88	88	6.5	1.28	1.28
7/21/2004	9:00 AM	40.98	1.37	90	81	80	80	80	5.5	1.27	1.27
7/28/2004	9:00 AM	47.98	1.49	92	86	86	87	87	2	1.45	1.46
8/11/2004	7:00 AM	61.90	1.59	78	82	83	82	79	0	1.59	1.59
8/11/2004	10:00 AM	62.02	1.91	96	86	85	84	85	6.5	1.76	1.80
8/11/2004	12:00 PM	62.10	1.64	109	91	89	90	91	9.5	1.45	1.48
8/24/2004	10:00 AM	75.02	1.71	96	87	86	86	84	6.5	1.58	1.60
9/9/2004	10:00 AM	91.02	1.69	93	86	85	85	86	4	1.60	1.62
9/21/2004	10:00 AM	103.02	1.71	75	74	74	75	75	0	1.71	1.71
10/5/2004	3:36 AM	116.75	1.76	88	82	84	82	80	4	1.68	1.69
10/26/2004	9:00 AM	137.98	1.76	77	72	72	71	70	4	1.68	1.69

AASHTO Type V 2											
CF _{therm} = 0.0037 1/°F											
Date	Time	Time After Release (Days)	Field Camber (in)	Top Flange Temp (°F)	Bottom Flange Temp (°F)	Web Temp (°F)	Top Bulb Temp (°F)	Bottom Bulb Temp (°F)	ΔT (°F)	Empirical Corrected Camber (in)	Analytical Corrected Camber (in)
9/28/2004	9:00 AM	0.00	0.90	81	78	79	79	79	0.5	0.90	0.90
9/28/2004	10:00 AM	0.04	0.90	89	82	82	82	83	3	0.89	0.87
10/5/2004	9:00 AM	7.00	1.28	89	82	85	85	83	1.5	1.27	1.26
10/12/2004	9:00 AM	14.00	1.30	74	73	74	74	74	0	1.30	1.30
10/19/2004	9:00 AM	21.00	1.30	79	77	79	81	75	0	1.30	1.30
10/19/2004	11:00 AM	21.08	1.35	89	82	82	81	78	6	1.32	1.28
10/19/2004	1:00 PM	21.17	1.35	100	86	82	81	80	12.5	1.29	1.20
10/26/2004	9:00 AM	28.00	1.28	71	71	73	75	71	0	1.28	1.28
AASHTO Type V 3											
CF _{therm} = 0.0061 1/°F											
Date	Time	Time After Release (Days)	Field Camber (in)	Top Flange Temp (°F)	Bottom Flange Temp (°F)	Web Temp (°F)	Top Bulb Temp (°F)	Bottom Bulb Temp (°F)	ΔT (°F)	Empirical Corrected Camber (in)	Analytical Corrected Camber (in)
9/28/2004	9:00 AM	0.00	0.85	78	80	80	80	80	0	0.85	0.85
9/28/2004	10:00 AM	0.04	1.00	87	82	83	83	83	1.5	0.99	0.98
10/5/2004	9:00 AM	7.00	1.25	87	82	84	84	83	1	1.24	1.24
10/12/2004	9:00 AM	14.00	1.28	74	73	73	74	74	0	1.28	1.28
10/19/2004	9:00 AM	21.00	1.33	81	76	78	77	75	2.5	1.30	1.30
10/19/2004	11:00 AM	21.08	1.40	91	82	80	80	78	7.5	1.34	1.31
10/19/2004	1:00 PM	21.17	1.43	102	86	83	82	80	13	1.31	1.27
10/26/2004	9:00 AM	28.00	1.33	76	71	74	73	71	1.5	1.31	1.31
AASHTO Type V 4											
CF _{therm} = 0.0075 1/°F											
Date	Time	Time After Release (Days)	Field Camber (in)	Top Flange Temp (°F)	Bottom Flange Temp (°F)	Web Temp (°F)	Top Bulb Temp (°F)	Bottom Bulb Temp (°F)	ΔT (°F)	Empirical Corrected Camber (in)	Analytical Corrected Camber (in)
9/28/2004	9:00 AM	0.00	0.70	79	78	80	79	79	0	0.70	0.70
9/28/2004	10:00 AM	0.04	0.73	90	82	83	82	81	4.5	0.70	0.67
10/5/2004	9:00 AM	7.00	1.20	88	82	85	84	82	2	1.18	1.18
10/12/2004	9:00 AM	14.00	1.25	74	72	73	74	74	0	1.25	1.25
10/19/2004	9:00 AM	21.00	1.10	80	76	77	76	75	2.5	1.08	1.07
10/19/2004	11:00 AM	21.08	1.15	87	80	79	79	78	5	1.11	1.09
10/19/2004	1:00 PM	21.17	1.20	99	86	82	81	80	12	1.09	1.06
10/26/2004	9:00 AM	28.00	1.15	71	71	74	74	71	0	1.15	1.15

APPENDIX C
EMPIRICAL THERMAL ANALYSIS

For the empirical thermal gradient camber correction method, a linear thermal gradient approximation was made. This was calculated by subtracting the average temperature of the bottom bulb from the average temperature of the top flange (Equation C-1).

$$\Delta T = \frac{T_A + T_B}{2} - \frac{T_D + T_E}{2} \quad (\text{C-1})$$

where:

T_i = temperature at location A , B , D , or E along the cross section ($^{\circ}\text{F}$)

In order to correct for the effect of the thermal gradient on the prestressed beam camber, a thermal correction factor needed to be determined. This factor was obtained by first determining the percent camber change relative to the early morning camber measurement ($\Delta C\%$) where there was essentially no gradient (Equation C-2).

$$\Delta C\% = \frac{C_i - C_o}{C_o} \quad (\text{C-2})$$

where:

C_o = morning field measured camber reading (in.)

C_i = subsequent field measured camber reading (in.)

The thermal gradient versus normalized camber reading was plotted and a linear regression of the data produced a thermal correction factor (Equation C-3) for the adjustment of the field measured camber values (Equation C-4).

$$CF_{therm} = \frac{\Delta C\% / 100}{\Delta T} \quad (C-3)$$

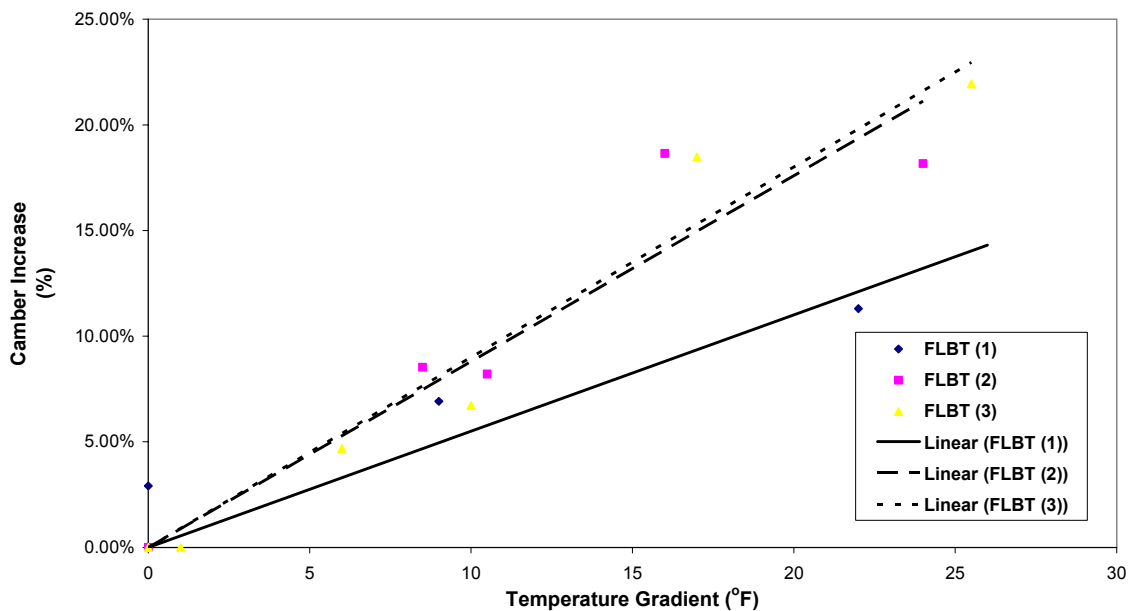
$$C_{corr} = C_{field} - (C_{field} \cdot CF_{therm} \cdot \Delta T) \quad (C-4)$$

where:

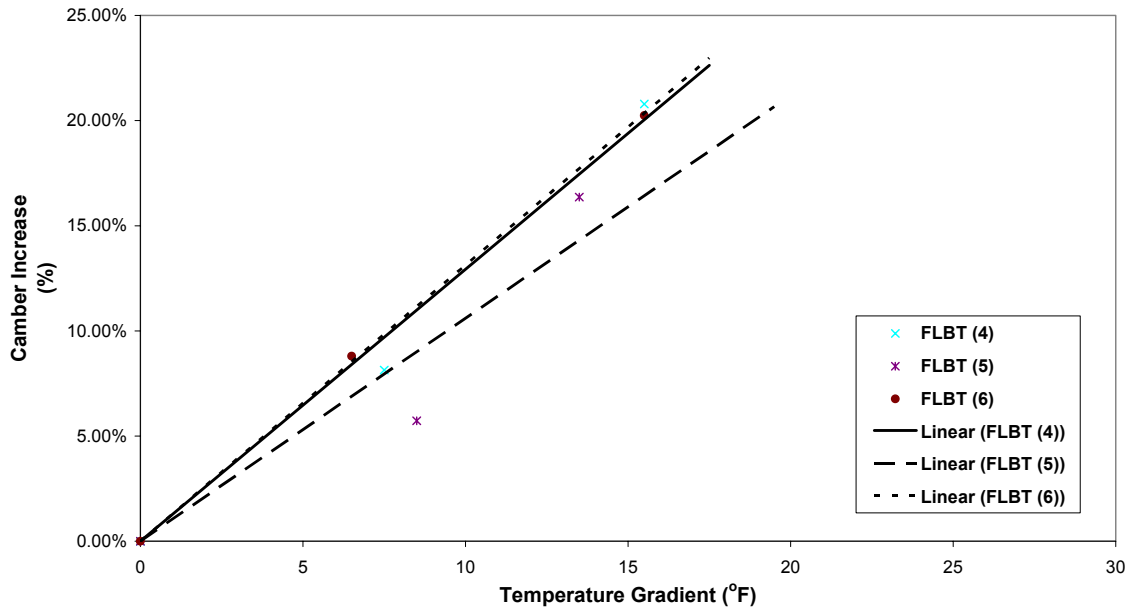
C_{field} = field measured camber reading (in.)

Assumptions made to obtain this thermal correction factor were that a thermal gradient of zero yielded no change in camber (i.e., the linear regression was forced through the origin) and that negative thermal gradients did not produce negative camber effects (i.e., an increase in camber). Temperature field measurements were not made for the first three camber readings of the 78-inch Bulb-Tee girders (girders 1, 2, and 3). The thermal gradients were estimated for these readings based on the time of reading and ambient temperature.

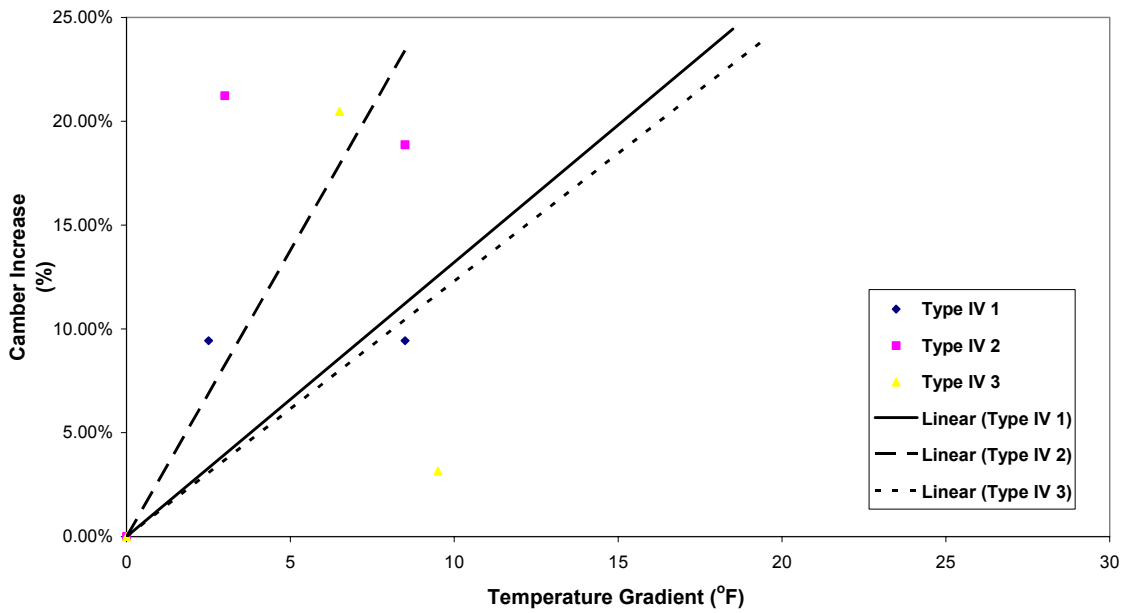
78" Bulb-Tee 1										
Date	Time	Field Measured Camber (in)	$\Delta C\%$ (%)	Top Flange Temp ($^{\circ}F$)	Bottom Flange Temp ($^{\circ}F$)	Web Temp ($^{\circ}F$)	Top Bulb Temp ($^{\circ}F$)	Bottom Bulb Temp ($^{\circ}F$)	ΔT ($^{\circ}F$)	CF_{therm} ($1/^{\circ}F$)
6/7/2004	7:30 AM	3.57	0.00%	75	73	78	74	75	0	0.0055
6/7/2004	9:30 AM	3.68	2.91%	94	79	78	85	90	0	
6/7/2004	12:30 PM	3.98	11.31%	117	99	83	86	86	22	
8/11/2004	7:00 AM	3.25	0.00%	81	79	82	83	81	0	
8/11/2004	10:00 AM	3.48	6.92%	100	88	85	86	84	9	
8/11/2004	12:00 PM	3.90	19.99%	110	97	88	87	87	16.5	
78" Bulb-Tee 2										
Date	Time	Field Measured Camber (in)	$\Delta C\%$ (%)	Top Flange Temp ($^{\circ}F$)	Bottom Flange Temp ($^{\circ}F$)	Web Temp ($^{\circ}F$)	Top Bulb Temp ($^{\circ}F$)	Bottom Bulb Temp ($^{\circ}F$)	ΔT ($^{\circ}F$)	CF_{therm} ($1/^{\circ}F$)
6/7/2004	7:30 AM	3.44	0.00%	75	72	75	74	77	0	0.0088
6/7/2004	9:30 AM	3.73	8.53%	94	80	79	80	77	8.5	
6/7/2004	12:30 PM	4.06	18.17%	119	104	88	89	86	24	
8/11/2004	7:00 AM	3.35	0.00%	81	79	82	83	81	0	
8/11/2004	10:00 AM	3.63	8.20%	101	89	85	85	84	10.5	
8/11/2004	12:00 PM	3.98	18.65%	110	95	88	87	86	16	
78" Bulb-Tee 3										
Date	Time	Field Measured Camber (in)	$\Delta C\%$ (%)	Top Flange Temp ($^{\circ}F$)	Bottom Flange Temp ($^{\circ}F$)	Web Temp ($^{\circ}F$)	Top Bulb Temp ($^{\circ}F$)	Bottom Bulb Temp ($^{\circ}F$)	ΔT ($^{\circ}F$)	CF_{therm} ($1/^{\circ}F$)
6/7/2004	7:30 AM	2.99	0.00%	78	73	75	74	75	1	0.009
6/7/2004	9:30 AM	3.13	4.68%	91	75	74	76	78	6	
6/7/2004	12:30 PM	3.65	21.95%	118	103	84	85	85	25.5	
8/11/2004	7:00 AM	2.98	0.00%	82	79	82	82	81	0	
8/11/2004	10:00 AM	3.18	6.72%	101	88	85	85	84	10	
8/11/2004	12:00 PM	3.53	18.47%	111	97	88	87	87	17	



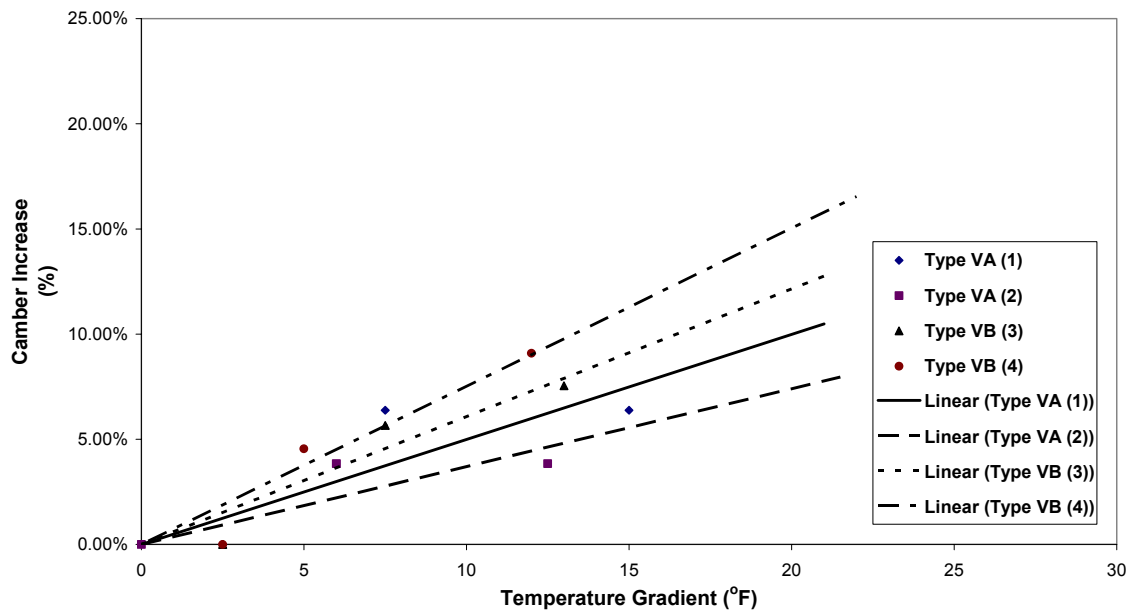
78" Bulb-Tee 4										
Date	Time	Field Measured Camber (in)	$\Delta C\%$ (%)	Top Flange Temp ($^{\circ}F$)	Bottom Flange Temp ($^{\circ}F$)	Web Temp ($^{\circ}F$)	Top Bulb Temp ($^{\circ}F$)	Bottom Bulb Temp ($^{\circ}F$)	ΔT ($^{\circ}F$)	CF_{therm} (1/ $^{\circ}F$)
8/11/2004	7:00 AM	2.77	0.00%	81	79	82	82	81	0	0.0129
8/11/2004	10:00 AM	2.99	8.14%	99	92	89	90	86	7.5	
8/11/2004	12:00 PM	3.34	20.79%	109	99	92	90	87	15.5	
78" Bulb-Tee 5										
Date	Time	Field Measured Camber (in)	$\Delta C\%$ (%)	Top Flange Temp ($^{\circ}F$)	Bottom Flange Temp ($^{\circ}F$)	Web Temp ($^{\circ}F$)	Top Bulb Temp ($^{\circ}F$)	Bottom Bulb Temp ($^{\circ}F$)	ΔT ($^{\circ}F$)	CF_{therm} (1/ $^{\circ}F$)
8/11/2004	7:00 AM	3.06	0.00%	80	79	85	83	82	0	0.0106
8/11/2004	10:00 AM	3.23	5.73%	98	87	84	84	84	8.5	
8/11/2004	12:00 PM	3.56	16.36%	107	94	88	87	87	13.5	
78" Bulb-Tee 6										
Date	Time	Field Measured Camber (in)	$\Delta C\%$ (%)	Top Flange Temp ($^{\circ}F$)	Bottom Flange Temp ($^{\circ}F$)	Web Temp ($^{\circ}F$)	Top Bulb Temp ($^{\circ}F$)	Bottom Bulb Temp ($^{\circ}F$)	ΔT ($^{\circ}F$)	CF_{therm} (1/ $^{\circ}F$)
8/11/2004	7:00 AM	2.84	0.00%	83	79	82	82	82	0	0.0131
8/11/2004	10:00 AM	3.09	8.80%	94	87	85	85	83	6.5	
8/11/2004	12:00 PM	3.42	20.24%	109	98	90	89	87	15.5	



AASHTO Type IV 1										
Date	Time	Field Measured Camber (in)	$\Delta C\%$ (%)	Top Flange Temp ($^{\circ}F$)	Bottom Flange Temp ($^{\circ}F$)	Web Temp ($^{\circ}F$)	Top Bulb Temp ($^{\circ}F$)	Bottom Bulb Temp ($^{\circ}F$)	ΔT ($^{\circ}F$)	CF_{therm} ($1/^{\circ}F$)
8/11/2004	7:00 AM	1.33	0.00%	79	82	83	82	79	0	0.0132
8/11/2004	10:00 AM	1.45	9.43%	95	87	87	88	89	2.5	
8/11/2004	12:00 PM	1.45	9.43%	107	91	90	90	91	8.5	
AASHTO Type IV 2										
Date	Time	Field Measured Camber (in)	$\Delta C\%$ (%)	Top Flange Temp ($^{\circ}F$)	Bottom Flange Temp ($^{\circ}F$)	Web Temp ($^{\circ}F$)	Top Bulb Temp ($^{\circ}F$)	Bottom Bulb Temp ($^{\circ}F$)	ΔT ($^{\circ}F$)	CF_{therm} ($1/^{\circ}F$)
8/11/2004	7:00 AM	1.06	0.00%	79	82	83	82	79	0	0.0276
8/11/2004	10:00 AM	1.29	21.23%	93	84	85	85	86	3	
8/11/2004	12:00 PM	1.26	18.87%	107	91	89	90	91	8.5	
AASHTO Type IV 3										
Date	Time	Field Measured Camber (in)	$\Delta C\%$ (%)	Top Flange Temp ($^{\circ}F$)	Bottom Flange Temp ($^{\circ}F$)	Web Temp ($^{\circ}F$)	Top Bulb Temp ($^{\circ}F$)	Bottom Bulb Temp ($^{\circ}F$)	ΔT ($^{\circ}F$)	CF_{therm} ($1/^{\circ}F$)
8/11/2004	7:00 AM	1.59	0.00%	78	82	83	82	79	0	0.0123
8/11/2004	10:00 AM	1.91	20.47%	96	86	85	84	85	6.5	
8/11/2004	12:00 PM	1.64	3.15%	109	91	89	90	91	9.5	



AASHTO Type V 1										
Date	Time	Field Measured Camber (in)	$\Delta C\%$ (%)	Top Flange Temp ($^{\circ}F$)	Bottom Flange Temp ($^{\circ}F$)	Web Temp ($^{\circ}F$)	Top Bulb Temp ($^{\circ}F$)	Bottom Bulb Temp ($^{\circ}F$)	ΔT ($^{\circ}F$)	CF_{therm} ($1/^{\circ}F$)
10/19/2004	9:00 AM	1.18	0.00%	81	77	78	78	75	2.5	0.005
10/19/2004	11:00 AM	1.25	6.38%	91	82	80	80	78	7.5	
10/19/2004	1:00 PM	1.25	6.38%	103	88	82	81	80	15	
AASHTO Type V 2										
Date	Time	Field Measured Camber (in)	$\Delta C\%$ (%)	Top Flange Temp ($^{\circ}F$)	Bottom Flange Temp ($^{\circ}F$)	Web Temp ($^{\circ}F$)	Top Bulb Temp ($^{\circ}F$)	Bottom Bulb Temp ($^{\circ}F$)	ΔT ($^{\circ}F$)	CF_{therm} ($1/^{\circ}F$)
10/19/2004	9:00 AM	1.30	0.00%	79	77	79	81	75	0	0.0037
10/19/2004	11:00 AM	1.35	3.85%	89	82	82	81	78	6	
10/19/2004	1:00 PM	1.35	3.85%	100	86	82	81	80	12.5	
AASHTO Type V 3										
Date	Time	Field Measured Camber (in)	$\Delta C\%$ (%)	Top Flange Temp ($^{\circ}F$)	Bottom Flange Temp ($^{\circ}F$)	Web Temp ($^{\circ}F$)	Top Bulb Temp ($^{\circ}F$)	Bottom Bulb Temp ($^{\circ}F$)	ΔT ($^{\circ}F$)	CF_{therm} ($1/^{\circ}F$)
10/19/2004	9:00 AM	1.33	0.00%	81	76	78	77	75	2.5	0.0061
10/19/2004	11:00 AM	1.40	5.66%	91	82	80	80	78	7.5	
10/19/2004	1:00 PM	1.43	7.55%	102	86	83	82	80	13	
AASHTO Type V 4										
Date	Time	Field Measured Camber (in)	$\Delta C\%$ (%)	Top Flange Temp ($^{\circ}F$)	Bottom Flange Temp ($^{\circ}F$)	Web Temp ($^{\circ}F$)	Top Bulb Temp ($^{\circ}F$)	Bottom Bulb Temp ($^{\circ}F$)	ΔT ($^{\circ}F$)	CF_{therm} ($1/^{\circ}F$)
10/19/2004	9:00 AM	1.10	0.00%	80	76	77	76	75	2.5	0.0075
10/19/2004	11:00 AM	1.15	4.55%	87	80	79	79	78	5	
10/19/2004	1:00 PM	1.20	9.09%	99	86	82	81	80	12	



APPENDIX D
ANALYTICAL THERMAL ANALYSIS

Analytical Thermal Analysis

--written by Jonathan Sanek, University of Florida Department of Civil and Coastal Engineering

78" Bulb-Tee Girder, Pour A

ORIGIN= 1 Ξ = ORIGIN

Input Field Temperature Measurements

$t_{\text{camber}} :=$	0.00 0.13 7.17 14.08 14.17 14.25 20.13 28.13 42.13 58.98 59.06 59.19 69.13 84.125 96.125 110.0416667 123.96 124.08 124.17 137.0833333 153.0833333 165.0833333 179.0416667 200.0416667	FLBT1:=	0 91 78 74 74 74 93 78 74 74 74 93 80 77 77 77 75 73 78 74 75 94 79 78 85 90 117 99 83 86 86 99 86 83 83 82 104 90 86 86 85 104 94 87 89 86 97 90 86 88 85 81 79 82 83 81 100 88 85 86 84 110 97 88 87 87 97 86 84 84 83 88 82 82 82 81 72 73 74 74 75 82 79 81 81 79 70 69 74 73 69	FLBT2:=	0 97 79 75 74 73 100 85 79 78 78 92 80 76 75 74 75 72 75 74 77 94 80 79 80 77 119 104 88 89 86 106 94 90 88 86 109 95 89 90 86 108 92 89 89 86 98 90 86 88 85 81 79 82 83 81 101 89 85 85 84 110 95 88 87 86 100 86 82 82 82 89 82 82 81 82 72 73 74 74 75 80 78 81 80 79 70 69 73 72 69
------------------------	--	---------	---	---------	---

Input Field Temperature Measurements (cont...)

Height vector
corresponding to
temperature readings

$$H_{\text{vec}} := \begin{pmatrix} 0 \\ 5 \\ 35 \\ 65 \\ 78 \end{pmatrix} \quad (\text{in})$$

$$\text{FLBT3} := \begin{pmatrix} 0 & 0 & 0 & 0 & 0 \\ 0 & 0 & 0 & 0 & 0 \\ 0 & 0 & 0 & 0 & 0 \\ 0 & 0 & 0 & 0 & 0 \\ 0 & 0 & 0 & 0 & 0 \\ 94 & 80 & 76 & 75 & 74 \\ 102 & 89 & 80 & 78 & 78 \\ 101 & 87 & 80 & 77 & 76 \\ 78 & 73 & 75 & 74 & 75 \\ 91 & 75 & 74 & 76 & 78 \\ 118 & 103 & 84 & 85 & 85 \\ 106 & 95 & 87 & 86 & 87 \\ 112 & 96 & 87 & 88 & 85 \\ 106 & 95 & 87 & 87 & 86 \\ 97 & 90 & 86 & 87 & 89 \\ 82 & 79 & 82 & 82 & 81 \\ 101 & 88 & 85 & 85 & 84 \\ 111 & 97 & 88 & 87 & 87 \\ 98 & 86 & 83 & 82 & 82 \\ 88 & 82 & 83 & 83 & 82 \\ 72 & 73 & 74 & 74 & 75 \\ 82 & 80 & 82 & 82 & 79 \\ 71 & 70 & 75 & 74 & 69 \end{pmatrix}$$

Input Material Testing Data

$$\alpha := 5.3 \times 10^{-6} \quad \text{taken from Table 5 of NCHRP Report 276}$$

$$t_{\text{emod}} := \begin{pmatrix} 0 \\ 7 \\ 14 \\ 21 \\ 28 \\ 42 \\ 84 \\ 109 \\ 136 \\ 200 \end{pmatrix} \text{ (days)} \quad E_c := \begin{pmatrix} 4309 \\ 5228 \\ 5304 \\ 5336 \\ 5444 \\ 5588 \\ 6005 \\ 6070 \\ 6126 \\ 6017 \end{pmatrix} \text{ (ksi)} \quad E(t) := \begin{cases} \text{for } i \in \Xi \dots \text{last}(t) \\ \text{out}_i \leftarrow \text{linterp}(t_{\text{emod}}, E_c, t_i) \\ \text{out} \end{cases}$$

Section Properties

$$H := 78 \quad \text{(in)}$$

$$L := 1942.625 \quad \text{(in)}$$

Section Shape

$$b(z) := \begin{cases} 60 & \text{if } 0 \leq z \leq 3 \\ [60 - 11.75(z - 3)] & \text{if } 3 < z \leq 7 \\ [13 - 2 \cdot (z - 7)] & \text{if } 7 < z \leq 10 \\ 7 & \text{if } 10 < z \leq 60 \\ [7 + 2.1 \cdot (z - 60)] & \text{if } 60 < z \leq 70 \\ 28 & \text{if } 70 < z \leq H \end{cases}$$

$$A := \int_0^H b(z) dz \quad A = 1105.007 \quad \text{(in}^2\text{) Cross-Sectional Area}$$

$$Q_y := \int_0^H z \cdot b(z) dz \quad Q_y = 41563.094 \quad \text{(in}^3\text{) First Moment Area}$$

$$c := \frac{Q_y}{A} \quad c = 37.613 \quad \text{(in) Location of Neutral Axis from top of member}$$

$$I_g := \int_0^H (z - c)^2 \cdot b(z) dz \quad I_g = 935547.485 \quad \text{(in}^4\text{) Gross Moment of Inertia}$$

Calculations

Extract Thermal Gradient and Normalized based on Minimum Measured Temperature Along Profile...

$$T_{\text{vec}}(\text{Beam}) := \left| \begin{array}{l} \text{for } i \in \Xi \dots \text{rows}(\text{Beam}) \\ \quad \left| \begin{array}{l} \min_1 \leftarrow \min(\text{submatrix}(\text{Beam}, i, i, \Xi, \text{cols}(\text{Beam}))) \\ \text{for } j \in \Xi \dots \text{cols}(\text{Beam}) \\ \quad \left| \begin{array}{l} T_{g_{i,j}} \leftarrow \text{Beam}_{i,j} - \min_1 \\ T_{g_{i,j}} \leftarrow T_{g_{i,j}} \text{ if } T_{g_{i,j}} \geq 0 \\ T_{g_{i,j}} \leftarrow 0 \text{ otherwise} \end{array} \right. \\ \text{out}_i \leftarrow \left(\left(\text{submatrix}(T_g, i, i, \Xi, \text{cols}(T_g)) \right) \right)^T \end{array} \right. \\ \text{out} \end{array} \right.$$

Linear Interpolation of Thermal Gradient for variable, z...

$$T_{\text{grad}}(\text{Beam}, z) := \left| \begin{array}{l} \text{for } i \in \Xi \dots \text{rows}(\text{Beam}) \\ \quad \text{out}_i \leftarrow \text{linterp}(H_{\text{vec}}, T_{\text{vec}}(\text{Beam})_i, z) \\ \text{out} \end{array} \right.$$

Example Calculation of Internal Moment Due to Positive Thermal Gradient

$$\text{time} := 15 \quad \text{Beam} := \text{FLBT1}$$

$$T(z) := T_{\text{grad}}(\text{Beam}, z)_{\text{time}} \quad (\text{deg F})$$

$$\sigma_T(z) := -E(t_{\text{camber}})_{\text{time}} \cdot \alpha \cdot T(z) \quad (\text{ksi})$$

$$M_{\text{int}} := \int_0^H \sigma_T(z) \cdot b(z) \cdot (z - c) \, dz \quad M_{\text{int}} = 4.429 \times 10^3 \quad (\text{kip}\cdot\text{in})$$

$$\Delta_{\text{corr}} := \frac{-M_{\text{int}} \cdot L^2}{8 \cdot E(t_{\text{camber}})_{\text{time}} \cdot I_g} \quad \Delta_{\text{corr}} = -0.37 \quad (\text{in})$$

Analytical Thermal Analysis

--written by Jonathan Sanek, University of Florida Department of Civil and Coastal Engineering

78" Bulb-Tee Girder, Pour B

ORIGIN=1 Ξ = ORIGIN

Input Field Temperature Measurements

$$t_{\text{camber}} := \begin{pmatrix} 0.00 \\ 0.10 \\ 4.23 \\ 16.23 \\ 23.23 \\ 30.10 \\ 44.02 \\ 44.15 \\ 44.23 \\ 57.15 \\ 73.15 \\ 85.15 \\ 99.10 \\ 120.10 \end{pmatrix} \quad \text{FLBT4} := \begin{pmatrix} 75 & 79 & 81 & 80 & 80 \\ 79 & 79 & 82 & 81 & 81 \\ 110 & 104 & 96 & 93 & 91 \\ 104 & 101 & 93 & 92 & 92 \\ 102 & 94 & 87 & 87 & 85 \\ 95 & 88 & 86 & 87 & 85 \\ 81 & 79 & 82 & 82 & 81 \\ 99 & 92 & 89 & 90 & 86 \\ 109 & 99 & 92 & 90 & 87 \\ 98 & 86 & 84 & 83 & 82 \\ 88 & 81 & 82 & 82 & 81 \\ 72 & 73 & 74 & 74 & 74 \\ 80 & 78 & 80 & 80 & 79 \\ 69 & 69 & 72 & 71 & 69 \end{pmatrix} \quad \text{FLBT5} := \begin{pmatrix} 75 & 78 & 81 & 80 & 80 \\ 79 & 80 & 82 & 82 & 81 \\ 114 & 103 & 94 & 92 & 89 \\ 111 & 95 & 91 & 90 & 89 \\ 100 & 89 & 84 & 84 & 84 \\ 94 & 89 & 86 & 87 & 86 \\ 80 & 79 & 85 & 83 & 82 \\ 98 & 87 & 84 & 84 & 84 \\ 107 & 94 & 88 & 87 & 87 \\ 95 & 84 & 83 & 82 & 83 \\ 85 & 83 & 84 & 86 & 83 \\ 72 & 73 & 74 & 74 & 75 \\ 81 & 79 & 81 & 82 & 79 \\ 71 & 69 & 74 & 74 & 69 \end{pmatrix}$$

Height vector
corresponding to
temperature readings

$$H_{\text{vec}} := \begin{pmatrix} 0 \\ 5 \\ 35 \\ 65 \\ 78 \end{pmatrix} \quad (\text{in}) \quad \text{FLBT6} := \begin{pmatrix} 77 & 79 & 82 & 81 & 80 \\ 81 & 79 & 81 & 82 & 81 \\ 112 & 105 & 96 & 94 & 91 \\ 113 & 104 & 96 & 93 & 92 \\ 108 & 94 & 86 & 88 & 84 \\ 95 & 88 & 86 & 85 & 84 \\ 83 & 79 & 82 & 82 & 82 \\ 94 & 87 & 85 & 85 & 83 \\ 109 & 98 & 90 & 89 & 87 \\ 102 & 88 & 85 & 84 & 83 \\ 92 & 87 & 88 & 88 & 85 \\ 73 & 73 & 74 & 74 & 75 \\ 83 & 80 & 81 & 81 & 79 \\ 71 & 69 & 72 & 71 & 68 \end{pmatrix}$$

Input Material Testing Data

$$\alpha := 5.3 \times 10^{-6} \quad \text{taken from Table 5 of NCHRP Report 276}$$

$$t_{\text{emod}} := \begin{pmatrix} 0 \\ 4 \\ 16 \\ 22 \\ 34 \\ 43 \\ 56 \\ 72 \\ 84 \\ 120 \end{pmatrix} \text{ (days)} \quad E_c := \begin{pmatrix} 4759 \\ 4677 \\ 4813 \\ 5099 \\ 4932 \\ 5133 \\ 5222 \\ 5370 \\ 5365 \\ 5160 \end{pmatrix} \text{ (ksi)} \quad E(t) := \begin{cases} \text{for } i \in \Xi \dots \text{last}(t) \\ \text{out}_i \leftarrow \text{interp}(t_{\text{emod}}, E_c, t_i) \\ \text{out} \end{cases}$$

Section Properties

$$H := 78 \quad \text{(in)}$$

$$L := 1942.625 \quad \text{(in)}$$

Section Shape

$$b(z) := \begin{cases} 60 & \text{if } 0 \leq z \leq 3 \\ [60 - 11.75(z - 3)] & \text{if } 3 < z \leq 7 \\ [13 - 2 \cdot (z - 7)] & \text{if } 7 < z \leq 10 \\ 7 & \text{if } 10 < z \leq 60 \\ [7 + 2.1 \cdot (z - 60)] & \text{if } 60 < z \leq 70 \\ 28 & \text{if } 70 < z \leq H \end{cases}$$

$$A := \int_0^H b(z) dz \quad A = 1105.007 \quad \text{(in}^2\text{) Cross-Sectional Area}$$

$$Q_y := \int_0^H z \cdot b(z) dz \quad Q_y = 41563.094 \quad \text{(in}^3\text{) First Moment Area}$$

$$c := \frac{Q_y}{A} \quad c = 37.613 \quad \text{(in) Location of Neutral Axis from top of member}$$

$$I_g := \int_0^H (z - c)^2 \cdot b(z) dz \quad I_g = 935547.485 \quad \text{(in}^4\text{) Gross Moment of Inertia}$$

Calculations

Extract Thermal Gradient and Normalized based on Minimum Measured Temperature Along Profile...

$$T_{\text{vec}}(\text{Beam}) := \left| \begin{array}{l} \text{for } i \in \Xi \dots \text{rows}(\text{Beam}) \\ \quad \left| \begin{array}{l} \min_1 \leftarrow \min(\text{submatrix}(\text{Beam}, i, i, \Xi, \text{cols}(\text{Beam}))) \\ \text{for } j \in \Xi \dots \text{cols}(\text{Beam}) \\ \quad \left| \begin{array}{l} T_{g_{i,j}} \leftarrow \text{Beam}_{i,j} - \min_1 \\ T_{g_{i,j}} \leftarrow T_{g_{i,j}} \text{ if } T_{g_{i,j}} \geq 0 \\ T_{g_{i,j}} \leftarrow 0 \text{ otherwise} \end{array} \right. \\ \text{out}_i \leftarrow \left(\left(\text{submatrix}(T_g, i, i, \Xi, \text{cols}(T_g)) \right) \right)^T \end{array} \right. \\ \text{out} \end{array} \right.$$

Linear Interpolation of Thermal Gradient for variable, z...

$$T_{\text{grad}}(\text{Beam}, z) := \left| \begin{array}{l} \text{for } i \in \Xi \dots \text{rows}(\text{Beam}) \\ \quad \text{out}_i \leftarrow \text{linterp}(H_{\text{vec}}, T_{\text{vec}}(\text{Beam})_i, z) \\ \text{out} \end{array} \right.$$

Example Calculation of Internal Moment Due to Positive Thermal Gradient

$$\text{time} := 8 \quad \text{Beam} := \text{FLBT4}$$

$$T(z) := T_{\text{grad}}(\text{Beam}, z)_{\text{time}} \quad (\text{deg F})$$

$$\sigma_T(z) := -E(t_{\text{camber}})_{\text{time}} \cdot \alpha \cdot T(z) \quad (\text{ksi})$$

$$M_{\text{int}} := \int_0^H \sigma_T(z) \cdot b(z) \cdot (z - c) \, dz \quad M_{\text{int}} = 2.431 \times 10^3 \text{ (kip}\cdot\text{in)}$$

$$\Delta_{\text{corr}} := \frac{-M_{\text{int}} \cdot L^2}{8 \cdot E(t_{\text{camber}})_{\text{time}} \cdot I_g} \quad \Delta_{\text{corr}} = -0.238 \text{ (in)}$$

Analytical Thermal Analysis

--written by Jonathan Sanek, University of Florida Department of Civil and Coastal Engineering

AASHTO Type IV Girder, Pour A

ORIGIN= 1 Ξ = ORIGIN

Input Field Temperature Measurements

$$t_{\text{camber}} := \begin{pmatrix} 0.00 \\ 0.08 \\ 6.98 \\ 14.23 \\ 21.98 \\ 34.02 \\ 40.98 \\ 47.98 \\ 61.90 \\ 62.02 \\ 62.10 \\ 75.02 \\ 91.02 \\ 103.02 \\ 116.98 \\ 137.98 \end{pmatrix} \quad \text{TYPEIV1} := \begin{pmatrix} 83 & 83 & 85 & 88 & 85 \\ 104 & 88 & 87 & 98 & 92 \\ 87 & 85 & 85 & 84 & 82 \\ 117 & 100 & 95 & 96 & 95 \\ 98 & 88 & 87 & 86 & 85 \\ 101 & 90 & 90 & 89 & 88 \\ 92 & 85 & 86 & 86 & 85 \\ 92 & 85 & 86 & 87 & 87 \\ 79 & 82 & 83 & 82 & 79 \\ 95 & 87 & 87 & 88 & 89 \\ 107 & 91 & 90 & 90 & 91 \\ 93 & 86 & 87 & 87 & 84 \\ 94 & 86 & 86 & 86 & 86 \\ 75 & 74 & 75 & 75 & 75 \\ 88 & 84 & 85 & 84 & 80 \\ 81 & 74 & 74 & 73 & 70 \end{pmatrix} \quad \text{TYPEIV2} := \begin{pmatrix} 87 & 85 & 88 & 93 & 87 \\ 105 & 87 & 85 & 86 & 87 \\ 92 & 84 & 84 & 89 & 84 \\ 120 & 99 & 96 & 103 & 96 \\ 93 & 88 & 88 & 86 & 84 \\ 101 & 93 & 92 & 89 & 88 \\ 87 & 82 & 82 & 82 & 80 \\ 93 & 85 & 86 & 87 & 87 \\ 79 & 82 & 83 & 82 & 79 \\ 93 & 84 & 85 & 85 & 86 \\ 107 & 91 & 89 & 90 & 91 \\ 94 & 86 & 86 & 86 & 84 \\ 92 & 86 & 86 & 86 & 86 \\ 75 & 74 & 75 & 75 & 75 \\ 89 & 84 & 84 & 84 & 80 \\ 78 & 76 & 76 & 75 & 70 \end{pmatrix}$$

*Height vector
corresponding to
temperature readings*

$$H_{\text{vec}} := \begin{pmatrix} 0 \\ 11.02 \\ 25.51 \\ 41.5 \\ 54.02 \end{pmatrix} \text{ (in)} \quad \text{TYPEIV3} := \begin{pmatrix} 86 & 84 & 87 & 95 & 89 \\ 104 & 88 & 85 & 84 & 87 \\ 95 & 87 & 86 & 84 & 84 \\ 116 & 103 & 99 & 105 & 100 \\ 95 & 89 & 89 & 87 & 84 \\ 101 & 88 & 88 & 88 & 88 \\ 90 & 81 & 80 & 80 & 80 \\ 92 & 86 & 86 & 87 & 87 \\ 78 & 82 & 83 & 82 & 79 \\ 96 & 86 & 85 & 84 & 85 \\ 109 & 91 & 89 & 90 & 91 \\ 96 & 87 & 86 & 86 & 84 \\ 93 & 86 & 85 & 85 & 86 \\ 75 & 74 & 74 & 75 & 75 \\ 88 & 82 & 84 & 82 & 80 \\ 77 & 72 & 72 & 71 & 70 \end{pmatrix}$$

Input Material Testing Data

$$\alpha := 5.3 \times 10^{-6} \quad \text{taken from Table 5 of NCHRP Report 276}$$

$$t_{\text{emod}} := \begin{pmatrix} 0 \\ 7 \\ 14 \\ 21 \\ 34 \\ 40 \\ 61 \\ 74 \\ 102 \\ 138 \end{pmatrix} \text{ (days)} \quad E_c := \begin{pmatrix} 4506 \\ 4911 \\ 5390 \\ 5191 \\ 5456 \\ 5830 \\ 5886 \\ 5672 \\ 5853 \\ 5887 \end{pmatrix} \text{ (ksi)} \quad E(t) := \begin{cases} \text{for } i \in \Xi \dots \text{last}(t) \\ \text{out}_i \leftarrow \text{interp}(t_{\text{emod}}, E_c, t_i) \\ \text{out} \end{cases}$$

Section Properties

$$H := 54.02 \quad (\text{in})$$

$$L := 1092.32 \quad (\text{in})$$

Section Shape

$$b(z) := \begin{cases} 20.08 & \text{if } 0 \leq z \leq 8.03 \\ [20.08 - 2.015(z - 8.03)] & \text{if } 8.03 < z \leq 14.01 \\ 8.03 & \text{if } 14.01 < z \leq 37 \\ [8.03 + 2 \cdot (z - 37)] & \text{if } 37 < z \leq 45.98 \\ 28 & \text{if } 45.98 < z \leq H \end{cases}$$

$$A := \int_0^H b(z) dz \quad A = 807.739 \quad (\text{in}^2) \text{ Cross-Sectional Area}$$

$$Q_y := \int_0^H z \cdot b(z) dz \quad Q_y = 23960.324 \quad (\text{in}^3) \text{ First Moment Area}$$

$$c := \frac{Q_y}{A} \quad c = 29.663 \quad (\text{in}) \text{ Location of Neutral Axis from top of member}$$

$$I_g := \int_0^H (z - c)^2 \cdot b(z) dz \quad I_g = 268621.613 \quad (\text{in}^4) \text{ Gross Moment of Inertia}$$

Calculations

Extract Thermal Gradient and Normalized based on Minimum Measured Temperature Along Profile...

$$T_{\text{vec}}(\text{Beam}) := \left| \begin{array}{l} \text{for } i \in \Xi \dots \text{rows}(\text{Beam}) \\ \quad \left| \begin{array}{l} \min_i \leftarrow \min(\text{submatrix}(\text{Beam}, i, i, \Xi, \text{cols}(\text{Beam}))) \\ \text{for } j \in \Xi \dots \text{cols}(\text{Beam}) \\ \quad \left| \begin{array}{l} T_{g_{i,j}} \leftarrow \text{Beam}_{i,j} - \min_i \\ T_{g_{i,j}} \leftarrow T_{g_{i,j}} \text{ if } T_{g_{i,j}} \geq 0 \\ T_{g_{i,j}} \leftarrow 0 \text{ otherwise} \end{array} \right. \\ \text{out}_i \leftarrow \left(\left(\text{submatrix}(T_g, i, i, \Xi, \text{cols}(T_g)) \right) \right)^T \end{array} \right. \\ \text{out} \end{array} \right.$$

Linear Interpolation of Thermal Gradient for variable, z...

$$T_{\text{grad}}(\text{Beam}, z) := \left| \begin{array}{l} \text{for } i \in \Xi \dots \text{rows}(\text{Beam}) \\ \quad \left| \begin{array}{l} \text{out}_i \leftarrow \text{linterp}(H_{\text{vec}}, T_{\text{vec}}(\text{Beam})_i, z) \end{array} \right. \\ \text{out} \end{array} \right.$$

Example Calculation of Internal Moment Due to Positive Thermal Gradient

$$\text{time} := 12 \quad \text{Beam} := \text{TYPEIV1}$$

$$T(z) := T_{\text{grad}}(\text{Beam}, z)_{\text{time}} \quad (\text{deg F})$$

$$\sigma_T(z) := -E(t_{\text{camber}})_{\text{time}} \cdot \alpha \cdot T(z) \quad (\text{ksi})$$

$$M_{\text{int}} := \int_0^H \sigma_T(z) \cdot b(z) \cdot (z - c) \, dz \quad M_{\text{int}} = 732.438 \quad (\text{kip}\cdot\text{in})$$

$$\Delta_{\text{corr}} := \frac{-M_{\text{int}} \cdot L^2}{8 \cdot E(t_{\text{camber}})_{\text{time}} \cdot I_g} \quad \Delta_{\text{corr}} = -0.072 \quad (\text{in})$$

Analytical Thermal Analysis

--written by Jonathan Sanek, University of Florida Department of Civil and Coastal Engineering

AASHTO Type V Girder, Pour A

ORIGIN = 1 Ξ = ORIGIN

Input Field Temperature Measurements

$$t_{\text{camber}} := \begin{pmatrix} 0.00 \\ 0.04 \\ 7.00 \\ 14.00 \\ 21.00 \\ 21.08 \\ 21.17 \\ 28.00 \end{pmatrix} \quad \text{TYPEV1} := \begin{pmatrix} 82 & 79 & 80 & 79 & 79 \\ 89 & 82 & 82 & 82 & 82 \\ 88 & 83 & 85 & 86 & 83 \\ 74 & 73 & 74 & 74 & 74 \\ 81 & 77 & 78 & 78 & 75 \\ 91 & 82 & 80 & 80 & 78 \\ 103 & 88 & 82 & 81 & 80 \\ 76 & 72 & 73 & 72 & 71 \end{pmatrix} \quad \text{TYPEV2} := \begin{pmatrix} 81 & 78 & 79 & 79 & 79 \\ 89 & 82 & 82 & 82 & 83 \\ 89 & 82 & 85 & 85 & 83 \\ 74 & 73 & 74 & 74 & 74 \\ 79 & 77 & 79 & 81 & 75 \\ 89 & 82 & 82 & 81 & 78 \\ 100 & 86 & 82 & 81 & 80 \\ 71 & 71 & 73 & 75 & 71 \end{pmatrix}$$

Height vector
corresponding to
temperature readings

$$H_{\text{vec}} := \begin{pmatrix} 0 \\ 8.5 \\ 28.5 \\ 50 \\ 63 \end{pmatrix} \text{ (in)} \quad \text{TYPEV3} := \begin{pmatrix} 78 & 80 & 80 & 80 & 80 \\ 87 & 82 & 83 & 83 & 83 \\ 87 & 82 & 84 & 84 & 83 \\ 74 & 73 & 73 & 74 & 74 \\ 81 & 76 & 78 & 77 & 75 \\ 91 & 82 & 80 & 80 & 78 \\ 102 & 86 & 83 & 82 & 80 \\ 76 & 71 & 74 & 73 & 71 \end{pmatrix} \quad \text{TYPEV4} := \begin{pmatrix} 79 & 78 & 80 & 79 & 79 \\ 90 & 82 & 83 & 82 & 81 \\ 88 & 82 & 85 & 84 & 82 \\ 74 & 72 & 73 & 74 & 74 \\ 80 & 76 & 77 & 76 & 75 \\ 87 & 80 & 79 & 79 & 78 \\ 99 & 86 & 82 & 81 & 80 \\ 71 & 71 & 74 & 74 & 71 \end{pmatrix}$$

Input Material Testing Data

$\alpha := 5.3 \times 10^{-6}$ taken from Table 5 of NCHRP Report 276

$$t_{\text{emod}} := \begin{pmatrix} 0 \\ 7 \\ 14 \\ 22 \\ 28 \end{pmatrix} \text{ (days)} \quad E_c := \begin{pmatrix} 4909 \\ 5130 \\ 5361 \\ 5419 \\ 5323 \end{pmatrix} \text{ (ksi)} \quad E(t) := \begin{cases} \text{for } i \in \Xi \dots \text{last}(t) \\ \text{out}_i \leftarrow \text{linterp}(t_{\text{emod}}, E_c, t_i) \\ \text{out} \end{cases}$$

Section Properties

$$H := 63 \quad (\text{in})$$

$$L := 972.625 \quad (\text{in})$$

Section Shape

$$b(z) := \begin{cases} 42 & \text{if } 0 \leq z \leq 5 \\ [42 - 8.667 \cdot (z - 5)] & \text{if } 5 < z \leq 8 \\ [16 - 2 \cdot (z - 8)] & \text{if } 8 < z \leq 12 \\ 8 & \text{if } 12 < z \leq 45 \\ [8 + 2 \cdot (z - 45)] & \text{if } 45 < z \leq 55 \\ 28 & \text{if } 55 < z \leq H \end{cases}$$

$$A := \int_0^H b(z) \, dz \quad A = 1013.107 \quad (\text{in}^2) \text{ Cross-Sectional Area}$$

$$Q_y := \int_0^H z \cdot b(z) \, dz \quad Q_y = 31446.978 \quad (\text{in}^3) \text{ First Moment Area}$$

$$c := \frac{Q_y}{A} \quad c = 31.04 \quad (\text{in}) \text{ Location of Neutral Axis from top of member}$$

$$I_g := \int_0^H (z - c)^2 \cdot b(z) \, dz \quad I_g = 521157.365 \quad (\text{in}^4) \text{ Gross Moment of Inertia}$$

Calculations

Extract Thermal Gradient and Normalized based on Minimum Measured Temperature Along Profile...

$$T_{\text{vec}}(\text{Beam}) := \left| \begin{array}{l} \text{for } i \in \Xi \dots \text{rows}(\text{Beam}) \\ \quad \left| \begin{array}{l} \min_i \leftarrow \min(\text{submatrix}(\text{Beam}, i, i, \Xi, \text{cols}(\text{Beam}))) \\ \text{for } j \in \Xi \dots \text{cols}(\text{Beam}) \\ \quad \left| \begin{array}{l} T_{g_{i,j}} \leftarrow \text{Beam}_{i,j} - \min_i \\ T_{g_{i,j}} \leftarrow T_{g_{i,j}} \text{ if } T_{g_{i,j}} \geq 0 \\ T_{g_{i,j}} \leftarrow 0 \text{ otherwise} \end{array} \right. \\ \text{out}_i \leftarrow \left(\left(\text{submatrix}(T_g, i, i, \Xi, \text{cols}(T_g)) \right) \right)^T \end{array} \right. \\ \text{out} \end{array} \right.$$

Linear Interpolation of Thermal Gradient for variable, z...

$$T_{\text{grad}}(\text{Beam}, z) := \left| \begin{array}{l} \text{for } i \in \Xi \dots \text{rows}(\text{Beam}) \\ \quad \text{out}_i \leftarrow \text{linterp}(H_{\text{vec}}, T_{\text{vec}}(\text{Beam})_i, z) \\ \text{out} \end{array} \right.$$

Example Calculation of Internal Moment Due to Positive Thermal Gradient

$$\text{time} := 6 \quad \text{Beam} := \text{TYPEV1}$$

$$T(z) := T_{\text{grad}}(\text{Beam}, z)_{\text{time}} \quad (\text{deg F})$$

$$\sigma_T(z) := -E(t_{\text{camber}})_{\text{time}} \cdot \alpha \cdot T(z) \quad (\text{ksi})$$

$$M_{\text{int}} := \int_0^H \sigma_T(z) \cdot b(z) \cdot (z - c) \, dz \quad M_{\text{int}} = 2.103 \times 10^3 \quad (\text{kip} \cdot \text{in})$$

$$\Delta_{\text{corr}} := \frac{-M_{\text{int}} \cdot L^2}{8 \cdot E(t_{\text{camber}})_{\text{time}} \cdot I_g} \quad \Delta_{\text{corr}} = -0.088 \quad (\text{in})$$

Analytical Thermal Analysis

--written by Jonathan Sanek, University of Florida Department of Civil and Coastal Engineering

AASHTO Type V Girder, Pour B

ORIGIN = 1 Ξ = ORIGIN

Input Field Temperature Measurements

$$t_{\text{camber}} := \begin{pmatrix} 0.00 \\ 0.04 \\ 7.00 \\ 14.00 \\ 21.00 \\ 21.08 \\ 21.17 \\ 28.00 \end{pmatrix} \quad \text{TYPEV1} := \begin{pmatrix} 82 & 79 & 80 & 79 & 79 \\ 89 & 82 & 82 & 82 & 82 \\ 88 & 83 & 85 & 86 & 83 \\ 74 & 73 & 74 & 74 & 74 \\ 81 & 77 & 78 & 78 & 75 \\ 91 & 82 & 80 & 80 & 78 \\ 103 & 88 & 82 & 81 & 80 \\ 76 & 72 & 73 & 72 & 71 \end{pmatrix} \quad \text{TYPEV2} := \begin{pmatrix} 81 & 78 & 79 & 79 & 79 \\ 89 & 82 & 82 & 82 & 83 \\ 89 & 82 & 85 & 85 & 83 \\ 74 & 73 & 74 & 74 & 74 \\ 79 & 77 & 79 & 81 & 75 \\ 89 & 82 & 82 & 81 & 78 \\ 100 & 86 & 82 & 81 & 80 \\ 71 & 71 & 73 & 75 & 71 \end{pmatrix}$$

Height vector
corresponding to
temperature readings

$$H_{\text{vec}} := \begin{pmatrix} 0 \\ 8.5 \\ 28.5 \\ 50 \\ 63 \end{pmatrix} \text{ (in)} \quad \text{TYPEV3} := \begin{pmatrix} 78 & 80 & 80 & 80 & 80 \\ 87 & 82 & 83 & 83 & 83 \\ 87 & 82 & 84 & 84 & 83 \\ 74 & 73 & 73 & 74 & 74 \\ 81 & 76 & 78 & 77 & 75 \\ 91 & 82 & 80 & 80 & 78 \\ 102 & 86 & 83 & 82 & 80 \\ 76 & 71 & 74 & 73 & 71 \end{pmatrix} \quad \text{TYPEV4} := \begin{pmatrix} 79 & 78 & 80 & 79 & 79 \\ 90 & 82 & 83 & 82 & 81 \\ 88 & 82 & 85 & 84 & 82 \\ 74 & 72 & 73 & 74 & 74 \\ 80 & 76 & 77 & 76 & 75 \\ 87 & 80 & 79 & 79 & 78 \\ 99 & 86 & 82 & 81 & 80 \\ 71 & 71 & 74 & 74 & 71 \end{pmatrix}$$

Input Material Testing Data

$\alpha := 5.3 \times 10^{-6}$ taken from Table 5 of NCHRP Report 276

$$t_{\text{emod}} := \begin{pmatrix} 0 \\ 7 \\ 14 \\ 22 \\ 28 \end{pmatrix} \text{ (days)} \quad E_c := \begin{pmatrix} 4796 \\ 5164 \\ 5331 \\ 5466 \\ 5313 \end{pmatrix} \text{ (ksi)} \quad E(t) := \begin{cases} \text{for } i \in \Xi \dots \text{last}(t) \\ \text{out}_i \leftarrow \text{linterp}(t_{\text{emod}}, E_c, t_i) \\ \text{out} \end{cases}$$

Section Properties

$$H := 63 \quad (\text{in})$$

$$L := 972.625 \quad (\text{in})$$

Section Shape

$$b(z) := \begin{cases} 42 & \text{if } 0 \leq z \leq 5 \\ [42 - 8.667 \cdot (z - 5)] & \text{if } 5 < z \leq 8 \\ [16 - 2 \cdot (z - 8)] & \text{if } 8 < z \leq 12 \\ 8 & \text{if } 12 < z \leq 45 \\ [8 + 2 \cdot (z - 45)] & \text{if } 45 < z \leq 55 \\ 28 & \text{if } 55 < z \leq H \end{cases}$$

$$A := \int_0^H b(z) dz \quad A = 1013.107 \quad (\text{in}^2) \text{ Cross-Sectional Area}$$

$$Q_y := \int_0^H z \cdot b(z) dz \quad Q_y = 31446.978 \quad (\text{in}^3) \text{ First Moment Area}$$

$$c := \frac{Q_y}{A} \quad c = 31.04 \quad (\text{in}) \text{ Location of Neutral Axis from top of member}$$

$$I_g := \int_0^H (z - c)^2 \cdot b(z) dz \quad I_g = 521157.365 \quad (\text{in}^4) \text{ Gross Moment of Inertia}$$

Calculations

Extract Thermal Gradient and Normalized based on Minimum Measured Temperature Along Profile...

$$T_{\text{vec}}(\text{Beam}) := \left| \begin{array}{l} \text{for } i \in \Xi \dots \text{rows}(\text{Beam}) \\ \quad \left| \begin{array}{l} \min_i \leftarrow \min(\text{submatrix}(\text{Beam}, i, i, \Xi, \text{cols}(\text{Beam}))) \\ \text{for } j \in \Xi \dots \text{cols}(\text{Beam}) \\ \quad \left| \begin{array}{l} T_{g_{i,j}} \leftarrow \text{Beam}_{i,j} - \min_i \\ T_{g_{i,j}} \leftarrow T_{g_{i,j}} \text{ if } T_{g_{i,j}} \geq 0 \\ T_{g_{i,j}} \leftarrow 0 \text{ otherwise} \end{array} \right. \\ \text{out}_i \leftarrow \left(\left(\text{submatrix}(T_g, i, i, \Xi, \text{cols}(T_g)) \right) \right)^T \end{array} \right. \\ \text{out} \end{array} \right.$$

Linear Interpolation of Thermal Gradient for variable, z...

$$T_{\text{grad}}(\text{Beam}, z) := \left| \begin{array}{l} \text{for } i \in \Xi \dots \text{rows}(\text{Beam}) \\ \quad \text{out}_i \leftarrow \text{linterp}(H_{\text{vec}}, T_{\text{vec}}(\text{Beam})_i, z) \\ \text{out} \end{array} \right.$$

Example Calculation of Internal Moment Due to Positive Thermal Gradient

$$\text{time} := 6 \quad \text{Beam} := \text{TYPEV4}$$

$$T(z) := T_{\text{grad}}(\text{Beam}, z)_{\text{time}} \quad (\text{deg F})$$

$$\sigma_T(z) := -E(t_{\text{camber}})_{\text{time}} \cdot \alpha \cdot T(z) \quad (\text{ksi})$$

$$M_{\text{int}} := \int_0^H \sigma_T(z) \cdot b(z) \cdot (z - c) \, dz \quad M_{\text{int}} = 1.41 \times 10^3 \quad (\text{kip} \cdot \text{in})$$

$$\Delta_{\text{corr}} := \frac{-M_{\text{int}} \cdot L^2}{8 \cdot E(t_{\text{camber}})_{\text{time}} \cdot I_g} \quad \Delta_{\text{corr}} = -0.059 \quad (\text{in})$$

APPENDIX E
TABULATED AMBIENT DATA

2

Year	Month	Day	Hour	Temp (°C) (60 cm)	Temp (°F) (60 cm)	Temp (°C) (200 cm)	Temp (°F) (200 cm)	RH (%)	SOLRD (W/m2)
2004	4	9	0	19.07	66.33	19.47	67.05	95	0
2004	4	9	1	18.96	66.13	19.32	66.78	96	0
2004	4	9	2	18.94	66.09	19.23	66.61	96	0
2004	4	9	3	19.15	66.47	19.36	66.85	96	0
2004	4	9	4	19.14	66.45	19.32	66.78	96	0
2004	4	9	5	19.09	66.36	19.32	66.78	95	0
2004	4	9	6	19.17	66.51	19.37	66.87	95	12
2004	4	9	7	19.57	67.23	19.70	67.46	93	77
2004	4	9	8	21.01	69.82	20.88	69.58	87	288
2004	4	9	9	22.11	71.80	21.78	71.20	81	329
2004	4	9	10	23.74	74.73	23.14	73.65	74	622
2004	4	9	11	25.70	78.26	24.81	76.66	65	760
2004	4	9	12	26.57	79.83	25.84	78.51	61	825
2004	4	9	13	26.82	80.28	26.60	79.88	55	577
2004	4	9	14	27.89	82.20	27.50	81.50	51	637
2004	4	9	15	28.99	84.18	28.68	83.62	43	685
2004	4	9	16	28.93	84.07	29.20	84.56	39	490
2004	4	9	17	28.75	83.75	29.12	84.42	35	286
2004	4	9	18	26.50	79.70	27.10	80.78	42	82
2004	4	9	19	23.25	73.85	24.07	75.33	59	0
2004	4	9	20	21.54	70.77	22.46	72.43	71	0
2004	4	9	21	19.80	67.64	20.71	69.28	76	0
2004	4	9	22	18.73	65.71	19.55	67.19	84	0
2004	4	9	23	17.82	64.08	18.45	65.21	90	0

Bulb-Tee A At Release

² Highlighted entries are when field measurements were made (▨ 78" Bulb-Tee A, ▩ 78" Bulb-Tee B, ▧ AASHTO Type IV A, ▦ AASHTO V A and B, and ▨ All Girders)

Year	Month	Day	Hour	Temp (°C) (60 cm)	Temp (°F) (60 cm)	Temp (°C) (200 cm)	Temp (°F) (200 cm)	RH (%)	SOLRD (W/m2)	
2004	4	16	0	9.70	49.46	10.10	50.18	83	0	Bulb-Tee A 7-Day Reading
2004	4	16	1	8.38	47.08	8.71	47.68	89	0	
2004	4	16	2	7.68	45.82	8.06	46.51	91	0	
2004	4	16	3	7.23	45.01	7.48	45.46	92	0	
2004	4	16	4	6.93	44.47	7.15	44.87	92	0	
2004	4	16	5	6.82	44.28	7.07	44.73	93	0	
2004	4	16	6	7.31	45.16	7.37	45.27	94	35	
2004	4	16	7	13.27	55.89	12.44	54.39	85	222	
2004	4	16	8	18.23	64.81	17.57	63.63	59	447	
2004	4	16	9	20.86	69.55	19.97	67.95	48	649	
2004	4	16	10	21.82	71.28	20.94	69.69	46	747	
2004	4	16	11	22.74	72.93	22.00	71.60	45	874	
2004	4	16	12	23.85	74.93	23.02	73.44	44	945	
2004	4	16	13	24.72	76.50	23.94	75.09	42	950	
2004	4	16	14	25.20	77.36	24.59	76.26	39	903	
2004	4	16	15	24.78	76.60	24.44	75.99	40	659	
2004	4	16	16	24.24	75.63	24.26	75.67	40	530	
2004	4	16	17	23.59	74.46	23.66	74.59	40	299	
2004	4	16	18	22.14	71.85	22.45	72.41	46	84	
2004	4	16	19	20.38	68.68	20.84	69.51	53	1	
2004	4	16	20	19.18	66.52	19.68	67.42	59	0	
2004	4	16	21	18.12	64.62	18.62	65.52	66	0	
2004	4	16	22	17.16	62.89	17.66	63.79	70	0	
2004	4	16	23	16.95	62.51	17.43	63.37	72	0	
2004	4	23	0	18.36	65.05	18.99	66.18	85	0	
2004	4	23	1	17.07	62.73	17.64	63.75	90	0	
2004	4	23	2	16.90	62.42	17.36	63.25	92	0	
2004	4	23	3	17.70	63.86	18.28	64.90	92	0	
2004	4	23	4	17.85	64.13	18.32	64.98	92	0	
2004	4	23	5	17.71	63.88	18.22	64.80	93	0	
2004	4	23	6	17.19	62.94	17.48	63.46	94	39	
2004	4	23	7	20.78	69.40	20.40	68.72	88	210	
2004	4	23	8	23.79	74.82	23.30	73.94	76	438	
2004	4	23	9	25.97	78.75	25.35	77.63	64	634	
2004	4	23	10	27.50	81.50	26.75	80.15	53	845	
2004	4	23	11	28.35	83.03	27.44	81.39	46	945	
2004	4	23	12	29.06	84.31	28.12	82.62	41	833	
2004	4	23	13	29.90	85.82	28.77	83.79	39	899	
2004	4	23	14	29.91	85.84	28.98	84.16	39	821	
2004	4	23	15	29.61	85.30	29.04	84.27	41	687	
2004	4	23	16	29.21	84.58	29.07	84.33	40	461	
2004	4	23	17	29.09	84.36	28.97	84.15	40	312	
2004	4	23	18	27.87	82.17	28.17	82.71	43	101	
2004	4	23	19	25.42	77.76	25.98	78.76	48	2	
2004	4	23	20	23.72	74.70	24.25	75.65	54	0	
2004	4	23	21	22.18	71.92	22.77	72.99	62	0	
2004	4	23	22	20.72	69.30	21.35	70.43	70	0	
2004	4	23	23	19.86	67.75	20.48	68.86	78	0	
										Bulb-Tee A 14-Day Reading

³Highlighted entries are when field measurements were made (78" Bulb-Tee A, 78" Bulb-Tee B, AASHTO Type IV A, AASHTO V A and B, and All Girders)

4

Year	Month	Day	Hour	Temp (°C) (60 cm)	Temp (°F) (60 cm)	Temp (°C) (200 cm)	Temp (°F) (200 cm)	RH (%)	SOLRD (W/m2)	
2004	4	29	0	19.81	67.66	20.26	68.47	72	0	Bulb-Tee A 20-Day Reading
2004	4	29	1	19.71	67.48	20.14	68.25	71	0	
2004	4	29	2	19.38	66.88	19.88	67.78	76	0	
2004	4	29	3	19.36	66.85	19.81	67.66	77	0	
2004	4	29	4	19.71	67.48	20.10	68.18	74	0	
2004	4	29	5	19.89	67.80	20.28	68.50	75	0	
2004	4	29	6	19.91	67.84	20.23	68.41	76	52	
2004	4	29	7	20.87	69.57	20.90	69.62	75	223	
2004	4	29	8	23.15	73.67	22.97	73.35	67	459	
2004	4	29	9	25.01	77.02	24.79	76.62	59	596	
2004	4	29	10	26.70	80.06	26.24	79.23	56	766	
2004	4	29	11	27.58	81.64	27.16	80.89	54	644	
2004	4	29	12	27.25	81.05	27.06	80.71	54	395	
2004	4	29	13	27.53	81.55	27.32	81.18	53	431	
2004	4	29	14	26.77	80.19	26.74	80.13	56	313	
2004	4	29	15	26.24	79.23	26.26	79.27	60	255	
2004	4	29	16	26.17	79.11	26.16	79.09	62	312	
2004	4	29	17	25.25	77.45	25.44	77.79	67	128	
2004	4	29	18	24.09	75.36	24.36	75.85	73	46	
2004	4	29	19	23.33	73.99	23.69	74.64	76	1	
2004	4	29	20	22.88	73.18	23.22	73.80	79	0	
2004	4	29	21	22.90	73.22	23.18	73.72	81	0	
2004	4	29	22	22.58	72.64	22.89	73.20	85	0	
2004	4	29	23	22.31	72.16	22.60	72.68	87	0	
2004	4	30	0	22.12	71.82	22.40	72.32	88	0	
2004	5	7	0	18.60	65.48	19.31	66.76	84	0	Bulb-Tee A 28-Day Reading
2004	5	7	1	18.03	64.45	18.58	65.44	88	0	
2004	5	7	2	17.68	63.82	18.20	64.76	91	0	
2004	5	7	3	17.21	62.98	17.73	63.91	92	0	
2004	5	7	4	16.59	61.86	16.97	62.55	94	0	
2004	5	7	5	16.28	61.30	16.66	61.99	95	0	
2004	5	7	6	16.84	62.31	17.00	62.60	95	53	
2004	5	7	7	20.90	69.62	20.68	69.22	88	200	
2004	5	7	8	23.75	74.75	23.45	74.21	73	470	
2004	5	7	9	26.36	79.45	25.79	78.42	60	648	
2004	5	7	10	27.54	81.57	26.95	80.51	52	799	
2004	5	7	11	28.77	83.79	28.06	82.51	47	904	
2004	5	7	12	29.43	84.97	28.70	83.66	41	942	
2004	5	7	13	29.89	85.80	29.15	84.47	40	912	
2004	5	7	14	30.53	86.95	29.89	85.80	38	829	
2004	5	7	15	30.52	86.94	30.21	86.38	38	688	
2004	5	7	16	30.85	87.53	30.64	87.15	35	539	
2004	5	7	17	30.80	87.44	30.82	87.48	34	336	
2004	5	7	18	30.09	86.16	30.47	86.85	38	128	
2004	5	7	19	27.17	80.91	27.88	82.18	47	3	
2004	5	7	20	24.93	76.87	25.60	78.08	53	0	
2004	5	7	21	23.54	74.37	24.17	75.51	58	0	
2004	5	7	22	21.88	71.38	22.73	72.91	63	0	
2004	5	7	23	20.18	68.32	20.99	69.78	74	0	
2004	5	8	0	19.83	67.69	20.66	69.19	74	0	

⁴Highlighted entries are when field measurements were made (▨ 78" Bulb-Tee A, ▩ 78" Bulb-Tee B, ▧ AASHTO Type IV A, ▦ AASHTO V A and B, and ▨ All Girders)

5

Year	Month	Day	Hour	Temp (°C) (60 cm)	Temp (°F) (60 cm)	Temp (°C) (200 cm)	Temp (°F) (200 cm)	RH (%)	SOLRD (W/m ²)	
2004	5	21	0	20.87	69.57	21.58	70.84	82	0	
2004	5	21	1	19.00	66.20	19.51	67.12	89	0	
2004	5	21	2	18.60	65.48	19.07	66.33	91	0	
2004	5	21	3	17.97	64.35	18.45	65.21	92	0	
2004	5	21	4	17.30	63.14	17.69	63.84	93	0	
2004	5	21	5	16.97	62.55	17.34	63.21	94	1	
2004	5	21	6	18.35	65.03	18.35	65.03	93	68	
2004	5	21	7	23.63	74.53	23.36	74.05	83	251	
2004	5	21	8	25.18	77.32	24.91	76.84	76	467	
2004	5	21	9	26.49	79.68	26.10	78.98	66	556	
2004	5	21	10	28.13	82.63	27.42	81.36	56	829	
2004	5	21	11	29.74	85.53	28.67	83.61	44	952	
2004	5	21	12	30.32	86.58	29.33	84.79	44	923	
2004	5	21	13	31.26	88.27	30.13	86.23	40	970	
2004	5	21	14	31.64	88.95	30.78	87.40	36	764	
2004	5	21	15	31.81	89.26	31.34	88.41	37	731	
2004	5	21	16	31.91	89.44	31.56	88.81	37	567	
2004	5	21	17	31.23	88.21	31.17	88.11	42	332	
2004	5	21	18	28.91	84.04	29.30	84.74	50	81	
2004	5	21	19	27.03	80.65	27.61	81.70	57	9	
2004	5	21	20	25.20	77.36	25.78	78.40	65	0	
2004	5	21	21	24.00	75.20	24.56	76.21	71	0	
2004	5	21	22	23.16	73.69	23.67	74.61	77	0	
2004	5	21	23	22.25	72.05	22.89	73.20	81	0	
2004	5	22	0	21.72	71.10	22.45	72.41	84	0	
2004	6	7	0	21.7	71.06	22.32	72.18	89	0	
2004	6	7	1	20.98	69.76	21.53	70.75	92	0	
2004	6	7	2	20.57	69.03	21.07	69.93	94	0	
2004	6	7	3	20.36	68.65	20.85	69.53	95	0	
2004	6	7	4	20.39	68.70	20.91	69.64	96	0	
2004	6	7	5	20.18	68.32	20.72	69.30	96	2	
2004	6	7	6	21.56	70.81	21.74	71.13	96	92	
2004	6	7	7	24.47	76.05	24.17	75.51	85	242	
2004	6	7	8	26.66	79.99	26.32	79.38	73	466	
2004	6	7	9	28.11	82.60	27.73	81.91	65	642	
2004	6	7	10	29.66	85.39	29.11	84.40	60	784	
2004	6	7	11	30.82	87.48	30.03	86.05	57	899	
2004	6	7	12	31.8	89.24	31.04	87.87	53	728	
2004	6	7	13	32.34	90.21	31.77	89.19	50	266	
2004	6	7	14	32.7	90.86	32.32	90.18	46	582	
2004	6	7	15	31.22	88.20	31.52	88.74	48	163	
2004	6	7	16	28.6	83.48	29.06	84.31	58	106	
2004	6	7	17	27.43	81.37	27.54	81.57	65	181	
2004	6	7	18	24.78	76.60	25.07	77.13	78	97	
2004	6	7	19	22.09	71.76	22.43	72.37	89	4	
2004	6	7	20	21.82	71.28	22.16	71.89	92	0	
2004	6	7	21	21.87	71.37	22.31	72.16	89	0	
2004	6	7	22	21.78	71.20	22.29	72.12	90	0	
2004	6	7	23	21.55	70.79	22.01	71.62	92	0	
2004	6	8	0	21.44	70.59	21.92	71.46	92	0	

Bulb-Tee A 42-Day Reading

Bulb-Tee A 59-Day Reading

⁵Highlighted entries are when field measurements were made (▨ 78" Bulb-Tee A, ▩ 78" Bulb-Tee B, ▧ AASHTO Type IV A, ▦ AASHTO V A and B, and ▨ All Girders)

6

Year	Month	Day	Hour	Temp (°C) (60 cm)	Temp (°F) (60 cm)	Temp (°C) (200 cm)	Temp (°F) (200 cm)	RH (%)	SOLRD (W/m ²)	
2004	6	10	0	22.74	72.93	23.06	73.51	97	0	Type IV Release
2004	6	10	1	22.36	72.25	22.74	72.93	97	0	
2004	6	10	2	22.4	72.32	22.74	72.93	98	0	
2004	6	10	3	22.42	72.36	22.77	72.99	98	0	
2004	6	10	4	22.42	72.36	22.78	73.00	98	0	
2004	6	10	5	22.24	72.03	22.63	72.73	98	1	
2004	6	10	6	23.19	73.74	23.32	73.98	98	93	
2004	6	10	7	25.76	78.37	24.78	76.60	92	312	
2004	6	10	8	27.52	81.54	27.09	80.76	74	493	
2004	6	10	9	28.71	83.68	28.33	82.99	71	668	
2004	6	10	10	29.56	85.21	29.24	84.63	66	787	
2004	6	10	11	30.41	86.74	30.02	86.04	62	690	
2004	6	10	12	30.56	87.01	30.26	86.47	60	499	
2004	6	10	13	32.04	89.67	31.45	88.61	55	237	
2004	6	10	14	32.91	91.24	32.38	90.28	51	736	
2004	6	10	15	27.76	81.97	28.3	82.94	67	86	
2004	6	10	16	25.4	77.72	25.72	78.30	78	37	
2004	6	10	17	25.65	78.17	25.96	78.73	75	45	
2004	6	10	18	24.92	76.86	25.26	77.47	82	36	
2004	6	10	19	24.18	75.52	24.52	76.14	83	8	
2004	6	10	20	23.35	74.03	23.72	74.70	87	0	
2004	6	10	21	23.07	73.53	23.43	74.17	88	0	
2004	6	10	22	22.57	72.63	23.01	73.42	89	0	
2004	6	10	23	22.09	71.76	22.51	72.52	91	0	
2004	6	11	0	21.83	71.29	22.23	72.01	93	0	
2004	6	17	0	24.68	76.42	25.21	77.38	83	0	
2004	6	17	1	24.24	75.63	24.74	76.53	85	0	
2004	6	17	2	23.61	74.50	24.18	75.52	88	0	
2004	6	17	3	22.75	72.95	23.31	73.96	91	0	
2004	6	17	4	22.81	73.06	23.4	74.12	93	0	
2004	6	17	5	23.38	74.08	23.92	75.06	91	3	
2004	6	17	6	24.41	75.94	24.65	76.37	89	77	
2004	6	17	7	26.35	79.43	26.3	79.34	81	268	
2004	6	17	8	27.57	81.63	27.48	81.46	74	464	
2004	6	17	9	28.45	83.21	28.27	82.89	68	707	
2004	6	17	10	29.18	84.52	29.01	84.22	62	624	
2004	6	17	11	30.33	86.59	30.01	86.02	56	734	
2004	6	17	12	31.27	88.29	30.93	87.67	51	705	
2004	6	17	13	31.58	88.84	31.49	88.68	48	219	
2004	6	17	14	31.73	89.11	31.71	89.08	48	657	
2004	6	17	15	31.91	89.44	31.99	89.58	48	603	
2004	6	17	16	31.4	88.52	31.49	88.68	53	538	
2004	6	17	17	30.1	86.18	30.51	86.92	55	175	
2004	6	17	18	29.24	84.63	29.64	85.35	59	122	
2004	6	17	19	28.12	82.62	28.71	83.68	62	19	
2004	6	17	20	26.91	80.44	27.54	81.57	67	0	
2004	6	17	21	25.96	78.73	26.57	79.83	74	0	
2004	6	17	22	25.3	77.54	25.92	78.66	79	0	
2004	6	17	23	24.65	76.37	25.22	77.40	83	0	
2004	6	18	0	24.11	75.40	24.67	76.41	86	0	
										Type IV 7-Day Reading

⁶Highlighted entries are when field measurements were made (▨ 78" Bulb-Tee A, ▩ 78" Bulb-Tee B, ▧ AASHTO Type IV A, ▦ AASHTO V A and B, and ▨ All Girders)

7

Year	Month	Day	Hour	Temp (°C) (60 cm)	Temp (°F) (60 cm)	Temp (°C) (200 cm)	Temp (°F) (200 cm)	RH (%)	SOLRD (W/m ²)	Type IV 14-Day Reading	Bulb-Tee B Release
2004	6	24	0	25.45	77.81	26.33	79.39	81	0		
2004	6	24	1	25.46	77.83	26.2	79.16	80	0		
2004	6	24	2	24.18	75.52	24.93	76.87	86	0		
2004	6	24	3	23.54	74.37	24.08	75.34	90	0		
2004	6	24	4	23.42	74.16	23.9	75.02	90	0		
2004	6	24	5	23.16	73.69	23.68	74.62	91	2		
2004	6	24	6	24.24	75.63	24.41	75.94	91	73		
2004	6	24	7	28.07	82.53	27.9	82.22	78	266		
2004	6	24	8	29.5	85.10	29.37	84.87	70	436		
2004	6	24	9	30.95	87.71	30.64	87.15	65	642		
2004	6	24	10	32.21	89.98	31.78	89.20	57	790		
2004	6	24	11	33.41	92.14	32.92	91.26	41	889		
2004	6	24	12	34.2	93.56	33.73	92.71	37	740		
2004	6	24	13	34.97	94.95	34.5	94.10	32	248		
2004	6	24	14	34.84	94.71	34.41	93.94	39	837		
2004	6	24	15	34.75	94.55	34.49	94.08	40	688		
2004	6	24	16	34.43	93.97	34.4	93.92	38	539		
2004	6	24	17	34.03	93.25	34.15	93.47	41	350		
2004	6	24	18	33.09	91.56	33.5	92.30	42	155		
2004	6	24	19	31.23	88.21	31.95	89.51	52	21		
2004	6	24	20	29.54	85.17	30.19	86.34	58	0		
2004	6	24	21	25.72	78.30	26.36	79.45	65	0		
2004	6	24	22	24.96	76.93	25.64	78.15	73	0		
2004	6	24	23	24.33	75.79	25.07	77.13	75	0		
2004	6	25	0	24.09	75.36	24.83	76.69	76	0		
2004	6	28	0	24.38	75.88	24.88	76.78	84	0		
2004	6	28	1	24.22	75.60	24.84	76.71	83	0		
2004	6	28	2	24.04	75.27	24.58	76.24	85	0		
2004	6	28	3	24.14	75.45	24.62	76.32	86	0		
2004	6	28	4	24.49	76.08	25.02	77.04	86	0		
2004	6	28	5	23.85	74.93	24.34	75.81	88	0		
2004	6	28	6	24.33	75.79	24.66	76.39	87	48		
2004	6	28	7	25.26	77.47	25.51	77.92	81	87		
2004	6	28	8	25.77	78.39	26.1	78.98	77	97		
2004	6	28	9	26.54	79.77	26.86	80.35	69	130		
2004	6	28	10	27.92	82.26	27.97	82.35	65	265		
2004	6	28	11	29.01	84.22	28.86	83.95	67	379		
2004	6	28	12	29.92	85.86	29.75	85.55	63	414		
2004	6	28	13	29.75	85.55	29.85	85.73	64	331		
2004	6	28	14	29.51	85.12	29.65	85.37	65	346		
2004	6	28	15	31.35	88.43	30.98	87.76	62	800		
2004	6	28	16	30.09	86.16	30.11	86.20	59	417		
2004	6	28	17	24.51	76.12	24.94	76.89	73	25		
2004	6	28	18	22.94	73.29	23.42	74.16	77	4		
2004	6	28	19	21.84	71.31	22.25	72.05	89	2		
2004	6	28	20	22.04	71.67	22.33	72.19	94	0		
2004	6	28	21	22.74	72.93	23.05	73.49	95	0		
2004	6	28	22	23.05	73.49	23.38	74.08	95	0		
2004	6	28	23	23.19	73.74	23.56	74.41	95	0		
2004	6	29	0	23.06	73.51	23.46	74.23	96	0		

⁷Highlighted entries are when field measurements were made (▨ 78" Bulb-Tee A, ▩ 78" Bulb-Tee B, ▧ AASHTO Type IV A, ▦ AASHTO V A and B, and ▨ All Girders)

Year	Month	Day	Hour	Temp (°C) (60 cm)	Temp (°F) (60 cm)	Temp (°C) (200 cm)	Temp (°F) (200 cm)	RH (%)	SOLRD (W/m2)			
2004	7	2	0	24.97	76.95	25.53	77.95	85	0			
2004	7	2	1	24.12	75.42	24.7	76.46	89	0			
2004	7	2	2	23.55	74.39	24.11	75.40	91	0			
2004	7	2	3	23.27	73.89	23.79	74.82	93	0			
2004	7	2	4	23.15	73.67	23.59	74.46	94	0			
2004	7	2	5	22.83	73.09	23.25	73.85	95	1			
2004	7	2	6	23.46	74.23	23.7	74.66	95	47			
2004	7	2	7	27.36	81.25	26.86	80.35	83	276			
2004	7	2	8	29	84.20	28.61	83.50	74	455			
2004	7	2	9	30.3	86.54	29.68	85.42	71	589			
2004	7	2	10	31.93	89.47	31.09	87.96	61	862			
2004	7	2	11	32.3	90.14	31.51	88.72	60	822			
2004	7	2	12	32.6	90.68	31.96	89.53	58	524			
2004	7	2	13	32.92	91.26	32.36	90.25	54	292			
2004	7	2	14	33.52	92.34	33.04	91.47	51	803			
2004	7	2	15	28.05	82.49	28.29	82.92	67	167			
2004	7	2	16	24.53	76.15	24.91	76.84	79	18			
2004	7	2	17	23.37	74.07	23.48	74.26	93	11			
2004	7	2	18	23.77	74.79	23.95	75.11	93	6			
2004	7	2	19	23.54	74.37	23.79	74.82	93	1			
2004	7	2	20	23.36	74.05	23.59	74.46	94	0			
2004	7	2	21	23.45	74.21	23.71	74.68	93	0			
2004	7	2	22	23.11	73.60	23.48	74.26	93	0			
2004	7	2	23	22.71	72.88	23.07	73.53	95	0			
2004	7	3	0	22.68	72.82	23.04	73.47	96	0			
2004	7	14	0	26.08	78.94	26.68	80.02	82	0			
2004	7	14	1	25.74	78.33	26.27	79.29	86	0			
2004	7	14	2	25.38	77.68	25.89	78.60	88	0			
2004	7	14	3	25.2	77.36	25.7	78.26	88	0			
2004	7	14	4	25.09	77.16	25.61	78.10	89	0			
2004	7	14	5	24.99	76.98	25.56	78.01	89	0			
2004	7	14	6	25.01	77.02	25.46	77.83	89	23			
2004	7	14	7	26.36	79.45	26.47	79.65	86	99			
2004	7	14	8	28.14	82.65	28.05	82.49	79	322			
2004	7	14	9	30.24	86.43	29.94	85.89	69	588			
2004	7	14	10	31.07	87.93	30.82	87.48	65	585			
2004	7	14	11	32.49	90.48	32.01	89.62	58	767			
2004	7	14	12	34.13	93.43	33.5	92.30	51	871			
2004	7	14	13	34.49	94.08	33.85	92.93	49	184			
2004	7	14	14	34.45	94.01	33.96	93.13	51	819			
2004	7	14	15	32.73	90.91	32.59	90.66	57	460			
2004	7	14	16	33.75	92.75	33.61	92.50	51	547			
2004	7	14	17	32.95	91.31	33.04	91.47	53	338			
2004	7	14	18	31.63	88.93	31.97	89.55	57	155			
2004	7	14	19	29.83	85.69	30.43	86.77	63	16			
2004	7	14	20	28.88	83.98	29.48	85.06	70	0			
2004	7	14	21	28.19	82.74	28.79	83.82	74	0			
2004	7	14	22	27.33	81.19	27.97	82.35	78	0			
2004	7	14	23	26.85	80.33	27.41	81.34	80	0			
2004	7	15	0	26.6	79.88	27.19	80.94	81	0			

⁸Highlighted entries are when field measurements were made (78" Bulb-Tee A, 78" Bulb-Tee B, AASHTO Type IV A, AASHTO V A and B, and All Girders)

9

Year	Month	Day	Hour	Temp (°C) (60 cm)	Temp (°F) (60 cm)	Temp (°C) (200 cm)	Temp (°F) (200 cm)	RH (%)	SOLRD (W/m ²)			
2004	7	21	0	23.16	73.69	23.58	74.44	95	0			
2004	7	21	1	22.86	73.15	23.23	73.81	96	0			
2004	7	21	2	23.5	74.30	23.78	74.80	97	0			
2004	7	21	3	23.65	74.57	23.89	75.00	97	0			
2004	7	21	4	23.24	73.83	23.44	74.19	97	0			
2004	7	21	5	23.28	73.90	23.5	74.30	97	0			
2004	7	21	6	23.37	74.07	23.57	74.43	98	22			
2004	7	21	7	23.7	74.66	23.78	74.80	98	94			
2004	7	21	8	25.04	77.07	24.57	76.23	97	359			
2004	7	21	9	27.58	81.64	26.95	80.51	84	581			
2004	7	21	10	29.53	85.15	29.03	84.25	74	781			
2004	7	21	11	30.6	87.08	30.18	86.32	67	766			
2004	7	21	12	32.23	90.01	31.76	89.17	54	781			
2004	7	21	13	32.77	90.99	32.43	90.37	47	879			
2004	7	21	14	33.17	91.71	32.94	91.29	45	754			
2004	7	21	15	32.66	90.79	32.69	90.84	47	406			
2004	7	21	16	32.76	90.97	32.85	91.13	45	355			
2004	7	21	17	32.29	90.12	32.51	90.52	49	297			
2004	7	21	18	30.66	87.19	31.1	87.98	52	108			
2004	7	21	19	29.08	84.34	29.72	85.50	57	13			
2004	7	21	20	27.58	81.64	28.39	83.10	64	0			
2004	7	21	21	26.73	80.11	27.48	81.46	70	0			
2004	7	21	22	25.36	77.65	26.11	79.00	79	0			
2004	7	21	23	23.67	74.61	24.38	75.88	86	0			
2004	7	22	0	22.86	73.15	23.38	74.08	91	0			
2004	7	28	0	24.3	75.74	24.72	76.50	87	0			
2004	7	28	1	23.85	74.93	24.25	75.65	90	0			
2004	7	28	2	23.67	74.61	24.04	75.27	92	0			
2004	7	28	3	23.32	73.98	23.74	74.73	94	0			
2004	7	28	4	23.26	73.87	23.68	74.62	94	0			
2004	7	28	5	23.16	73.69	23.57	74.43	94	0			
2004	7	28	6	23.58	74.44	23.82	74.88	94	39			
2004	7	28	7	26	78.80	25.69	78.24	85	157			
2004	7	28	8	28.04	82.47	27.59	81.66	77	414			
2004	7	28	9	30.21	86.38	29.43	84.97	70	530			
2004	7	28	10	29.76	85.57	29.48	85.06	69	399			
2004	7	28	11	31.9	89.42	30.86	87.55	61	713			
2004	7	28	12	30.85	87.53	30.76	87.37	61	185			
2004	7	28	13	29.87	85.77	29.8	85.64	69	367			
2004	7	28	14	32	89.60	31.26	88.27	60	634			
2004	7	28	15	29.78	85.60	29.45	85.01	71	493			
2004	7	28	16	29.93	85.87	29.9	85.82	69	278			
2004	7	28	17	29.04	84.27	29.24	84.63	72	105			
2004	7	28	18	27.6	81.68	27.98	82.36	78	17			
2004	7	28	19	25.15	77.27	25.42	77.76	90	0			
2004	7	28	20	24.18	75.52	24.44	75.99	92	0			
2004	7	28	21	23.94	75.09	24.24	75.63	94	0			
2004	7	28	22	23.85	74.93	24.23	75.61	94	0			
2004	7	28	23	23.62	74.52	24	75.20	95	0			
2004	7	29	0	23.44	74.19	23.74	74.73	95	0			

⁹Highlighted entries are when field measurements were made (78" Bulb-Tee A, 78" Bulb-Tee B, AASHTO Type IV A, AASHTO V A and B, and All Girders)

Year	Month	Day	Hour	Temp (°C) (60 cm)	Temp (°F) (60 cm)	Temp (°C) (200 cm)	Temp (°F) (200 cm)	RH (%)	SOLRD (W/m2)			
2004	8	11	0	24.57	76.23	24.90	76.82	89	0			
2004	8	11	1	24.58	76.24	24.88	76.78	90	0			
2004	8	11	2	24.21	75.58	24.43	75.97	92	0			
2004	8	11	3	24.47	76.05	24.76	76.57	91	0			
2004	8	11	4	24.33	75.79	24.60	76.28	91	0			
2004	8	11	5	23.97	75.15	24.22	75.60	92	0			
2004	8	11	6	24.20	75.56	24.27	75.69	92	42			
2004	8	11	7	25.86	78.55	25.55	77.99	87	163			
2004	8	11	8	27.06	80.71	26.70	80.06	83	322			
2004	8	11	9	28.00	82.40	27.67	81.81	79	344			
2004	8	11	10	30.36	86.65	29.63	85.33	72	772			
2004	8	11	11	32.02	89.64	31.35	88.43	62	797			
2004	8	11	12	32.62	90.72	32.12	89.82	58	790			
2004	8	11	13	33.88	92.98	33.12	91.62	55	874			
2004	8	11	14	33.13	91.63	33.07	91.53	53	431			
2004	8	11	15	27.93	82.27	28.36	83.05	73	80			
2004	8	11	16	29.26	84.67	28.86	83.95	72	470			
2004	8	11	17	28.02	82.44	28.20	82.76	77	118			
2004	8	11	18	28.32	82.98	28.38	83.08	76	153			
2004	8	11	19	26.28	79.30	26.63	79.93	80	3			
2004	8	11	20	25.18	77.32	25.45	77.81	85	0			
2004	8	11	21	24.60	76.28	24.94	76.89	82	0			
2004	8	11	22	24.10	75.38	24.45	76.01	85	0			
2004	8	11	23	24.24	75.63	24.54	76.17	88	0			
2004	8	12	0	24.60	76.28	25.02	77.04	85	0			
2004	8	24	0	24.16	75.49	24.40	75.92	91	0			
2004	8	24	1	23.55	74.39	23.81	74.86	92	0			
2004	8	24	2	23.30	73.94	23.56	74.41	92	0			
2004	8	24	3	23.07	73.53	23.32	73.98	93	0			
2004	8	24	4	22.85	73.13	23.07	73.53	94	0			
2004	8	24	5	22.85	73.13	23.01	73.42	95	0			
2004	8	24	6	23.11	73.60	23.16	73.69	95	11			
2004	8	24	7	24.63	76.33	24.35	75.83	92	128			
2004	8	24	8	27.46	81.43	27.09	80.76	81	370			
2004	8	24	9	29.07	84.33	28.62	83.52	73	569			
2004	8	24	10	30.04	86.02	29.62	85.32	69	546			
2004	8	24	11	30.42	86.76	30.05	86.09	65	578			
2004	8	24	12	31.21	88.18	30.85	87.53	62	583			
2004	8	24	13	32.25	90.05	31.63	88.93	57	816			
2004	8	24	14	32.91	91.24	32.43	90.37	53	763			
2004	8	24	15	31.28	88.30	31.43	88.57	57	273			
2004	8	24	16	28.18	82.72	28.30	82.94	73	256			
2004	8	24	17	26.95	80.51	27.17	80.91	78	95			
2004	8	24	18	24.12	75.42	24.34	75.81	89	2			
2004	8	24	19	23.72	74.70	23.64	74.55	95	0			
2004	8	24	20	24.08	75.34	24.03	75.25	96	0			
2004	8	24	21	24.28	75.70	24.21	75.58	96	0			
2004	8	24	22	24.54	76.17	24.49	76.08	96	0			
2004	8	24	23	24.26	75.67	24.21	75.58	96	0			
2004	8	25	0	24.33	75.79	24.30	75.74	96	0			

¹⁰Highlighted entries are when field measurements were made (78" Bulb-Tee A, 78" Bulb-Tee B, AASHTO Type IV A, AASHTO V A and B, and All Girders)

Year	Month	Day	Hour	Temp (°C) (60 cm)	Temp (°F) (60 cm)	Temp (°C) (200 cm)	Temp (°F) (200 cm)	RH (%)	SOLRD (W/m2)			
2004	9	9	0	24.53	76.15	24.69	76.44	91	0	Bulb-Tee A 153-Day Reading	Type IV 91-Day Reading	Bulb-Tee B 73-Day Reading
2004	9	9	1	24.13	75.43	24.14	75.45	93	0			
2004	9	9	2	24.27	75.69	24.07	75.33	94	0			
2004	9	9	3	24.62	76.32	24.06	75.31	95	0			
2004	9	9	4	24.59	76.26	23.91	75.04	96	0			
2004	9	9	5	24.53	76.15	23.73	74.71	96	0			
2004	9	9	6	24.58	76.24	23.72	74.70	96	4			
2004	9	9	7	25.01	77.02	23.92	75.06	95	31			
2004	9	9	8	26.05	78.89	25.02	77.04	89	253			
2004	9	9	9	27.35	81.23	26.59	79.86	85	392			
2004	9	9	10	29.82	85.68	28.92	84.06	74	740			
2004	9	9	11	30.53	86.95	30.00	86.00	69	415			
2004	9	9	12	31.41	88.54	30.78	87.40	64	731			
2004	9	9	13	29.74	85.53	29.63	85.33	66	352			
2004	9	9	14	27.85	82.13	28.13	82.63	74	100			
2004	9	9	15	26.53	79.75	26.46	79.63	87	127			
2004	9	9	16	27.00	80.60	26.94	80.49	86	81			
2004	9	9	17	24.75	76.55	24.64	76.35	93	11			
2004	9	9	18	24.59	76.26	24.15	75.47	95	3			
2004	9	9	19	24.68	76.42	24.13	75.43	96	0			
2004	9	9	20	24.51	76.12	23.79	74.82	96	0			
2004	9	9	21	24.22	75.60	23.41	74.14	96	0			
2004	9	9	22	23.99	75.18	23.12	73.62	97	0			
2004	9	9	23	23.98	75.16	23.01	73.42	97	0			
2004	9	10	0	23.85	74.93	22.81	73.06	97	0			
2004	9	21	0	23.50	74.30	23.41	74.14	86	0			
2004	9	21	1	23.83	74.89	24.05	75.29	78	0			
2004	9	21	2	23.60	74.48	23.92	75.06	76	0			
2004	9	21	3	23.49	74.28	23.82	74.88	76	0			
2004	9	21	4	23.27	73.89	23.52	74.34	79	0			
2004	9	21	5	23.43	74.17	23.64	74.55	79	0			
2004	9	21	6	23.47	74.25	23.81	74.86	78	4			
2004	9	21	7	23.78	74.80	23.99	75.18	79	65			
2004	9	21	8	24.73	76.51	24.89	76.80	74	155			
2004	9	21	9	27.17	80.91	27.08	80.74	64	555			
2004	9	21	10	27.69	81.84	27.82	82.08	59	427			
2004	9	21	11	27.73	81.91	27.91	82.24	58	418			
2004	9	21	12	28.30	82.94	28.40	83.12	57	529			
2004	9	21	13	27.52	81.54	27.82	82.08	61	269			
2004	9	21	14	27.14	80.85	27.37	81.27	64	280			
2004	9	21	15	26.55	79.79	26.72	80.10	70	266			
2004	9	21	16	26.38	79.48	26.55	79.79	71	225			
2004	9	21	17	26.05	78.89	26.39	79.50	69	139			
2004	9	21	18	24.78	76.60	25.16	77.29	73	12			
2004	9	21	19	24.68	76.42	25.15	77.27	72	0			
2004	9	21	20	24.77	76.59	25.25	77.45	73	0			
2004	9	21	21	24.76	76.57	25.22	77.40	73	0			
2004	9	21	22	24.57	76.23	25.03	77.05	75	0			
2004	9	21	23	24.34	75.81	24.78	76.60	76	0			
2004	9	22	0	24.61	76.30	25.07	77.13	75	0			
										Bulb-Tee A 165-Day Reading	Type IV 103-Day Reading	Bulb-Tee B 85-Day Reading

¹¹Highlighted entries are when field measurements were made (78" Bulb-Tee A, 78" Bulb-Tee B, AASHTO Type IV A, AASHTO V A and B, and All Girders)

Year	Month	Day	Hour	Temp (°C) (60 cm)	Temp (°F) (60 cm)	Temp (°C) (200 cm)	Temp (°F) (200 cm)	RH (%)	SOLRD (W/m2)				
2004	9	28	0	24.15	75.47	23.97	75.15	92	0				
2004	9	28	1	23.79	74.82	23.43	74.17	93	0				
2004	9	28	2	23.50	74.30	22.89	73.20	94	0				
2004	9	28	3	23.44	74.19	22.48	72.46	95	0				
2004	9	28	4	23.25	73.85	22.16	71.89	96	0				
2004	9	28	5	23.05	73.49	21.87	71.37	96	0				
2004	9	28	6	22.89	73.20	21.68	71.02	96	7				
2004	9	28	7	24.08	75.34	22.44	72.39	94	134				
2004	9	28	8	26.13	79.03	24.87	76.77	87	347				
2004	9	28	9	27.73	81.91	27.20	80.96	78	535				
2004	9	28	10	28.75	83.75	28.49	83.28	70	710				
2004	9	28	11	29.94	85.89	29.65	85.37	65	788				
2004	9	28	12	30.41	86.74	30.23	86.41	62	739				
2004	9	28	13	31.08	87.94	30.92	87.66	59	762				
2004	9	28	14	31.52	88.74	31.48	88.66	55	713				
2004	9	28	15	31.32	88.38	31.47	88.65	54	560				
2004	9	28	16	30.55	86.99	30.97	87.75	56	371				
2004	9	28	17	29.28	84.70	29.85	85.73	62	162				
2004	9	28	18	27.13	80.83	27.81	82.06	70	14				
2004	9	28	19	25.51	77.92	26.21	79.18	78	0				
2004	9	28	20	24.52	76.14	25.05	77.09	84	0				
2004	9	28	21	23.73	74.71	24.10	75.38	88	0				
2004	9	28	22	23.13	73.63	23.34	74.01	91	0				
2004	9	28	23	23.00	73.40	22.99	73.38	93	0				
2004	9	29	0	22.82	73.08	22.61	72.70	94	0				
2004	10	5	0	23.36	74.05	23.29	73.92	91	0				
2004	10	5	1	23.34	74.01	22.95	73.31	93	0				
2004	10	5	2	22.99	73.38	22.57	72.63	93	0				
2004	10	5	3	22.45	72.41	21.92	71.46	94	0				
2004	10	5	4	21.77	71.19	21.12	70.02	95	0				
2004	10	5	5	22.03	71.65	21.00	69.80	96	0				
2004	10	5	6	21.86	71.35	20.73	69.31	96	7				
2004	10	5	7	23.92	75.06	22.39	72.30	91	117				
2004	10	5	8	26.12	79.02	25.38	77.68	82	264				
2004	10	5	9	27.68	81.82	27.07	80.73	76	464				
2004	10	5	10	28.02	82.44	27.68	81.82	71	376				
2004	10	5	11	29.71	85.48	29.08	84.34	64	775				
2004	10	5	12	29.71	85.48	29.47	85.05	62	494				
2004	10	5	13	29.97	85.95	29.89	85.80	58	518				
2004	10	5	14	29.30	84.74	29.45	85.01	60	283				
2004	10	5	15	29.16	84.49	29.14	84.45	61	406				
2004	10	5	16	28.32	82.98	28.62	83.52	63	186				
2004	10	5	17	25.07	77.13	25.42	77.76	78	39				
2004	10	5	18	25.10	77.18	25.54	77.97	74	2				
2004	10	5	19	24.88	76.78	25.16	77.29	80	0				
2004	10	5	20	24.54	76.17	24.77	76.59	81	0				
2004	10	5	21	23.83	74.89	24.05	75.29	84	0				
2004	10	5	22	23.45	74.21	23.56	74.41	86	0				
2004	10	5	23	23.21	73.78	23.13	73.63	88	0				
2004	10	6	0	23.17	73.71	23.04	73.47	89	0				

¹²Highlighted entries are when field measurements were made (78" Bulb-Tee A, 78" Bulb-Tee B, AASHTO Type IV A, AASHTO V A and B, and All Girders)

Year	Month	Day	Hour	Temp (°C) (60 cm)	Temp (°F) (60 cm)	Temp (°C) (200 cm)	Temp (°F) (200 cm)	RH (%)	SOLRD (W/m2)				
2004	10	12	0	21.50	70.70	20.31	68.56	91	0				
2004	10	12	1	21.62	70.92	20.62	69.12	90	0				
2004	10	12	2	21.84	71.31	21.05	69.89	89	0				
2004	10	12	3	21.77	71.19	21.22	70.20	88	0				
2004	10	12	4	21.76	71.17	21.22	70.20	89	0				
2004	10	12	5	21.95	71.51	21.33	70.39	90	0				
2004	10	12	6	22.27	72.09	21.69	71.04	88	1				
2004	10	12	7	22.69	72.84	22.17	71.91	86	29				
2004	10	12	8	23.39	74.10	22.89	73.20	85	88				
2004	10	12	9	23.52	74.34	23.12	73.62	84	111				
2004	10	12	10	23.14	73.65	22.18	71.92	91	226				
2004	10	12	11	23.79	74.82	23.07	73.53	86	241				
2004	10	12	12	24.88	76.78	24.16	75.49	83	315				
2004	10	12	13	26.31	79.36	25.76	78.37	77	390				
2004	10	12	14	26.43	79.57	26.11	79.00	77	314				
2004	10	12	15	27.41	81.34	27.00	80.60	73	417				
2004	10	12	16	27.28	81.10	27.19	80.94	72	303				
2004	10	12	17	26.78	80.20	26.94	80.49	74	97				
2004	10	12	18	25.20	77.36	25.37	77.67	81	2				
2004	10	12	19	24.25	75.65	24.10	75.38	87	0				
2004	10	12	20	23.56	74.41	23.07	73.53	90	0				
2004	10	12	21	23.52	74.34	22.87	73.17	91	0				
2004	10	12	22	22.70	72.86	22.06	71.71	93	0				
2004	10	12	23	21.82	71.28	20.91	69.64	95	0				
2004	10	13	0	21.53	70.75	20.52	68.94	96	0				
2004	10	19	0	22.12	71.816	22.26	72.068	86	0				
2004	10	19	1	22.35	72.23	22.36	72.248	87	0				
2004	10	19	2	22.1	71.78	22.07	71.726	87	0				
2004	10	19	3	21.41	70.538	21.3	70.34	91	0				
2004	10	19	4	20.98	69.764	20.58	69.044	93	0				
2004	10	19	5	20.88	69.584	20.26	68.468	94	0				
2004	10	19	6	21.35	70.43	20.41	68.738	94	1				
2004	10	19	7	21.75	71.15	20.52	68.936	94	49				
2004	10	19	8	24.58	76.244	23.12	73.616	88	248				
2004	10	19	9	26.86	80.348	25.87	78.566	80	449				
2004	10	19	10	28.93	84.074	28.3	82.94	71	596				
2004	10	19	11	29.89	85.802	29.29	84.722	66	603				
2004	10	19	12	30.35	86.63	29.83	85.694	62	592				
2004	10	19	13	30.38	86.684	30.14	86.252	60	484				
2004	10	19	14	30.59	87.062	30.47	86.846	58	498				
2004	10	19	15	30.12	86.216	30.26	86.468	59	277				
2004	10	19	16	28.53	83.354	29.1	84.38	63	44				
2004	10	19	17	22.62	72.716	22.29	72.122	91	1				
2004	10	19	18	21.87	71.366	20.96	69.728	93	1				
2004	10	19	19	21.78	71.204	20.96	69.728	93	0				
2004	10	19	20	21.83	71.294	20.72	69.296	95	0				
2004	10	19	21	21.71	71.078	20.43	68.774	95	0				
2004	10	19	22	21.65	70.97	20.32	68.576	95	0				
2004	10	19	23	22.05	71.69	20.75	69.35	92	0				
2004	10	20	0	21.79	71.222	20.48	68.864	94	0				

Type V 14-Day Reading

Type V 21-Day Reading

¹³Highlighted entries are when field measurements were made (78" Bulb-Tee A, 78" Bulb-Tee B, AASHTO Type IV A, AASHTO V A and B, and All Girders)

Year	Month	Day	Hour	Temp (°C) (60 cm)	Temp (°F) (60 cm)	Temp (°C) (200 cm)	Temp (°F) (200 cm)	RH (%)	SOLRD (W/m2)				
2004	10	26	0	17.34	63.212	17.06	62.708	92	0				
2004	10	26	1	16.79	62.222	16.36	61.448	93	0				
2004	10	26	2	16.19	61.142	15.62	60.116	94	0				
2004	10	26	3	15.78	60.404	15.1	59.18	95	0				
2004	10	26	4	15.7	60.26	14.88	58.784	96	0				
2004	10	26	5	16.01	60.818	15.23	59.414	97	0				
2004	10	26	6	16.33	61.394	15.52	59.936	97	2				
2004	10	26	7	18.23	64.814	16.92	62.456	97	83				
2004	10	26	8	20.94	69.692	19.45	67.01	89	265				
2004	10	26	9	23.14	73.652	22.41	72.338	76	457				
2004	10	26	10	25.21	77.378	24.53	76.154	68	611				
2004	10	26	11	26.6	79.88	26.01	78.818	60	723				
2004	10	26	12	27.5	81.5	26.98	80.564	54	666				
2004	10	26	13	27.44	81.392	27.15	80.87	53	546				
2004	10	26	14	27.34	81.212	27.26	81.068	52	487				
2004	10	26	15	27.26	81.068	27.27	81.086	54	355				
2004	10	26	16	25.83	78.494	25.97	78.746	60	199				
2004	10	26	17	24.36	75.848	24.76	76.568	64	53				
2004	10	26	18	22.99	73.382	23.4	74.12	69	0				
2004	10	26	19	21.85	71.33	22.28	72.104	74	0				
2004	10	26	20	21.12	70.016	21.53	70.754	77	0				
2004	10	26	21	20.9	69.62	21.19	70.142	80	0				
2004	10	26	22	20.61	69.098	20.81	69.458	82	0				
2004	10	26	23	20.29	68.522	20.33	68.594	85	0				
2004	10	27	0	19.98	67.964	19.94	67.892	87	0				

Type V 28-Day Reading
 Bulb-Tee B 120-Day Reading
 Type IV 131-Day Reading
 Bulb-Tee A 200-Day Reading

Highlighted entries are when field measurements were made (▨ 78" Bulb-Tee A, ▩ 78" Bulb-Tee B, ▧ AASHTO Type IV A, ▦ AASHTO V A and B, and ▨ All Girders)

APPENDIX F
MIX DESIGNS

78" Bulb-Tee Girder Pour A					
Concrete Mix Design					
CLASS CONCRETE			: VI	DATE	: 4/1/2004
SPECIFIED 28-DAY COMP STRENGTH			: 8500 PSI		
SOURCE OF MATERIALS					
COURSE AGGREGATE	: ANDERSON COLUMBIA		GRADE	: 67	S.G. (SSD): 2.720
FINE AGGREGATE	: FLORIDA ROCK		F.M.	: 2.11	S.G. (SSD): 2.630
PIT NO. (COURSE)	: GA-553		TYPE	: CRUSHED GRANITE	
PIT NO. (FINE)	: 36-491		TYPE	: SILICA SAND	
CEMENT	: SUANEE AMERICAN (BRANFORD)		SPEC	: AASHTO M-85 TYPE II	
AIR ENTR. ADMIX	: DARAVAIR 1000	W.R. GRACE	SPEC	: AASHTO M-154	
1st ADMIX	: WRDA 60	W.R. GRACE	SPEC	: AASHTO M-194 TYPE D	
2nd ADMIX	: ADVA 540	W.R. GRACE	SPEC	: ASTM C-494 TYPE F	
3rd ADMIX	: N/A		SPEC	: N/A	
FLY ASH	: ISG	FERNANDIA BEACH	SPEC	: ASTM C-618 CLASS F	
HOT WEATHER DESIGN MIX	4 X 8 COMPRESSIVE STRENGTH 10050 PSI				
CEMENT (Kg) LBS	: 775	SLUMP RANGE	: 5.50 TO 8.50 (mm) IN		
COURSE AGG (Kg) LBS	: 1800	AIR CONTENT	: 1.0% TO 5.0%		
FINE AGG (Kg) LBS	: 855	UNIT WEIGHT (WET)	: 145.4	(Kg/m ³)PCF	
AIR ENT ADMX (mL) OZ	: 3.0	W/C RATIO (PLANT)	: 0.35	(Kg/Kg)LBS/LB	
1st ADMIX (mL) OZ	: 23.3	W/C RATIO (FIELD)	: 0.35	(Kg/Kg)LBS/LB	
2nd ADMIX (mL) OZ	: 46.5	THEO. YIELD	: 27.00	(m ³)CU FT	
3rd ADMIX (mL) OZ	: 0.0				
WATER (mL) GAL	: 39.30				
WATER (Kg) LBS	: 327.4				
FLY ASH (Kg) LBS	: 170				
PRODUCER TEST DATA					
CHLORIDE CONTENT	: 0.277	(Kg/m ³)LB/CY			
SLUMP	: 8.25	(mm) IN			
AIR CONTENT	: 2.90	%			
CONC. TEMPERATURE	: 74	DEG (C) F			
AMB. TEMPERATURE	: 55	DEG (C) F			
CALC W/B RATIO	: 0.35	(Kg/Kg)LBS/LB	< 0.40	HIGH STRENGTH CONCRETE	

78" Bulb-Tee Girder Pour B					
Concrete Mix Design					
CLASS CONCRETE			: VI	DATE	: 6/17/2004
SPECIFIED 28-DAY COMP STRENGTH			: 8500 PSI		
SOURCE OF MATERIALS					
COURSE AGGREGATE	: ANDERSON COLUMBIA		GRADE	: 67	S.G. (SSD): 2.720
FINE AGGREGATE	: FLORIDA ROCK		F.M.	: 2.11	S.G. (SSD): 2.630
PIT NO. (COURSE)	: GA-553		TYPE	: CRUSHED GRANITE	
PIT NO. (FINE)	: 36-491		TYPE	: SILICA SAND	
CEMENT	: SUANEE AMERICAN (BRANFORD)		SPEC	: AASHTO M-85 TYPE II	
AIR ENTR. ADMIX	: DARAVAIR 1000	W.R. GRACE	SPEC	: AASHTO M-154	
1st ADMIX	: WRDA 60	W.R. GRACE	SPEC	: AASHTO M-194 TYPE D	
2nd ADMIX	: ADVA 540	W.R. GRACE	SPEC	: ASTM C-494 TYPE F	
3rd ADMIX	: N/A		SPEC	: N/A	
FLY ASH	: ISG	FERNANDIA BEACH	SPEC	: ASTM C-618 CLASS F	
HOT WEATHER DESIGN MIX	4 X 8 COMPRESSIVE STRENGTH 10050 PSI				
CEMENT (Kg) LBS	: 775	SLUMP RANGE	: 5.50 TO 8.50 (mm) IN		
COURSE AGG (Kg) LBS	: 1800	AIR CONTENT	: 1.0% TO 5.0%		
FINE AGG (Kg) LBS	: 855	UNIT WEIGHT (WET)	: 145.4 (Kg/m ³)PCF		
AIR ENT ADMX (mL) OZ	: 3.0	W/C RATIO (PLANT)	: 0.35 Kg/Kg)LBS/LB		
1st ADMIX (mL) OZ	: 23.3	W/C RATIO (FIELD)	: 0.35 Kg/Kg)LBS/LB		
2nd ADMIX (mL) OZ	: 46.5	THEO. YIELD	: 27.00 (m ³)CU FT		
3rd ADMIX (mL) OZ	: 0.0				
WATER (mL) GAL	: 39.30				
WATER (Kg) LBS	: 327.4				
FLY ASH (Kg) LBS	: 170				
PRODUCER TEST DATA					
CHLORIDE CONTENT	: 0.277	(Kg/m ³)LB/CY			
SLUMP	: 6.75	(mm) IN			
AIR CONTENT	: 3.00	%			
CONC. TEMPERATURE	: 88	DEG (C) F			
AMB. TEMPERATURE	: 74	DEG (C) F			
CALC W/B RATIO	: 0.35	(Kg/Kg)LBS/LB	< 0.40	HIGH STRENGTH CONCRETE	

AASHTO Type IV Girder Pour A					
Concrete Mix Design					
CLASS CONCRETE			: IV	DATE	: 6/7/2004
SPECIFIED 28-DAY COMPRESSIVE STRENGTH			: 38 MPA		
SOURCE OF MATERIALS					
COURSE AGGREGATE	: ANDERSON COLUMBIA			GRADE	: 57 S.G. (SSD): 2.720
FINE AGGREGATE	: FLORIDA ROCK			F.M.	: 2.11 S.G. (SSD): 2.630
PIT NO. (COURSE)	: GA-553			TYPE	: CRUSHED GRANITE
PIT NO. (FINE)	: 36-491			TYPE	: SILICA SAND
CEMENT	: SUANEE AMERICAN			SPEC	: AASHTO M-85 TYPE II
AIR ENTR. ADMIX	: DARAVAIR 1000	W.R. GRACE		SPEC	: AASHTO M-154
1st ADMIX	: WRDA 60	W.R. GRACE		SPEC	: AASHTO M-194 TYPE D
2nd ADMIX	: ADVA 540	W.R. GRACE		SPEC	: ASTM C-494 TYPE F
3rd ADMIX	: N/A			SPEC	: N/A
FLY ASH	: ISG			SPEC	: ASTM C-618 CLASS F
HOT WEATHER METRIC DESIGN MIX				4 X 8 COMPRESSIVE STRENGTH @ 28 DAYS = 59.0 MPA	
CEMENT (Kg)	: 430.00			SLUMP RANGE	: 140 TO 220 (mm)
COURSE AGG (Kg)	: 1800.00			AIR CONTENT	: 1.00% TO 5.00%
FINE AGG (Kg)	: 544.00			UNIT WEIGHT (WET)	: 2337.00 (Kg/m ³)
AIR ENT ADMX (mL)	: 116.00			W/C RATIO (PLANT)	: 0.36 (Kg/Kg)
1st ADMIX (mL)	: 843.00			W/C RATIO (FIELD)	: 0.36 (Kg/Kg)
2nd ADMIX (mL)	: 1682.00			THEO. YIELD	: 1.01 (m ³)
3rd ADMIX (mL)	: 0.00				
WATER (L)	: 188.00				
WATER (Kg)	: 188.00				
FLY ASH (Kg)	: 95.00				
PRODUCER TEST DATA					
CHLORIDE CONTENT	: 0.18 (Kg/m ³)				
SLUMP	: 170.00 (mm)				
AIR CONTENT	: 1.90 %				
CONC. TEMPERATURE	: 34.00 DEG C				
AMB. TEMPERATURE	: 31.00 DEG C				
CALC W/B RATIO	: 0.36 (Kg/Kg)			< 0.40	HIGH STRENGTH CONCRETE

AASHTO Type V Girder Pour A					
Concrete Mix Design					
CLASS CONCRETE			: IV	DATE	: 9/17/2004
SPECIFIED 28-DAY COMP. STRENGTH			: 5500 PSI		
SOURCE OF MATERIALS					
COURSE AGGREGATE	: ANDERSON COLUMBIA		GRADE	: 67	S.G. (SSD): 2.720
FINE AGGREGATE	: FLORIDA ROCK		F.M.	: 2.11	S.G. (SSD): 2.630
PIT NO. (COURSE)	: GA-553		TYPE	: CRUSHED GRANITE	
PIT NO. (FINE)	: 36-491		TYPE	: SILICA SAND	
CEMENT	: SUANEE AMERICAN (BRANFORD)		SPEC	: AASHTO M-85 TYPE II	
AIR ENTR. ADMIX	: DARAVAIR 1000	W.R. GRACE	SPEC	: AASHTO M-154	
1st ADMIX	: WRDA 60	W.R. GRACE	SPEC	: AASHTO M-194 TYPE D	
2nd ADMIX	: ADVA 540	W.R. GRACE	SPEC	: ASTM C-494 TYPE F	
3rd ADMIX	: N/A		SPEC	: N/A	
FLY ASH	: ISG	FERNANDIA BEACH	SPEC	: ASTM C-618 CLASS F	
HOT WEATHER DESIGN MIX			4 X 8 COMPRESSIVE STRENGTH	10050 PSI	
CEMENT (Kg) LBS	: 725		SLUMP RANGE	: 5.50 TO 8.50 (mm) IN	
COURSE AGG (Kg) LBS	: 1820		AIR CONTENT	: 1.0% TO 6.0%	
FINE AGG (Kg) LBS	: 917		UNIT WEIGHT (WET)	: 145.9 (Kg/m ³)PCF	
AIR ENT ADMX (mL) OZ	: 3.0		W/C RATIO (PLANT)	: 0.36 (Kg/Kg)LBS/LB	
1st ADMIX (mL) OZ	: 21.8		W/C RATIO (FIELD)	: 0.32 (Kg/Kg)LBS/LB	
2nd ADMIX (mL) OZ	: 43.5		THEO. YIELD	: 27.00 (m ³)CU FT	
3rd ADMIX (mL) OZ	: 0.0				
WATER (mL) GAL	: 38.00				
WATER (Kg) LBS	: 316.5				
FLY ASH (Kg) LBS	: 160				
PRODUCER TEST DATA					
CHLORIDE CONTENT	: 0.296 (Kg/m ³)LB/CY				
SLUMP	: 7.25 (mm) IN				
AIR CONTENT	: 2.70 %				
CONC. TEMPERATURE	: 91 DEG (C) F				
AMB. TEMPERATURE	: 85 DEG (C) F				
CALC W/B RATIO	: 0.36 (Kg/Kg)LBS/LB		< 0.40		HIGH STRENGTH CONCRETE

AASHTO Type V Girder Pour B					
Concrete Mix Design					
CLASS CONCRETE			: IV	DATE	: 9/21/2004
SPECIFIED 28-DAY COMP. STRENGTH			: 5500 PSI		
SOURCE OF MATERIALS					
COURSE AGGREGATE	: ANDERSON COLUMBIA		GRADE	: 67	S.G. (SSD): 2.720
FINE AGGREGATE	: FLORIDA ROCK		F.M.	: 2.11	S.G. (SSD): 2.630
PIT NO. (COURSE)	: GA-553		TYPE	: CRUSHED GRANITE	
PIT NO. (FINE)	: 36-491		TYPE	: SILICA SAND	
CEMENT	: SUANEE AMERICAN (BRANFORD)		SPEC	: AASHTO M-85 TYPE II	
AIR ENTR. ADMIX	: DARAVAIR 1000	W.R. GRACE	SPEC	: AASHTO M-154	
1st ADMIX	: WRDA 60	W.R. GRACE	SPEC	: AASHTO M-194 TYPE D	
2nd ADMIX	: ADVA 540	W.R. GRACE	SPEC	: ASTM C-494 TYPE F	
3rd ADMIX	: N/A		SPEC	: N/A	
FLY ASH	: ISG	FERNANDIA BEACH	SPEC	: ASTM C-618 CLASS F	
HOT WEATHER DESIGN MIX		4 X 8 COMPRESSIVE STRENGTH	10050 PSI		
CEMENT (Kg) LBS	: 725	SLUMP RANGE	: 5.50 TO 8.50 (mm) IN		
COURSE AGG (Kg) LBS	: 1820	AIR CONTENT	: 1.0% TO 6.0%		
FINE AGG (Kg) LBS	: 917	UNIT WEIGHT (WET)	: 145.9 (Kg/m ³)PCF		
AIR ENT ADMX (mL) OZ	: 3.0	W/C RATIO (PLANT)	: 0.36 (Kg/Kg)LBS/LB		
1st ADMIX (mL) OZ	: 21.8	W/C RATIO (FIELD)	: 0.31 (Kg/Kg)LBS/LB		
2nd ADMIX (mL) OZ	: 43.5	THEO. YIELD	: 27.00 (m ³)CU FT		
3rd ADMIX (mL) OZ	: 0.0				
WATER (mL) GAL	: 38.00				
WATER (Kg) LBS	: 316.5				
FLY ASH (Kg) LBS	: 160				
PRODUCER TEST DATA					
CHLORIDE CONTENT	: 0.296 (Kg/m ³)LB/CY				
SLUMP	: 7.75 (mm) IN				
AIR CONTENT	: 4.50 %				
CONC. TEMPERATURE	: 83 DEG (C) F				
AMB. TEMPERATURE	: 73 DEG (C) F				
CALC W/B RATIO	: 0.36 (Kg/Kg)LBS/LB	< 0.40			HIGH STRENGTH CONCRETE

APPENDIX G
TABULATED MATERIAL TESTING DATA

78" Bulb-Tee Pour "A"						
4" x 8" Cylinder Specimens						
Time After Release (day)	Time After Casting (day)	Average Compressive Strength (psi)	Elastic Modulus (Linear Regression) (ksi)	Elastic Modulus (ASTM) (ksi)	Elastic Modulus (ACI) (ksi)	Elastic Modulus (AASHTO) (ksi)
-	0	0	0	0	0	0
0	7	6903	4309	4341	4807	4782
7	14	8117	5228	4670	5213	5185
14	21	8680	5304	4718	5390	5362
21	28	8827	5336	4722	5436	5407
28	35	9326	5444	4843	5587	5558
42	49	9766	5588	4949	5718	5687
84	91	10107	6005	6002	5817	5786
109	116	10575	6070	6082	5950	5919
136	143	10509	6126	6226	5931	5900
200	207	10538	6017	5969	5939	5908
6" x 12" Cylinder Specimens						
Time After Release (day)	Time After Casting (day)	Average Compressive Strength (psi)	Elastic Modulus (Linear Regression) (ksi)	Elastic Modulus (ASTM) (ksi)	Elastic Modulus (ACI) (ksi)	Elastic Modulus (AASHTO) (ksi)
-	0	0	0	0	0	0
0	7	7230	4924	4942	4920	4894
18	25	8760	5442	5320	5415	5387
23	30	9377	5348	5345	5603	5573
31	38	9407	5575	5577	5611	5582
200	207				0	0
$t_j =$ 7 days after casting to release						

78" Bulb-Tee Pour "B"						
4" x 8" Cylinder Specimens						
Time After Release (day)	Time After Casting (day)	Average Compressive Strength (psi)	Elastic Modulus (Linear Regression) (ksi)	Elastic Modulus (ASTM) (ksi)	Elastic Modulus (ACI) (ksi)	Elastic Modulus (AASHTO) (ksi)
-	0	0	0	0	0	0
0	9	7014	4759	4709	4845	4820
4	13	7578	4677	4666	5037	5010
16	25	8053	4813	4773	5192	5165
22	31	8344	5099	5085	5285	5257
34	43	8678	4932	4917	5390	5362
43	52	8624	5133	5131	5373	5345
56	65	8899	5222	5195	5458	5429
72	81	9092	5370	5344	5517	5488
84	93	9115	5365	5374	5524	5495
120	129	9093	5160	5160	5517	5488
6" x 12" Cylinder Specimens						
Time After Release (day)	Time After Casting (day)	Average Compressive Strength (psi)	Elastic Modulus (Linear Regression) (ksi)	Elastic Modulus (ASTM) (ksi)	Elastic Modulus (ACI) (ksi)	Elastic Modulus (AASHTO) (ksi)
-	0	0	0	0	0	0
0	9	6653	4806	4766	4719	4695
$t_j =$ 9 days after casting to release						

AASHTO Type IV Pour "A"						
4" x 8" Cylinder Specimens						
Time After Release (day)	Time After Casting (day)	Average Compressive Strength (psi)	Elastic Modulus (Linear Regression) (ksi)	Elastic Modulus (ASTM) (ksi)	Elastic Modulus (ACI) (ksi)	Elastic Modulus (AASHTO) (ksi)
-	0	0	0	0	0	0
0	3	5410	4506	4438	4279	4233
7	10	6793	4911	4847	4795	4744
14	17	8305	5390	5385	5302	5245
21	24	8281	5191	5196	5295	5237
34	37	8440	5456	5447	5345	5288
40	43	8440	5830	5781	5345	5287
61	64	9135	5886	5855	5561	5501
74	77	8880	5672	5634	5483	5423
102	105	9069	5853	5813	5541	5481
138	141	9399	5887	5887	5641	5580
6" x 12" Cylinder Specimens						
Time After Release (day)	Time After Casting (day)	Average Compressive Strength (psi)	Elastic Modulus (Linear Regression) (ksi)	Elastic Modulus (ASTM) (ksi)	Elastic Modulus (ACI) (ksi)	Elastic Modulus (AASHTO) (ksi)
-	0	0	0	0	0	0
4	7	5910	4726	4729	4473	4425
34	37	8540	5481	5551	5377	5319
138	141				0	0
$t_j =$ 3 days after casting to release						

AASHTO Type V Pour "A"						
4" x 8" Cylinder Specimens						
Time After Release (day)	Time After Casting (day)	Average Compressive Strength (psi)	Elastic Modulus (Linear Regression) (ksi)	Elastic Modulus (ASTM) (ksi)	Elastic Modulus (ACI) (ksi)	Elastic Modulus (AASHTO) (ksi)
-	0	0	0	0	0	0
0	10	6336	4909	4854	4629	4581
7	17	7289	5130	5105	4965	4914
14	24	7862	5361	5327	5157	5103
22	32	8616	5419	5412	5398	5342
28	38	8478	5323	5310	5355	5299
$t_j =$ 10 days after casting to release						

AASHTO Type V Pour "B"						
4" x 8" Cylinder Specimens						
Time After Release (day)	Time After Casting (day)	Average Compressive Strength (psi)	Elastic Modulus (Linear Regression) (ksi)	Elastic Modulus (ASTM) (ksi)	Elastic Modulus (ACI) (ksi)	Elastic Modulus (AASHTO) (ksi)
-	0	0	0	0	0	0
0	7	5683	4796	4751	4384	4339
7	14	7045	5164	5137	4881	4831
14	21	7510	5331	5326	5040	4988
22	29	8188	5466	5336	5262	5208
28	35	8172	5313	5313	5257	5203
$t_j =$ 7 days after casting to release						

APPENDIX H
78" BULB-TEE CAMBER PREDICTION METHOD

**Recommended Camber Growth Model Using LRFD Creep
Coefficient for 78" Florida Bulb-Tee Girder**

--written by Jonathan Sanek, University of Florida Department of Civil and Coastal Engineering

Given Structural Parameters

78-inch Bulb-Tee Properties

<i>Bulb-Tee Section Properties</i>	<i>Bulb-Tee Material Properties</i>
Perim := 295 (in)	$\gamma_c := 145$ (pcf)
Area := 1105 (in ²)	$f_c := 8.5$ (ksi) <i>Mean tested value</i>
I := 935544 (in ⁴)	$E_c := 5146$ (ksi) <i>Mean tested value</i>
L := 1942.625 (in)	$E_{ci} := 4534$ (ksi) <i>Mean tested value</i>
$I_{top} := 2496944$ (in ⁴)	<i>moment of inertia about top of section</i>
$B_{top} := -41566$ (in ³)	<i>first moment area about top of section</i>

Bulb-Tee Tendon Properties

PrestressType := "Low Relaxation"

$y_{cgt} := 70.7$ (in)

$y_{NA} := 37.6$ (in)

$e_{cgt} := y_{cgt} - y_{NA}$ (in) *(straight tendon configuration)*

$A_{ps} := 11.5$ (in²)

$f_{pu} := 270$ (ksi)

$f_{py} := \begin{cases} 0.9 f_{pu} & \text{if PrestressType} = \text{"Low Relaxation"} \\ 0.85 f_{pu} & \text{if PrestressType} = \text{"Stress Relieved"} \end{cases}$

$f_{pj} := \begin{cases} 0.75 f_{pu} & \text{if PrestressType} = \text{"Low Relaxation"} \\ 0.70 f_{pu} & \text{if PrestressType} = \text{"Stress Relieved"} \end{cases}$

$E_p := 28500$ (ksi)

Bulb-Tee Calculated Properties

$w_{sw} := \frac{\text{Area}}{1728} \cdot \frac{\gamma_c}{1000}$ $w_{sw} = 0.093$ (kip/in)

$VS := \frac{\text{Area}}{\text{Perim}}$ $VS = 3.746$ (in)

Assumed Conditions

H := 65 Relative Humidity

$t_j := 8$ (days from jacking to transfer)

FDOT/LFRD Prestress Loss Calculation (Section 5.9.5.4)

i. Prestress Loss due to Initial Relaxation of the Prestressing Steel

$$\Delta f_{pR1} := \begin{cases} \frac{\log(24.0t_j)}{40.0} \cdot \left(\frac{f_{pj}}{f_{py}} - 0.55 \right) \cdot f_{pj} & \text{if PrestressType} = \text{"Low Relaxation"} \\ \frac{\log(24.0t_j)}{10.0} \cdot \left(\frac{f_{pj}}{f_{py}} - 0.55 \right) \cdot f_{pj} & \text{if PrestressType} = \text{"Stress Relieved"} \end{cases}$$

$$\Delta f_{pR1} = 3.275 \quad (\text{ksi})$$

$$\Delta f_{pR1.\%} := \frac{\Delta f_{pR1}}{f_{pj}} \cdot 100 \quad \Delta f_{pR1.\%} = 1.6 \quad (\%)$$

ii. Prestress Loss due to Elastic Shortening (assume initially 5% due to elastic shorting)

P_e effective prestress force after elastic shortening and relaxation losses

B first moment area about top

y_{cgp} distance from top flange to c.g. of prestressing steel

I moment of inertia about top

Iteration 1

$$\Delta f_{pES} := 0.05 \cdot f_{pj} \quad \Delta f_{pES} = 10.125 \quad (\text{ksi})$$

$$f_{pe.ES} := f_{pj} - (\Delta f_{pES} + \Delta f_{pR1}) \quad f_{pe.ES} = 189.1 \quad (\text{ksi})$$

$$M_g := \frac{w_{sw} \cdot L^2}{8} \quad M_g = 43740 \quad (\text{kip} \cdot \text{in})$$

$$P_e := f_{pe.ES} \cdot A_{ps} \quad P_e = 2174.649 \quad (\text{kip})$$

$$M_{pe.top} := P_e \cdot y_{cgt} \quad M_{pe.top} = 153748 \quad (\text{kip} \cdot \text{in})$$

$$f_{cgp} := - \frac{I_{top} \cdot P_e + B_{top} \cdot (M_g - M_{pe.top}) + [Area \cdot (M_g - M_{pe.top}) + B_{top} \cdot P_e] \cdot y_{cgt}}{Area \cdot I_{top} - (B_{top})^2}$$

$$f_{cgp} = 4.831 \quad (\text{ksi})$$

$$\Delta f_{pES} := \frac{E_p}{E_{ci}} \cdot f_{cgp} \quad \Delta f_{pES} = 30.365 \quad (\text{ksi})$$

ii. Prestress Loss due to Elastic Shortening (continued)

Iteration 2

$$f_{pe,ES} := f_{pj} - (\Delta f_{pES} + \Delta f_{pR1}) \quad f_{pe,ES} = 168.86 \quad (\text{ksi})$$

$$M_g := \frac{w_{sw} \cdot L^2}{8} \quad M_g = 43740 \quad (\text{kip} \cdot \text{in})$$

$$P_e := f_{pe,ES} \cdot A_{ps} \quad P_e = 1941.89 \quad (\text{kip})$$

$$M_{pe,top} := P_e \cdot y_{cgt} \quad M_{pe,top} = 137292 \quad (\text{kip} \cdot \text{in})$$

$$f_{cgp} := -\frac{I_{top} \cdot P_e + B_{top} \cdot (M_g - M_{pe,top}) + [\text{Area} \cdot (M_g - M_{pe,top}) + B_{top} \cdot P_e] \cdot y_{cgt}}{\text{Area} \cdot I_{top} - (B_{top})^2} \quad f_{cgp} = 4.148 \quad (\text{ksi})$$

$$\Delta f_{pES} := \frac{E_p}{E_{ci}} \cdot f_{cgp} \quad \Delta f_{pES} = 26.072 \quad (\text{ksi})$$

$$\Delta f_{pES,\%} := \frac{\Delta f_{pES}}{f_{pj}} \cdot 100 \quad \Delta f_{pES,\%} = 12.9 \quad (\%)$$

iii. *Prestress Loss due Shrinkage of Concrete*

$$\Delta f_{pSR} := 17.0 - 0.150H \quad \Delta f_{pSR} = 7.25 \quad (\text{ksi})$$

$$\Delta f_{pSR.\%} := \frac{\Delta f_{pSR}}{f_{pj}} \cdot 100 \quad \Delta f_{pSR.\%} = 3.6 \quad (\%)$$

iv. *Prestress Loss due Creep of Concrete*

$$f_{pe} := f_{pj} - (\Delta f_{pR1} + \Delta f_{pES}) \quad f_{pe} = 173.153 \quad (\text{ksi})$$

$$M_{pe} := (f_{pe} \cdot A_{ps}) \cdot e_{cgt} \quad M_{pe} = 65911 \quad (\text{kip} \cdot \text{in})$$

$$f_{cgp} := \frac{M_{pe} \cdot e_{cgt}}{I} \quad f_{cgp} = 2.332 \quad (\text{ksi})$$

$$\Delta f_{cdp} := \frac{M_g \cdot e_{cgt}}{I} \quad \Delta f_{cdp} = 1.548 \quad (\text{ksi})$$

$$\Delta f_{pCR} := \begin{cases} \text{out} \leftarrow 12.0 f_{cgp} - 7.0 \Delta f_{cdp} & \Delta f_{pCR} = 17.151 \quad (\text{ksi}) \\ \text{out} \leftarrow \text{out} & \text{if } \text{out} \geq 0 \\ \text{out} \leftarrow 0 & \text{otherwise} \end{cases}$$

$$\Delta f_{pCR.\%} := \frac{\Delta f_{pCR}}{f_{pj}} \cdot 100 \quad \Delta f_{pCR.\%} = 8.5 \quad (\%)$$

v. *Prestress Loss due to Relaxation of the Prestressing Steel After Transfer*

$$\Delta f_{pR2} := \begin{cases} R2 \leftarrow 20.0 - 0.4 \Delta f_{pES} - 0.2 (\Delta f_{pSR} + \Delta f_{pCR}) & \Delta f_{pR2} = 1.407 \quad (\text{ksi}) \\ R2 \leftarrow R2 \cdot 0.30 & \text{if } \text{PrestressType} = \text{"Low Relaxation"} \\ R2 \leftarrow R2 & \text{if } \text{PrestressType} = \text{"Stress Relieved"} \end{cases}$$

$$\Delta f_{pR2.\%} := \frac{\Delta f_{pR2}}{f_{pj}} \cdot 100 \quad \Delta f_{pR2.\%} = 0.695 \quad (\%)$$

v. *Effective Prestress After Initial Effects*

$$\Delta f_{pi} := \Delta f_{pR1} + \Delta f_{pES} \quad \Delta f_{pi} = 29.347 \quad (\text{ksi})$$

$$\Delta f_{pi.\%} := \frac{\Delta f_{pi}}{f_{pj}} \cdot 100 \quad \Delta f_{pi.\%} = 14.5 \quad (\%)$$

$$f_{pi} := f_{pj} - \Delta f_{pi} \quad f_{pi} = 173.153 \quad (\text{ksi})$$

vi. *Effective Prestress After Initial and Time-Dependent Effects*

$$f_{pTOT} := \Delta f_{pR1} + \Delta f_{pES} + \Delta f_{pSR} + \Delta f_{pCR} + \Delta f_{pR2} \quad f_{pTOT} = 55.155 \quad (\text{ksi})$$

$$\Delta f_{pTOT.\%} := \frac{f_{pTOT}}{f_{pj}} \cdot 100 \quad \Delta f_{pTOT.\%} = 27.2 \quad (\%)$$

$$f_{pe} := f_{pj} - f_{pTOT} \quad f_{pe} = 147.345 \quad (\text{ksi})$$

vii. *Creep Coefficient Cacluation (LRFD 5.4.2.3.2-1, Collins and Mitchell, 1991)*

$$k_c(t) := \left(\frac{45 + t}{26e^{0.36 \cdot VS} + t} \right) \cdot \left(\frac{1.80 + 1.77 \cdot e^{-0.54 \cdot VS}}{2.587} \right) \quad \text{LRFD C5.4.2.3.2-1}$$

$$k_f(f_c) := \frac{1}{0.67 + \left(\frac{f_c}{9} \right)} \quad \text{LRFD 5.4.2.3.2-2}$$

$$\psi(t_j, t, f_c) := 3.5 \cdot k_c(t) \cdot k_f(f_c) \cdot \left(1.58 - \frac{H}{120} \right) \cdot t_j^{-0.118} \cdot \frac{(t - t_j)^{0.6}}{10.0 + (t - t_j)^{0.6}} \quad \text{LRFD 5.4.2.3.2-1}$$

$$C_{\text{release}} := \psi(t_j, 0 + t_j, f_c) \quad C_{\text{release}} = 0$$

$$C_{30\text{day}} := \psi(t_j, 30 + t_j, f_c) \quad C_{30\text{day}} = 0.362$$

$$C_{60\text{day}} := \psi(t_j, 60 + t_j, f_c) \quad C_{60\text{day}} = 0.501$$

$$C_{120\text{day}} := \psi(t_j, 120 + t_j, f_c) \quad C_{120\text{day}} = 0.671$$

$$C_{240\text{day}} := \psi(t_j, 240 + t_j, f_c) \quad C_{240\text{day}} = 0.849$$

Camber Calculations

$$\Delta_{pi} := \frac{(f_{pi} \cdot A_{ps}) \cdot e_{cgt} \cdot L^2}{8 \cdot E_c \cdot I} \quad \Delta_{pi} = 7.33 \quad (\text{in}) \quad (\text{Camber due to applied prestressing force})$$

$$\Delta_{pe} := \frac{(f_{pe} \cdot A_{ps}) \cdot e_{cgt} \cdot L^2}{8 \cdot E_c \cdot I} \quad \Delta_{pe} = 5.496 \quad (\text{in}) \quad (\text{Camber due to effective prestressing force, i.e. after prestress losses})$$

$$\Delta_{sw} := \frac{5 \cdot w_{sw} \cdot L^4}{384 E_c \cdot I} \quad \Delta_{sw} = 3.571 \quad (\text{in}) \quad (\text{Deflection due to beam self-weight})$$

Application of calculated creep coefficients to camber and dead-load deflection

$$\Delta_{\text{release}} := \Delta_{pe} + \frac{\Delta_{pi} + \Delta_{pe}}{2} \cdot C_{\text{release}} - \Delta_{sw} \cdot (1 + C_{\text{release}}) \quad \Delta_{\text{release}} = 1.924 \quad (\text{in})$$

$$\Delta_{30\text{day}} := \Delta_{pe} + \frac{\Delta_{pi} + \Delta_{pe}}{2} \cdot C_{30\text{day}} - \Delta_{sw} \cdot (1 + C_{30\text{day}}) \quad \Delta_{30\text{day}} = 2.952 \quad (\text{in})$$

$$\Delta_{60\text{day}} := \Delta_{pe} + \frac{\Delta_{pi} + \Delta_{pe}}{2} \cdot C_{60\text{day}} - \Delta_{sw} \cdot (1 + C_{60\text{day}}) \quad \Delta_{60\text{day}} = 3.348 \quad (\text{in})$$

$$\Delta_{120\text{day}} := \Delta_{pe} + \frac{\Delta_{pi} + \Delta_{pe}}{2} \cdot C_{120\text{day}} - \Delta_{sw} \cdot (1 + C_{120\text{day}}) \quad \Delta_{120\text{day}} = 3.83 \quad (\text{in})$$

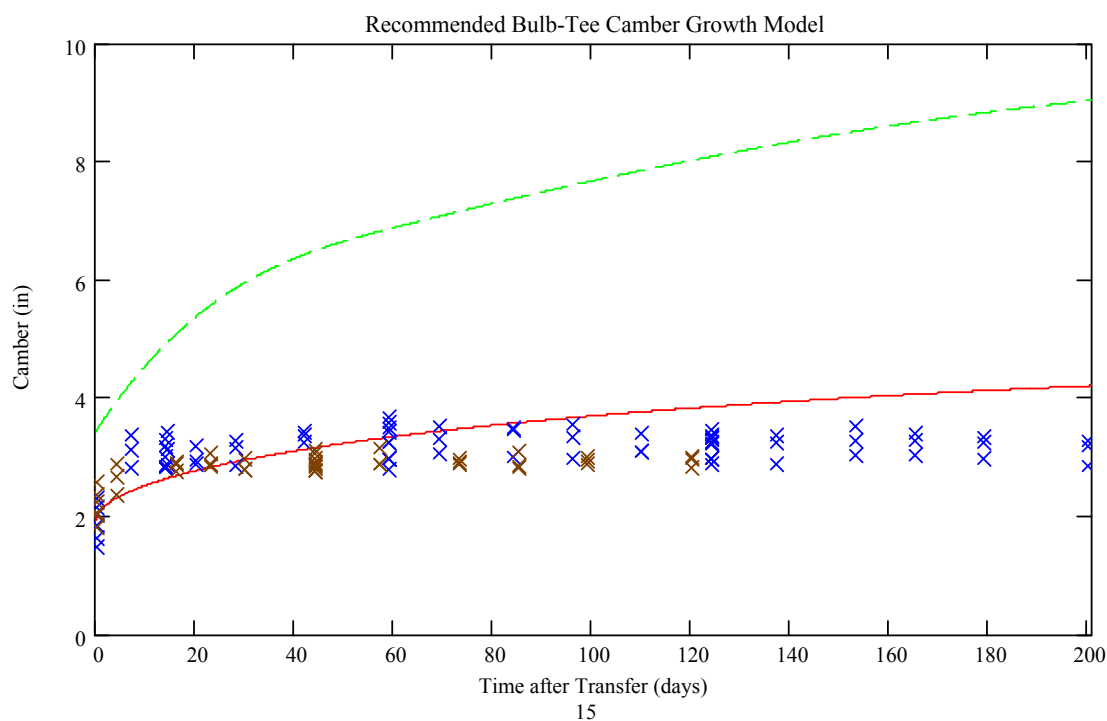
$$\Delta_{240\text{day}} := \Delta_{pe} + \frac{\Delta_{pi} + \Delta_{pe}}{2} \cdot C_{240\text{day}} - \Delta_{sw} \cdot (1 + C_{240\text{day}}) \quad \Delta_{240\text{day}} = 4.336 \quad (\text{in})$$

Time-Dependent Camber Growth Model

$$\Delta_{\text{camber}}(t_j, t, f_c) := \Delta_{pe} + \frac{\Delta_{pi} + \Delta_{pe}}{2} \cdot \psi(t_j, t + t_j, f_c) - \Delta_{sw} \cdot (1 + \psi(t_j, t + t_j, f_c))$$

] Field Camber Measurements

] FDOT Curve Fit



¹⁵ Note: Dashed line represents curve fit of FDOT produced values, the solid line represents recommended camber growth model, and the “X’s” represent the field measured values.

APPENDIX I
DOCUMENTED LIMROCK SPECIMEN DATA

AASHTO Type IV 1 (Limerock)			AASHTO Type IV 2 (Limerock)			AASHTO Type IV 3 (Limerock)		
Date	Time After Release (Days)	Field Camber (in)	Date	Time After Release (Days)	Field Camber (in)	Date	Time After Release (Days)	Field Camber (in)
8/26/2004	0	2.38	8/26/2004	0	2.38	8/26/2004	0	2.38
9/18/2004	23	4.00	9/18/2004	23	3.75	9/18/2004	23	4.00
10/20/2004	55	4.19	10/20/2004	55	4.31	10/20/2004	55	4.25
AASHTO Type IV 4 (Limerock)			AASHTO Type IV 5 (Limerock)			AASHTO Type IV 6 (Limerock)		
Date	Time After Release (Days)	Field Camber (in)	Date	Time After Release (Days)	Field Camber (in)	Date	Time After Release (Days)	Field Camber (in)
8/26/2004	0	2.25	8/26/2004	0	2.38	8/26/2004	0	2.38
9/18/2004	23	3.88	9/18/2004	23		9/18/2004	23	
10/20/2004	55	4.25	10/20/2004	55	4.13	10/20/2004	55	4.13
AASHTO Type IV 7 (Limerock)			AASHTO Type IV 8 (Limerock)			AASHTO Type IV 9 (Limerock)		
Date	Time After Release (Days)	Field Camber (in)	Date	Time After Release (Days)	Field Camber (in)	Date	Time After Release (Days)	Field Camber (in)
8/26/2004	0	2.38	8/26/2004	0	2.50	8/26/2004	0	2.38
9/18/2004	23		9/18/2004	23		9/18/2004	23	
10/20/2004	55	4.13	10/20/2004	55	4.25	10/20/2004	55	4.19
AASHTO Type IV 10 (Limerock)								
Date	Time After Release (Days)	Field Camber (in)						
8/26/2004	0	2.25						
9/18/2004	23							
10/20/2004	55	4.25						

72" Bulb-Tee 1 (Limerock)			72" Bulb-Tee 2 (Limerock)			72" Bulb-Tee 3 (Limerock)		
Date	Time After Release (Days)	Field Camber (in)	Date	Time After Release (Days)	Field Camber (in)	Date	Time After Release (Days)	Field Camber (in)
11/4/2003	0	2.50	11/4/2003	0	2.50	11/4/2003	0	2.50
7/9/2004	248	4.13	7/9/2004	248	4.13	7/9/2004	248	4.25
8/19/2004	289	4.50	8/19/2004	289	4.25	8/19/2004	289	4.25
9/18/2004	319	4.50	9/18/2004	319	4.25	9/18/2004	319	4.25
10/20/2004	351	4.50	10/20/2004	351	4.50	10/20/2004	351	4.50
11/19/2004	381	4.63	11/19/2004	381	4.38	11/19/2004	381	4.50
72" Bulb-Tee 4 (Limerock)			72" Bulb-Tee 5 (Limerock)			72" Bulb-Tee 6 (Limerock)		
Date	Time After Release (Days)	Field Camber (in)	Date	Time After Release (Days)	Field Camber (in)	Date	Time After Release (Days)	Field Camber (in)
11/4/2003	0	2.50	11/18/2003	0	2.63	11/18/2003	0	2.50
7/9/2004	248	4.38	7/9/2004	234	5.00	7/9/2004	234	5.25
8/19/2004	289	4.50	8/19/2004	275	5.50	8/19/2004	275	5.50
9/18/2004	319	4.25	9/18/2004	305	5.25	9/18/2004	305	5.50
10/20/2004	351	4.38	10/20/2004	337	5.75	10/20/2004	337	5.75
11/19/2004	381	4.38	11/19/2004	367	5.25	11/19/2004	367	5.25
72" Bulb-Tee 7 (Limerock)			72" Bulb-Tee 8 (Limerock)					
Date	Time After Release (Days)	Field Camber (in)	Date	Time After Release (Days)	Field Camber (in)			
11/18/2003	0	2.50	11/18/2003	0	2.50			
7/9/2004	234	5.25	7/9/2004	234	5.25			
8/19/2004	275	5.50	8/19/2004	275	5.75			
9/18/2004	305	5.50	9/18/2004	305	5.50			
10/20/2004	337	5.13	10/20/2004	337	5.75			
11/19/2004	367	5.25	11/19/2004	367	5.13			

AASHTO Type IV (Limerock)		72" Bulb-Tee (Limerock)	
Time After Transfer (days)	Average Compressive Strength (psi)	Time After Transfer (days)	Average Compressive Strength (psi)
0	6730	0	7063
28	9407	28	10068

REFERENCES

Referenced Standards and Reports

ASTM

C 157-93

C 512-87

ACI 318-02 Building Code and Commentary

Section 8.5.1

AASHTO LRFD Bridge Design Specification, 1998 ed.

Section 5.9.5.4

AASHTO Guide Specifications, 1989, "Thermal Effects in Concrete Bridge Superstructures (NCHRP R-276)," American Association of State Highway and Transportation Officials, Washington, D.C., 52 pp.

ACI Committee 209R, 1997, "Prediction of Creep, Shrinkage, and Temperature Effects in Concrete Structures (ACI 209R-92)," American Concrete Institute, Farmington Hills, MI, 47 pp.

Cited References

Aïtcin, P. C. and Mehta P. K., 1990, "Effect of Coarse Aggregate Characteristics on Mechanical Properties of High-Strength Concrete," American Concrete Institute Materials Journal, v. 87, is. 2, American Concrete Institute, Farmington Hills, MI, pp. 103-107.

Baalbaki, Walid; Aïcin, Pierre-Claude; and Ballivy, Gerard, 1992, "On Predicting Modulus of Elasticity in High-Strength Concrete," American Concrete Institute Materials Journal, v. 89, is. 5, American Concrete Institute, Farmington Hills, MI, pp. 517-520.

Branson, Dan E., 1977, *Deformation of Concrete Structures*, McGraw Hill, Inc., New York, NY, pp. 1-40.

- Byle, K.A.; Burns, Ned H.; Carrasquillo, Ramón L.; 1997. "Time-Dependent Deformation Behavior of Prestressed High Performance Concrete Bridge Beams," Center for Transportation Research, Bureau of Engineering Research, University of Texas, Austin, TX.
- Canadian Prestressed Concrete Institute, *Metric Design Manual – Precast and Prestressed Concrete*, 3rd ed., CPCI, Ottawa, 1996.
- Giaccio, G. and Zerbino, R., 1998, "Failure Mechanism of Concrete, Combined Effects of Coarse Aggregate and Strength Level," Elsevier Science, Elsevier Science Ltd., New York, NY, 8 pp.
- Illston, J.M. and England, L., 1970, "Creep and Shrinkage of Concrete and Their Influence on Structural Behavior—A Review of Methods of Analysis," Structural Engineer, Institution of Structural Engineers, London, UK, pp. 283-292.
- Kostmatka, Steven H. and Panarese, William C., 1988, *Design and Control of Concrete Mixtures*, 13th Ed., Portland Cement Association, Skokie, IL, pp. 153-159.
- Lybas, John M., 1990, "Reconciliation Study of Creep in Florida Concrete," Structures and Material Research Report, No. 90-1, University of Florida Department of Civil and Coastal Engineering, Gainesville, FL, 115 pp.
- Magura, Donald D.; Sozen, Mete A.; and Siess, Chester P., 1964, "A Study of Stress Relaxation in Prestressing Reinforcement," *Precast/Prestressed Concrete Institute Journal*, v. 9, is. 2, Precast/Prestressed Concrete Institute, Chicago, IL, pp. 13-57.
- Mehta, Kumar P., 1986, *Concrete: Structure, Properties, and Materials*, Prentice Hall, Inc., Englewood Cliffs, NJ.
- Mindness, Sidney; Young, J. Francis; and Darwin, David, 2003, Concrete, 2nd Ed., Pearson Education, Inc., Upper Saddle River, NJ, pp. 417-456.
- Naaman, A. E. and Hamza, A. M., 1993, "Prestress Losses in Partially Prestressed High Strength Concrete Beams," *Precast/Prestressed Concrete Institute Journal*, v. 38, is. 3, Precast/Prestressed Concrete Institute, Chicago, IL, pp. 98-114.
- Nawy, Edward G., 2003, *Prestressed Concrete, A Fundamental Approach*, 4th Ed., Pearson Education, Inc., pp. 403-480.
- Neville, Adam M., 1997, "Aggregate Bond and Modulus of Elasticity of Concrete," *American Concrete Institute Materials Journal*, v. 94, is. 1, American Concrete Institute, Farmington Hills, MI, pp. 71-74.

- Neville, Adam M., 1971, *Hardened Concrete: physical and mechanical aspects*, American Concrete Institute monograph, No. 6, American Concrete Institute, Detroit, MI, pp. 142-159, 359-433.
- Neville, A. M., 1963, *Properties of Concrete*, Sir Isaac Pitman & Sons Ltd., London, UK, pp. 95-170.
- Nilson, Arthur H., 1987, *Design of Prestressed Concrete*, 2nd Ed., John Wiley & Sons, Inc., New York, NY, pp. 33-36.
- Preston, H.K., 1975, "Recommendations for Estimating Prestress Losses," *Journal of the Prestressed Concrete Institute*, Prestressed Concrete Institute, Chicago, IL, pp. 43-75.
- Prestressed Concrete Institute, *PCI Design Handbook: Precast and Prestressed Concrete*, 5th ed., PCI, Chicago, 1999.
- R&A Products, January 20, 1996 *The Pro-Level™ Water Manometer*, "The Pro-Level™ Manometer Overview – Functions, Uses, Advantages, Accuracy: Operation" R&A Products, San Diego, CA, <<http://prolevel.com/operation.htm>> November 20, 2004.
- Sengul, Özkan; Tasdemir, Canan; and Tasdemir, Mehmet Ali, 2002, "Influence of Aggregate Type on Mechanical Behavior of Normal- and High-Strength Concretes," *American Concrete Institute Materials Journal*, v. 99, is. 6, American Concrete Institute, Farmington Hills, MI, pp. 528-533.
- Sinno, R. and Furr, H. L., 1970, "Hyperbolic Functions for Prestress Loss and Camber," *ASCE Journal of the Structural Division*, v. 96, no. ST4, American Society of Civil Engineers Publications, Reston, VA, pp. 803-821.
- Tadros, M. K.; Ghali, A.; and Meyer, A. W., 1985, "Prestress Loss and Deflection of Precast Concrete Members," *Precast/Prestressed Concrete Institute Journal*, v. 30, is. 1, Precast/Prestressed Concrete Institute, Chicago, IL, pp. 114-141.
- Troxell, George Earl; Davis, Harmer E.; and Kelly, Joe W., 1968, *Composition and Properties of Concrete*, 2nd Ed., McGraw Hill, Inc., New York, NY, pp. 290-351.
- Yazdani, N.; Mtenga, P.; and Richardson, N., 1999, "Camber Variation in Precast Girders," *Concrete International*, American Concrete Institute, Farmington Hills, MI, pp. 45-49.